

This file is part of the following work:

Dos Santos Antunes, Elsa Marisa (2017) *Investigations on biochar production from biosolids via microwave assisted pyrolysis and its potential applications*. PhD thesis, James Cook University.

Access to this file is available from:

<https://doi.org/10.4225/28/5ac5acab2251c>

Copyright © 2017 Elsa Marisa Dos Santos Antunes.

The author has certified to JCU that they have made a reasonable effort to gain permission and acknowledge the owner of any third party copyright material included in this document. If you believe that this is not the case, please email researchonline@jcu.edu.au

Investigations on Biochar Production from Biosolids
via Microwave Assisted Pyrolysis and its Potential
Applications

PhD Thesis

Elsa Marisa Dos Santos Antunes (BSc)

in September 2017

For the degree of Doctor of Philosophy
in the College of Science and Engineering

James Cook University

Townsville

Advisors: A/Prof Philip Schneider, A/Prof Mohan Jacob, Dr Madoc Sheehan

DECLARATION

I declare that this thesis is my own work and has not been submitted to elsewhere in whole or in part to obtain other degree award. The content of this thesis is the result of author work and the contribution of others has been acknowledged in the statement of contribution of others.

Elsa Dos Santos Antunes

September, 2017

STATEMENT OF ACCESS TO THIS THESIS

I, the under-signed, the author of this research work, understand that James Cook University will make this thesis available for use within the University Library and via the Australian Digital Thesis Network, for use elsewhere.

I understand that an unpublished work, a thesis has significant protection under the Copyright Act. I do not wish to place any restriction on access to this thesis, but any use of its content must be acknowledged.

Elsa Dos Santos Antunes

September, 2017

STATEMENT ON THE CONTRIBUTIONS OF OTHERS

Nature of assistance	Type of Contribution	Description of Contribution
Intellectual support	Editorial Assistance	I would like to thank my advisors (A/Prof Philip Schneider and A/Prof Mohan Jacob) for helping me with editing of my thesis and publications.
Financial Support	Fee offset	The Australian Government
	Research Costs	The Smart Water Fund
	Stipend	Graduate Research School, James Cook University
Data Collection	Research Assistance	I would like to thank James Schumann (master student at James Cook University) for assisting me in carrying out the pyrolysis experiments described in chapters 4 and 7.

AKNOWLEDGEMENTS

I would like to acknowledge the infinitive support from my advisor committee to my project thesis.

I wish to thank A/Prof Philip Schneider and A/Prof Mohan Jacob for trusting me and giving me freedom to develop my research project providing me the resources necessary to successfully develop my research work. I would like to thank both my advisors for being both a supporter and critic, and for steering me through my research and helping me to refine my writing.

I thank Dr Graham Brodie from The University of Melbourne for his unlimited support on microwave technology, helping me on modelling and simulation of single-mode microwave cavities. Also, I am grateful for helping me to access the Advanced Porous Materials Laboratory at The University of Melbourne, fundamental for surface area characterisation of my research materials.

I am very grateful to A/Prof Rachel Caruso and Dr William McMaster from The University of Melbourne for allowing me to use their laboratory for surface area characterisation and thermogravimetric analysis of biochar.

I thank James Schumann (master student at James Cook University) for helping me with some of the microwave assisted pyrolysis experiments and interesting discussions.

I would like to acknowledge the Advanced Analytical Centre at James Cook University for the access to scanning electron microscopy, X-ray diffraction and inductively coupled plasma.

I am grateful to the financial support – Australian Postgraduate Award scholarship provided by the Graduate Research School, James Cook University. I acknowledge the Smart Water fund for the extra financial support provided to this research, which was fundamental for the characterisation of biochar.

Finally, I would like to thank the enormous support from my family and husband Pedro, a great inspiration in my life.

ABSTRACT

Biosolids are the treated solid fraction produced in a municipal wastewater treatment plant. Biosolids production has been increasing every year mainly because of: 1) population increase, 2) more access to a sewage network, in particular in developing countries, and 3) more restrictive environmental regulations. Land application is typically used to manage biosolids, but contaminant leaching from biosolids to soil and groundwater has restricted this approach. Currently in Europe, biosolids are mainly incinerated, but in Australia there are no incineration plants, so a new environmental and sustainable solution for biosolids management has to be established in the near future. These new approaches must be focused on biosolids recycling and by-products valorisation, mitigating environmental impact and resource depletion.

This research studied microwave assisted pyrolysis (MWAP) as a methodology for biosolids treatment and investigated the potential applications of the final biochar. This study investigated the dielectric properties of biosolids and the impact of MWAP conditions on biosolids processing and biochar properties. The dielectric properties of compacted biosolids with varying moisture content were measured at different microwave frequencies using a network analyser. Results showed that as the moisture content increased in biosolids, the dielectric constant and dielectric loss factor both increased. Dry biosolids were almost transparent to microwaves, indicating that the ability to absorb microwave energy is very low. To overcome this problem, an addition of a microwave susceptor (activated carbon) was employed for the biosolids pyrolysis experiments.

As single-mode microwave cavities have just one “hot spot”, it is fundamental to place the biosolids sample in this area to maximize coupling between microwaves and the sample. Numerical simulations were carried out to assess the impact of biosolids load and moisture content on microwave field intensity and distribution. These simulations were done by using Inventor Professional 2015 software (AutoDesk Co., USA) and XFDTD software, version 7.5.1.3.r43518 (Remcom Co., USA) to solve the Maxwell’s electromagnetic equations for the pre-defined materials and microwave feed ports conditions in XFDTD. Results showed that distribution and intensity of the microwave field were significantly affected by moisture content. As the moisture increases the

intensity and distribution of microwave field decreased due to the adsorption of electromagnetic energy by the sample because water is a good microwave absorber. As the sample load increased, the electromagnetic field decreased, and its distribution was clearly affected due to field perturbation.

Pyrolysis conditions affect product yield and distribution, and the properties of the final by-products. Of all the conditions, temperature is the pyrolysis process variable with the greater impact on by-products properties. In this study, pyrolysis temperature impacted on biochar yield, surface area and resultant functional groups present on the biochar. Biochar yield decreased while surface area increased at higher pyrolysis temperatures. The heavy metals of biosolids accumulated in the final biochar and the percentage of heavy metals increased as the biochar yield decreased. Microwave susceptors affected the heating rate and consequently the pyrolysis energy consumption, biochar yield and properties. Activated carbon was the best option for biosolids MWAP due to the lower energy consumption, and the biochar had the highest stability and surface area, which are fundamental requirements for biochar soil application.

The biosolids biochar was successfully used for phosphorus and silver recovery from synthetic and real solutions. The phosphorus removal capacity by biochar was affected by the calcium content in biochar, contact time between biochar and phosphorus solution, pH and initial concentration of phosphorus of the aqueous solution. As the calcium content increased in biosolids, the phosphorus removal capacity increased due to more available calcium cations to complex with phosphate species. The phosphorus removal capacity of biochar (11.5% of Ca) was maximised at pH 4, corresponding to 147 mg-P/g of biochar. The main mechanism of phosphorus removal was precipitation, and the experimental data was well described by a pseudo second-order kinetic model and the isotherms followed the Langmuir model. Brushite (calcium hydrogen phosphate dehydrate: $\text{CaHPO}_4 \cdot 2\text{H}_2\text{O}$) was the main precipitation product resultant from the combination of calcium cations with phosphate species.

Silver is an emerging pollutant in wastewater treatment plants due to the wide use of this element as an anti-bacterial in final products. This element represents a serious threat to life even when present in very small amounts. This study showed that silver removal by biochar is a spontaneous process of physical adsorption. Silver removal

capacity increased with initial silver concentration and temperature of the silver aqueous solution. Experimental data fitted was well described by the pseudo second-order kinetic model and intra-particle diffusion model. The final composite (Ag-biochar) after silver adsorption can be further used for methylene blue degradation and adsorption.

The results of this study demonstrated that MWAP is an environmentally sustainable approach to deal with the anticipated increases in biosolids production. The final biochar can be used as adsorbent for contaminant removal, water pollution mitigation and resource recovery, thereby avoiding future natural resource depletion.

TABLE OF CONTENTS

DECLARATION.....	II
STATEMENT OF ACCESS TO THIS THESIS	III
STATEMENT ON THE CONTRIBUTIONS OF OTHERS	IV
AKNOWLEDGEMENTS	V
ABSTRACT	VI
TABLE OF CONTENTS	IX
LIST OF FIGURES	XVI
LIST OF TABLES	XIX
LIST OF PUBLICATONS	XXI
1 INTRODUCTION	1
1.1 Problem statement.....	1
1.2 Research Objectives.....	2
1.3 Thesis organisation	3
2 LITERATURE REVIEW	7
Abstract.....	7
2.1 Introduction.....	8
2.2 The value of biosolids.....	11

2.2.1	Nutrients value in biosolids	12
2.2.2	Energy value in biosolids	14
2.2.3	Chemical value in biosolids.....	14
2.3	Overview of current biosolids management methods.....	15
2.3.1	Incineration.....	15
2.3.2	Land application	16
2.3.3	Landfilling	17
2.3.4	Pyrolysis	18
2.4	Microwave Assisted Pyrolysis.....	21
2.4.1	Microwave Pyrolysis of Biosolids.....	23
2.4.2	Catalyst for MWAP	24
2.4.3	Temperature measurement inside microwave cavities.....	25
2.4.4	MWAP for nutrient recovery.....	26
2.4.5	MWAP for energy recovery	29
2.4.6	MWAP for chemicals recovery	31
2.5	Biochar.....	32
3	DIELECTRIC PROPERTIES OF BIOSOLIDS	45
	Abstract.....	45

Highlights	46
3.1 Introduction.....	47
3.2 Materials and methods	49
3.3 Results and discussion	51
3.3.1 Dielectric properties of biosolids and microwave susceptors	51
3.3.2 Microwave susceptor selection.....	57
3.3.3 Impact of microwave susceptors on pyrolysis heating rate and biochar properties	59
3.4 Conclusions.....	65
4 IMPACT OF PYROLYSIS TEMPERATURE ON BIOCHAR	66
Abstract.....	66
Highlights	67
4.1 Introduction.....	68
4.2 Materials and Methods.....	71
4.2.1 Materials	71
4.3 Methods	71
4.3.1 Pyrolysis experiments.....	71
4.3.2 Proximate analysis	74
4.3.3 Biochar yield	76

4.3.4	pH	76
4.3.5	Specific surface area	76
4.3.6	Thermogravimetric analysis	76
4.3.7	Chemical analyses	77
4.3.8	Phosphorus adsorption capacity	77
4.4	Results and discussion	78
4.4.1	Biosolids chemical composition	78
4.4.2	Biosolids proximate and ultimate analyses	79
4.4.3	Thermogravimetric analysis	79
4.4.4	Biochar yield	82
4.4.5	Volatiles, ash content, pH of biochar	84
4.4.6	Biochar specific surface area	85
4.4.7	Chemical analysis of biosolids and biochar	86
4.4.8	Phosphorus adsorption by biochar and biosolids	88
4.5	Conclusions.....	89
5	PHOSPHORUS RECOVERY FROM AQUEOUS SOLUTION BY Ca-DOPED BIOCHAR	91
	Abstract.....	91
	Highlights	92

5.1	Introduction.....	93
5.2	Materials and Methods.....	95
5.2.1	Biochar preparation	95
5.2.2	Biochar characterisation	96
5.2.3	Phosphorus removal capacity	96
5.3	Results and Discussion	98
5.3.1	Biochar characterisation	98
5.3.2	Phosphorus removal kinetics.....	100
5.3.3	Phosphate adsorption isotherms	102
5.3.4	Impact of initial pH of P-stock solution on phosphorus removal.....	105
5.4	Conclusions.....	112
6	SILVER REMOVAL FROM AQUEOUS SOLUTION BY BIOCHAR	114
	Abstract.....	114
	Highlights	115
6.1	Introduction.....	116
6.2	Materials and Methods.....	118
6.2.1	Biochar Preparation	119
6.2.2	Silver adsorption tests.....	120

6.2.3	Methylene blue (MB) adsorption and photodegradation.....	121
6.2.4	Biochar characterisation	123
6.3	Results and Discussion	123
6.3.1	The impact of pyrolysis conditions on biochar properties	123
6.3.2	Silver removal study.....	124
6.3.3	Adsorption kinetics.....	125
6.3.4	Adsorption isotherms and thermodynamics of adsorption	130
6.3.5	Characterisation of Ag-biochar	135
6.3.6	Applications of nanocomposite Ag-biochar	138
6.4	Conclusions.....	139
7	HEAVY METALS IN BIOSOLIDS	140
	Abstract.....	140
	Highlights	141
7.1	Introduction.....	142
7.2	Materials and Methods.....	144
7.2.1	Biochar production	144
7.2.2	Chemical composition of biochar.....	145
7.2.3	Heavy metal leaching	145

7.2.4	Statistical analysis	146
7.3	Results and discussion	146
7.3.1	Pyrolysis by-product yields	146
7.3.2	Heavy metal in biochar	148
7.3.3	Heavy metal leaching from biosolids and biochar	150
7.3.4	Metal leaching from biochar obtained from limed biosolids	151
7.3.5	SWOT analysis of biosolids management approaches.....	154
7.4	Conclusions.....	158
8	CONCLUSION AND RECOMMENDATIONS	159
8.1	Dielectric properties and microwave pyrolysis of biosolids.....	159
8.2	Impact of pyrolysis temperature on biochar properties	160
8.3	Phosphorus recovery by biochar	161
8.4	Silver removal by biochar	162
8.5	Heavy metals in biosolids and biochar	163
8.6	Implications of this research	164
8.7	Recommendations.....	165
	REFERENCES	167
	APPENDIX	189

LIST OF FIGURES

Figure 2.1 – Biosolids disposal methods in Australia (2013), The United States (2013) and Germany (2011) (adapted from [27, 28]).	10
Figure 2.2 – Biosolids disposal methods in The USA in 2008 and 2013 [27, 31].	11
Figure 2.3 – Microwave and conventional heating processes.	22
Figure 2.4 – Microwave heating process illustration, transferring energy from microwave susceptors to the cooler surroundings.	24
Figure 2.5 – Adsorption capacity of Cu(II) by sewage sludge adsorbents.	34
Figure 2.6 – Adsorption capacity of Pb(II) by sewage sludge adsorbents.	35
Figure 3.1 - Dielectric constant (a) and dielectric loss factor (b) of biosolids with varying moisture content measured at room temperature (23°C) between 1 to 10GHz.	52
Figure 3.2 – Electromagnetic field distribution and intensity in microwave cavity with 50 g of dry biosolids (a), 50 g of biosolids with 40% moisture content (b), 25 g of dry biosolids (c) and 25 g of biosolids with 40% moisture content (d).	54
Figure 3.3 – Penetration depth of dry biosolids and biosolids with varying moisture content at different microwave frequency.	57
Figure 3.4 – Temperature profile of microwave pyrolysis of biosolids mixed with 20% of a microwave susceptor.	60
Figure 3.5 – SEM of biochar produced from biosolids with different microwave absorbers: activated carbon (a), charcoal (b) and glycerol (c).	64
Figure 4.1 – Schematic of the single-mode microwave system used in this research.	73

Figure 4.2 – Thermogravimetric analysis of biosolids.....	80
Figure 4.3 – Temperature profile of biosolids MWAP.	81
Figure 4.4 – Microwave field intensity and distribution in empty chamber and with biosolids.....	84
Figure 4.5 – FTIR spectrum of biosolids and biochar obtained at different temperatures.	87
Figure 4.6 – XRD spectrum of biosolids and biochar obtained at different temperatures.	88
Figure 5.1 – Phosphorus removal kinetics of biochar.	101
Figure 5.2 – Phosphorus adsorption isotherm of biochar samples with Langmuir model superimposed.....	104
Figure 5.3 – Effect of pH on phosphorus removal by Ca-doped biochar.....	106
Figure 5.4 – Final pH of supernatant after 24 hours of reaction time of biochar with P-stock solution with different pH.....	106
Figure 5.5 – XRD spectrum of the four biochar samples before and after phosphorus removal tests (B – Brushite, Q – Quartz, C – Calcite) (Biochar – before adsorption; pH=2, 3, 4 and 12 – after adsorption).....	110
Figure 5.6 – Phosphorus removal by biochar from an effluent and P-stock solution. .	112
Figure 6.1 – Adsorption kinetics of silver by biochar.....	127
Figure 6.2 – Stages of intra-particle diffusion process of silver in biochar.....	127
Figure 6.3 – Adsorption isotherms of silver removal by biochar across a range of temperatures.....	132

Figure 6.4 – Biochar after silver adsorption (EDS mapping).....	135
Figure 6.5 – EDS of biochar before adsorption (A) and after silver adsorption (B). ...	136
Figure 6.6 – XRD spectrum of biochar before and after silver adsorption (Q: quartz, Ag: silver; K: kaolinite).....	138
Figure 7.1 – Pyrolysis by-product yields versus pyrolysis time at 500°C (a) and 700°C (b).	147
Figure 7.2 – Concentration of heavy metals As (a), Cr (b), Cu (c), Ni (d), Pb (e) and Zn (f) in biochar samples produced at 500°C and 700°C for different pyrolysis times. ...	149
Figure 7.3 – XRD of biochar samples produced from biosolids (BC) and limed biosolids (BC-L) (C – calcite; K – kaolinite; Q - quartz).	152

LIST OF TABLES

Table 2.1 - Composition of sewage sludge in different countries (adapted from [35]).	12
Table 2.2 – Microwave versus conventional pyrolysis (adapted from [65]).	20
Table 2.3 - Classification and main products of pyrolysis (adapted from [64]).	21
Table 2.4 - Heavy metals removal by biochar produced from sewage sludge or biosolids.	38
Table 2.5 – Dyes removal by biochar produced from sewage sludge or biosolids.	41
Table 2.6 – Contaminant removal by biochar produced from sewage sludge or biosolids.	43
Table 3.1 - Dielectric properties of microwave susceptors at 2.45 GHz.	58
Table 3.2 – Biochar yield and properties of the three samples produced with different microwave susceptors (20 wt% based on dry mass of biosolids).	62
Table 4.1 – Chemical composition of biosolids determined by ICP.	79
Table 4.2 – Proximate and ultimate analyses of the biosolids.	79
Table 4.3 – Summary of biochar yield and properties.	83
Table 5.1 – Biochar composition, specific surface area, pore size and volume.	99
Table 5.2 – Phosphorus removal kinetic parameters for the four biochar samples.	102
Table 5.3 – Phosphorus removal isotherm parameters for the four biochar samples.	104

Table 6.1 – Experimental design matrix (L9 orthogonal array), biochar characterisation and silver removal by biochar.	122
Table 6.2 – Ag-removal capacity of different adsorbents.	125
Table 6.3 – Adsorption kinetic parameters calculated using different kinetic models.	128
Table 6.4 – Isotherm parameters of Ag adsorption by biochar at different temperatures.	132
Table 6.5 – Thermodynamic parameters of the adsorption of Ag on biochar.	134
Table 7.1 – Heavy metal leaching from biosolids and biochar produced with different pyrolysis conditions using TCLP method.	151
Table 7.2 – Heavy metal leaching from biosolids and biochar produced from biosolids and lime biosolids at 700°C for 20 minutes, using TCLP method.	154
Table 7.3 – SWOT analysis of biosolids management methods.	156

LIST OF PUBLICATONS

Journal Publications

- E. Antunes, M. V. Jacob, G. Brodie, P. Schneider, *Silver removal from aqueous solution by biochar produced from biosolids via microwave pyrolysis*. Journal of Environmental Management, 2017, 203, 264-272.
- E. Antunes, J Schumann, G. Brodie, M. V. Jacob, P. Schneider, *Biochar produced from biosolids using a single-mode microwave: Characterisation and its potential for phosphorus removal*. Journal of Environmental Management, 2017, 196, 119-126.
- E. Antunes, M. V. Jacob, G. Brodie, P. Schneider, *kinetics and mechanism analysis of phosphorus recovery from aqueous solution by calcium-rich biochar produced from biosolids via microwave pyrolysis*. Korean Journal of Chemical Engineering (under review).
- E. Antunes, G. Brodie, M. V. Jacob, P. Schneider, *Microwave pyrolysis of sewage biosolids: dielectric properties, microwave susceptor role and its impact on biochar properties*. Journal of Analytical and Applied Pyrolysis (under review).
- E. Antunes, J Schumann, G. Brodie, M. V. Jacob, P. Schneider, *Heavy metal leaching from biochar produced from biosolids via microwave assisted pyrolysis: implications for land application*. Journal of Environmental Chemical Engineering (under review).

Conference Publications

- E. Antunes, J Schumann, P. Schneider, G. Brodie, M. V. Jacob, *Impact of microwave susceptor on biochar properties obtained from biosolids MWAP*. Oral presentation at the 3rd Global Congress on Microwave Energy Applications, Cartagena, Spain, July 2016.
- E. Antunes, J Schumann, P. Schneider, G. Brodie, M. V. Jacob, *Phosphorus recovery by Ca-modified biochar obtained from biosolids via microwave pyrolysis*. Oral presentation at the 2nd IWA Conference on Holistic Sludge Management, Malmo, Sweden, June 2016.
- J Schumann, E. Antunes, P. Schneider, G. Brodie, M. V. Jacob, et al., *Effects of holding time on bio-oil production from microwave assisted pyrolysis of sewage sludge*. Oral presentation at the 2nd IWA Conference on Holistic Sludge Management, Malmo, Sweden, June 2016.

1 INTRODUCTION

1.1 Problem statement

Biosolids are nutrient-rich organic stabilised solid residues from a municipal wastewater treatment plant [1]. Management and disposal of biosolids represents a significant problem due to pathogens and heavy metals content. Currently in Australia, land application and landfill are the main biosolids disposal methods. However, these solutions may impact on the environment and therefore humans in several ways: soil contamination with pathogens and heavy metals, ground water contamination, eutrophication due to phosphorus run-off, and greenhouse gas emissions during natural decomposition stage of biosolids. While land application is one way to recycle crucial nutrients for plant growth, landfill is a poor option, as it requires landfill sites and there is no beneficial reuse of biosolids. In Europe, incineration is one of the most popular approaches to deal with increasing biosolids production. Incineration reduces significantly the amount and volume of sludge, but suitable application for the final ashes and an appropriate control of dioxins must be considered to minimise impacts on the environment. With the exception of land application, the current solutions are not focused on resource recycling and beneficial biosolids reuse.

Microwave assisted pyrolysis (MWAP) is a potential solution for biosolids management and resource recovery. Pyrolysis is the thermal decomposition of biomass in an inert atmosphere at temperatures ranging between 300°C and 800°C. At these temperatures, all pathogens present in biosolids are destroyed, so the final pyrolysis products are safe to use. Another advantage of pyrolysis is the oxygen-free atmosphere, which does not produce dioxins, such as NO_x and SO_x. Thermal decomposition of biomass waste leads to three main products: biochar, biogas and bio-oil. While biogas and bio-oil fractions can be used for energy production, biochar has multiple applications, such as soil ameliorant, fertiliser, contaminant adsorbent, microwave susceptor, and can be also used for activated carbon production [2-4].

Using biochar produced from various types of biomass, such as rice husk, sugar cane bagasse, orange peel and cotton stalk for contaminant removal, has been well reported in the literature [5-8]. The biochar has been used for heavy metals removal (copper, zinc, lead, cadmium, nickel and mercury) [9-12], phosphorus and nitrogen [13, 14], and for organic contaminant removal (methylene blue, benzene derivatives, and phenols) [15-17]. However, the use of biochar produced from biosolids for contaminant removal has not been well explored. The advantages of using biosolids biochar are: biosolids are largely available and are considered waste. This approach utilises the free feedstock of biosolids and has no harmful environmental impacts.

Currently, after contaminant removal by biochar, chemical washing has been used for resource recovery and biochar regeneration [18, 19]. However, this is not an economical neither environmental solution, due to the amount of chemicals required, which depends on the concentration and type of contaminant in biochar and physical properties of biochar. These chemical solutions that are a waste product of this process have to be further processed to minimise the environmental impact. Also, the removal capacity of biochar is decreasing after each regeneration process. Finding new applications for the final material after contaminant removal (contaminant-biochar composite) is a new challenge to maximise the advantages of the overall process. As pyrolysis is a potential method for biosolids management, the biochar is a potential contaminant adsorbent and the contaminants in water, they can be recycled and applied as catalysts, fertilisers and/or anti-bacterials. This is a sustainable environmental approach to deal with waste and pollutants, and enhance global resource sustainability. As the reuse of the final material (contaminant-biochar composite) has not yet been investigated, one of this project's main objectives is to find value-added applications for the final composite.

1.2 Research Objectives

The main objectives of this research contribute to a better understanding of the microwave assisted pyrolysis process of biosolids, the impact of pyrolysis conditions on chemical and physical properties of biochar, and aim to study the potential applications of biochar. Part of this research was to design and commission the microwave system

unit before proceeding with the experimental work to ensure reproducible results and accurate measurements.

The specific objectives of this research thesis follow.

1. Study the dielectric properties of biosolids and the need of a microwave susceptor for microwave pyrolysis of biosolids.
2. Study the impact of pyrolysis conditions (pyrolysis temperature and time, microwave susceptor type and loading level) on the chemical and physical properties of the resultant biochar.
3. Investigate the use of biochar for phosphorus recovery from aqueous solution: removal kinetics and isotherms. Assess the impact of pH and calcium content in biochar on phosphorus recovery.
4. Evaluate the utility of biochar for silver removal from an aqueous solution: adsorption kinetics, isotherms and thermodynamics are investigated. Evaluate the potential of using the final composite (silver-biochar) for methylene blue adsorption and degradation.

1.3 Thesis organisation

This thesis contains eight chapters, each is based on a published journal article or submitted manuscript. As this thesis is a compilation of several journal articles, each containing a clearly described materials and methods section, so this thesis does not contain a stand-alone methodology chapter.

Chapter 1 – Introduction – includes the main motivations for this research and its potential benefits. This chapter also outlines the research objectives.

Chapter 2 – Literature Review – is a literature review on biochar production from biosolids and its applications, comparing biochar production from biosolids via conventional and microwave pyrolysis. A comparison between pyrolysis and other biosolids disposal approaches (incineration, land application and landfill) is made in

terms of an approach for biosolids management, resource recovery and impact on the environment. Biochar applications are also discussed in this section.

This chapter will be submitted as: Antunes, E., Jacob, M. V., Schneider, P., Biochar production from biosolids and its potential applications, Renewable and Sustainable Energy Reviews.

Chapter 3 – The impact of dielectric properties on biosolids microwave assisted pyrolysis – illustrates the impact of dielectric properties on MWAP of biosolids and the important role of a microwave susceptor on MWAP. Different microwave susceptors (activated carbon, charcoal, glycerol and biochar) were used and their effect on heating rate and biochar properties was analysed.

This work was submitted as: Antunes, E., Jacob, M. V., Schneider, P., Microwave pyrolysis of sewage biosolids: dielectric properties, microwave susceptor role and its impact on biochar properties, Journal of Analytical and Applied Pyrolysis.

Chapter 4 – Impact of pyrolysis temperature on biochar properties – describes the impact of pyrolysis temperature on biochar chemical and physical properties produced from biosolids via microwave assisted pyrolysis. The chemical characterisation of biochar comprises X-ray diffraction, elemental analysis, proximate analysis and chemical composition. The physical analysis includes specific surface area while the thermal characterisation includes thermogravimetric analysis. This chapter also contains a small section of the potential of using this biochar for phosphorus recovery from water streams.

This work has been published as: Antunes, E., Schumann, J., Brodie, G., Jacob, M. V., Schneider P. A., Biochar produced from biosolids using a single-mode microwave: characterisation and its potential for phosphorus removal. Journal of Environmental Management 2017, 196: 119-126.

Chapter 5 - Phosphorus recovery from aqueous solution by Ca-doped biochar – discusses the impact of calcium content in biochar on phosphorus removal capacity from aqueous solutions. Phosphorus removal kinetic and isotherm models were fitted to

the experimental data to improve the understanding of phosphorus removal by biochar. This section also includes the effect of calcium content in biochar and the initial pH of the phosphorus stock solution on phosphorus removal. This chapter also analyses the aluminium and heavy metal leaching from biosolids and biochar produced with different calcium contents.

This study has been submitted as: Antunes, E., Brodie, G., Jacob, M. V., Schneider P. A., Kinetics and mechanism analysis of phosphorus recovery from aqueous solution by calcium-rich biochar produced from biosolids via microwave pyrolysis. Korean Journal of Chemical Engineering.

Chapter 6 - Silver removal from aqueous solution by biochar – examines the use of biochar produced from biosolids for silver removal from aqueous solutions. Adsorption kinetic, isotherm and thermodynamic studies were carried out to gain a better insight to silver adsorption by biochar. The final nanocomposite (Ag-biochar) was efficiently used for methylene blue adsorption and photodegradation. The final application of the new nanocomposite formed from silver removal by biochar from aqueous solution shows the potential of the use of this new nanocomposite in value-added applications. As discussed in this chapter, reusing the final nanocomposite has more economical and environmental benefits than recovering the contaminant from biochar via chemical washing.

This study has been published as: Antunes, E., Brodie, G., Jacob, M. V., Schneider P. A., Silver removal from aqueous solution by biochar produced from biosolids via microwave pyrolysis, Journal of Environmental Management 2017, 203:264-272.

Chapter 7 – Heavy metals in biosolids and biochar – examines heavy metal leaching from biosolids and biochar. The impact of pyrolysis time and temperature on heavy metal leaching was studied. A comparison was made between heavy metal leaching from biochar produced from biosolids and lime-dosed biosolids. This study shows that microwave assisted pyrolysis is a promising technology to mitigate the impact of heavy metal in biosolids in the environment as well as for biosolids management. The SWOT analysis demonstrates that pyrolysis is a favourable approach for biosolids management as it reduces the environmental impact.

This study has been submitted as: Antunes, E., Schumann, J., Jacob, M. V., Schneider P. A., Heavy metal leaching from biochar produced from biosolids via microwave assisted pyrolysis: implications for land application, Journal of Environmental Chemical Engineering.

Chapter 8 – Conclusion and recommendations – presents the overall conclusions of this research and recommendations for future research and development.

2 LITERATURE REVIEW

Abstract

Biosolids production has been increasing every year. Management and disposal of biosolids are becoming a problem due to the high treatment costs to meet the requirements of more restrictive environmental legislation. However, with the current solutions for biosolids disposal is not possible to eliminate completely the negative impact of this biomass in the environment. Instead, biosolids can be converted into value-added products and can be a sustainable source of essential nutrients, energy and chemicals. Biosolids could be a renewable and sustainable source of phosphorus, which is a scarce and irreplaceable element. This review presents a summary of biosolids management methods, key risks and advantages. It also provides a review of the potential of nutrients, energy and chemicals recovery from biosolids, the main methodologies for this recovery, with special emphasis on microwave assisted pyrolysis. In the last section, biochar applications are discussed, in particular the use of biochar as an adsorbent for contaminant removal. Microwave pyrolysis is a promising sustainable approach for biosolids management while biochar can be beneficially used for contaminant removal mitigating water pollution and soil contamination and avoiding natural resources depletion.

Keywords: adsorption, biosolids, pyrolysis, resource recovery, waste management.

2.1 Introduction

The recovery and recycling of resources is a highly important issue currently facing the modern world. The global population is increasing constantly and non-renewable resources consumption per capita is also increasing. Peak oil and peak phosphorus are probably the major concerns in the near future; while oil can be replaced by other forms of energy for example, hydrogen, phosphorus has no substitute. Peak phosphorus will occur in the next 20 years, consequently a problem of food security may arise because this element is fundamental for plant growth and cannot be synthesised in a laboratory [20]. However, biosolids could be a sustainable source of energy and nutrients, such as nitrogen and phosphorus. As the biosolids generation rate is increasing rapidly due more restricted environmental regulations, urbanisation and population standards [21]. Recovering nutrients, energy and chemicals from biosolids could be a viable solution to manage the ever-increasing amounts of biosolids and to replace vital nutrients.

Petroleum consumption is rising around the globe and renewable alternatives need to be found in order to reduce petroleum consumption and eventually provide a replacement. The main use of petroleum is for heat and energy generation and a great deal of research has been done on identifying renewable energy sources. An often overlooked use of petroleum is the manufacture of base petrochemicals, which are used to manufacture plastics, chemicals for a wide variety of industries and other products that are essential to the modern world. Biosolids are a potential sustainable and renewable resource of energy, which can be used to produce syngas and bio-oil to generate energy or produce chemicals.

Biosolids are a potential source of nutrients, such as phosphorus, nitrogen and potassium. For example, phosphorus content in biosolids is generally between 1% and 5% (dry basis) [22]. Phosphorus is one of the most important elements for life; essential for humans, animals and plant growth. The majority of phosphorus comes from phosphate rock, which is a non-renewable resource, and its scarcity is increasing sharply due to its constant increase of consumption [23]. Fertiliser production consumes the majority of phosphorus, around 80% of global phosphorus extraction [24]. The quality of these phosphate rocks is decreasing while purification and extraction costs are rising [20]. Therefore, finding a renewable and sustainable methodology for phosphorus

recovery to support life into the future is urgent. It is estimated that the world's population will be around 9 billion people by 2050 and food security issues may arise due to the lack of phosphorus vital for food production [23].

Land application of biosolids is one way to recycle nutrients; nevertheless, biosolids could be harmful because of the concentration of pathogens, heavy metals and organic pollutants and subsequent leaching into soil and groundwater [25]. Therefore, land application of biosolids is contentious. There is no global consensus for biosolids disposal as can be observed in Figure 2.1. For example, in Germany where there is not much land available, incineration is the preferred disposal method; whereas in Australia land application is the most commonly used method to dispose biosolids while incineration is not used at all. Australia also stockpiles around 20% of biosolids production, which could be a problem in the future due to the high amount of accumulated biosolids to treat. Landfilling is the second most used biosolids disposal method in The United States. This solution may have some advantages when biosolids are applied to support tree growth, which minimises the potential of food chain contamination [26].

Figure 2.1 demonstrates that biosolids disposal is a relatively controversial topic; there is lack of a global consensus to deal with biosolids. Figure 2.2 shows the changes in biosolids management in The USA over five years period, between 2008 and 2013. Land application and landfill are decreasing slightly while other disposal uses are increasing, which could mean that some research and others methods have contributed to replacing the more conventional approaches. Finally, Figure 2.1 and Figure 2.2 illustrate the need for research to find a global and sustainable biosolids disposal policy to take advantage of biosolids value and to mitigate the negative environmental effects.

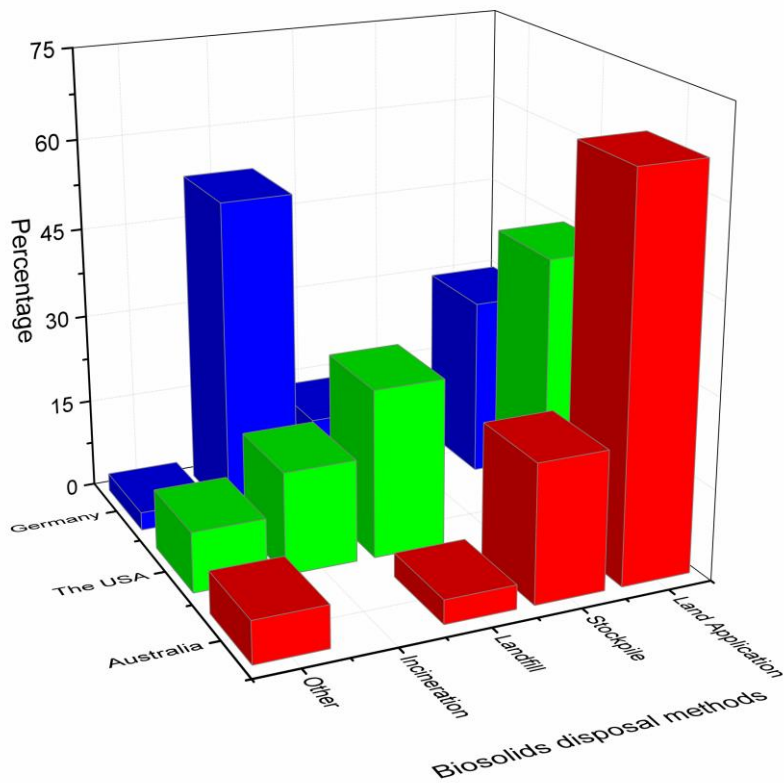


Figure 2.1 – Biosolids disposal methods in Australia (2013), The United States (2013) and Germany (2011) (adapted from [27, 28]).

Microwave assisted pyrolysis (MWAP) is a promising technology for nutrient and energy recovery from biosolids as well as a waste management method. One advantage of using MWAP as an approach for biosolids management is that microwave heating kills the pathogens present in biosolids, therefore the stabilisation step is avoided [29]. However, MWAP also has a few drawbacks, such as temperature measurement, possibly high but relatively unknown scale-up costs and some microwave mechanisms are not yet very well understood [30]. The impacts of these drawbacks may be overcome compared with the significant advantages of the MWAP process, which are detailed in section 2.3.4.

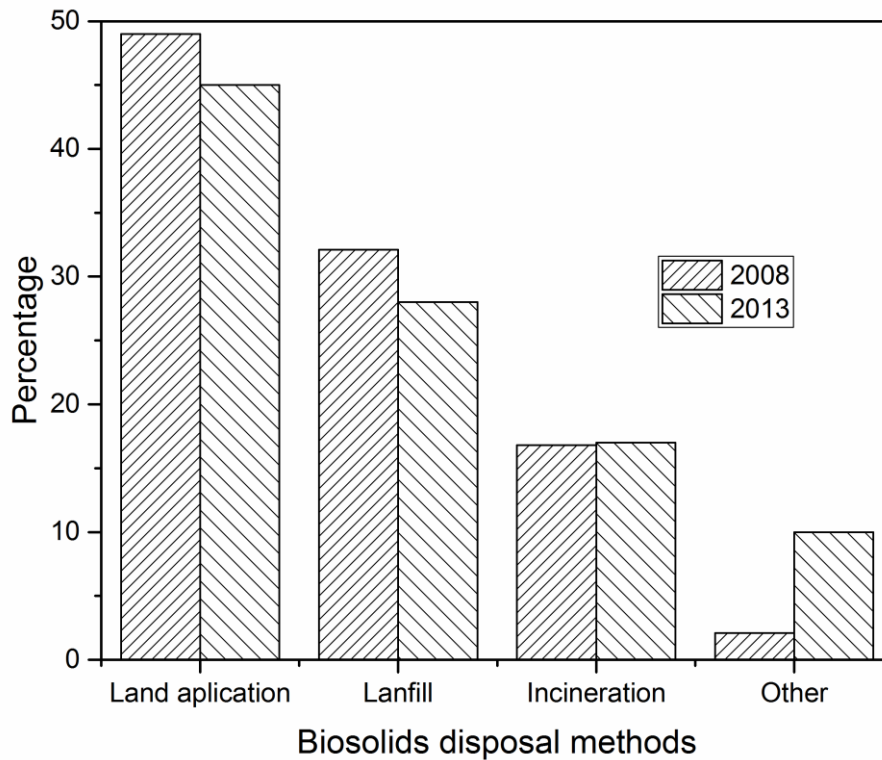


Figure 2.2 – Biosolids disposal methods in The USA in 2008 and 2013 [27, 31].

The present chapter contains five main sections: the value of nutrients, energy and chemicals in biosolids; biosolids management methods; microwave assisted pyrolysis – a general introduction, energy, chemicals and nutrients recovery from biosolids using MWAP; the advantages of using biochar for contaminant removal and the adsorption methods.

2.2 The value of biosolids

Biosolids are full or partially stabilised sewage sludge, which have a moisture content usually around 30% to 50% [32]. Biosolids should not be considered waste; they contain essential nutrients for life, traces of metals, organic and inorganic matter [28]. The composition of sewage sludge depends on the source as can be observed in Table 2.1, where the organic matter varies between 19.8 to 43.4%. Biosolids composition depends on population’s food habits, the type and percentage of industrial wastewater streams directed to domestic wastewater treatment plants, and previous wastewater treatment steps. Phosphorus, nitrogen and potassium are the most important nutrients in biosolids; nevertheless, the main focus of nutrient recovery from biosolids has been

concentrated on the first two due to high concentrations of these elements. Copper and zinc are also important micronutrients in biosolids for plant growth. Organic matter in biosolids could be used as a low-grade fertiliser and soil ameliorant to improve soil structure and water retention in case of land application. The organic matter can be also used for energy production by combustion or anaerobic digestion [28, 33]. Energy recovery from biosolids has been extensively studied; however, there is no consensus about benefits and profits, some researchers found that the energy balance of biosolids incineration is negative while others stated that biosolids incineration could be a profitable management approach [26, 34]. The inorganic matter in biosolids can be used to replace clay in brick production. In terms of chemicals, aromatics and alkenes are the most relevant hydrocarbons that could be recovered from biosolids.

Table 2.1 - Composition of sewage sludge in different countries (adapted from [35]).

Country	Organic matter (%)	Total N (%)	Total P (%)	K (%)	Zn (mg/kg)	Cu (mg/kg)	Mn (mg/kg)
India	23.2	2.6	1.34	0.42	1900	700	400
Spain	43.4	2.5	1.06	0.2	445	174	-
Thailand	19.82	3.43	-	-	1326	801	2621

All values based on dry weight.

2.2.1 Nutrients value in biosolids

Biosolids contain high amounts of phosphorus as well as nitrogen, a small concentration of potassium (0.1 – 0.6 wt%), and trace amounts of others macro and micronutrients, such as, zinc, calcium, magnesium and iron [36]. Phosphorus content in biosolids is generally between 1% to 5% dry weight basis [22]. However, the amount of phosphorus in biosolids depends on the previous wastewater treatment steps; for example, plants with a struvite crystallisation reactor produce biosolids with a lower percentage of phosphorus. Struvite crystallisation is the most used method for phosphorus recovery

from supernatant because of its high efficiency, with more than 90% of dissolved phosphorus possibly recovered, and the ability to produce up to 100 mg/l of struvite [24]. The major problem with this method is the lack of knowledge of the impact of kinetic thermodynamics and fluid dynamics on efficiency. Maximising struvite crystallisation yield requires a better understanding of complex mechanisms, such as, nucleation, crystal growth and agglomeration. Also, some process parameters such as operating temperature, load of suspended solids and concentration of phosphates in supernatant have a great impact on struvite crystallisation efficiency [37, 38]. The struvite crystallisation method can additionally recover some of the micronutrients present in supernatant, particularly magnesium and calcium.

Biosolids could be a sustainable source to replace phosphorus in the future. Recovering phosphorus from biosolids will be especially important for phosphate importer countries, which are dependent upon five countries (The USA, China, Morocco, Jordan and South Africa) that have 85% of worldwide phosphate reserves [39]. The analysis of phosphate rock imports and exports world region demonstrates that only Africa and West Asia have a positive balance export/import (Figure A2 – Appendix). The other countries depend mainly on these two regions to satisfy their phosphate demanding, so it is fundamental to recycle and recovery phosphorus. For example, it was estimated that in Germany, sewage sludge can replace 40% of total imported phosphorus [39].

Assuming a concentration of 2.5% (dry basis) of phosphorus in sewage sludge, the value of this resource could reach up to \$102/dry tonne [28]. However, this value will likely increase in the future due to the rise of consumption and phosphate rock scarcity. More importantly than the phosphorus value in biosolids, it is necessary to find a renewable source to replace this element in the future.

Nitrogen is one of the three fundamental elements for life and has the biggest demand in soil due to the highest consumption rate by plants [40]. Biosolids contain in general 4% of nitrogen (dry weight basis), which means a value of \$49 per tonne of dry biosolids [28]. However, the total nitrogen concentration in biosolids is variable, varying between 0.1% and 18% because the majority of nitrogen is organic and its concentration decreases over time after the final waste treatment [36]. However, there is less pressure for nitrogen recovery from biosolids than phosphorus recovery because nitrogen can be

produced from several sources, while the known phosphorus reserves will be depleted in 50 – 100 years [23, 41].

2.2.2 Energy value in biosolids

The energy produced from sewage sludge may cover the total energy needs of a wastewater treatment plant [42]. Organic matter content in sewage sludge is high, and can be used for energy production. Energy can be generated by several methods, such as, anaerobic digestion, combustion, gasification and pyrolysis. Anaerobic digestion produces methane from organic matter; therefore, this compound can be burnt to generate heat or power [28]. Combustion is the most well-established method for heat and power generation from renewable energy sources, where the heat produced from biomass is used to generate energy through a steam turbine [43]. Gasification and pyrolysis are less common; however, these methods are gaining attention in recent years [42]. The syngas produced by gasification and pyrolysis is mainly composed by CO, H₂, CO₂ and CH₄; although the composition and yield of these gases depend significantly on pyrolysis temperature and method [44]. The heating value of syngas fraction varies between 20 to 25 MJ/m³ [45].

Hydrogen production from sewage sludge can reach up to 11% in the syngas composition, which can replace fossil fuel energy and be used in fuel cells [42]. The organic liquid fraction could also have a reasonable heating value (22 to 28 MJ/kg), which is similar to some conventional fuels [45]. Using sewage sludge to generate energy has several economic and environmental advantages: lower formation of CO₂ and less disposal costs of ashes due to biosolids significant volume reduction [42]. For example, incineration reduces up to 90% of the initial volume of biosolids [39]. The final ashes can be used to produce clay bricks with a potential value of \$10 per tonne [28].

2.2.3 Chemical value in biosolids

The bio-oil produced from sewage sludge contains several types of hydrocarbons, such as, alkanes, alkenes, aromatics, phenols, carboxylic acids and N-compounds [46]. However, aromatics, alkanes and alkenes are the most important organic volatile

products due to their potential to replace petrochemicals for which global demand is increasing every year. Alkanes could reach up to 17 wt% (dry basis) in oil composition [47]. The economic value of the bio-oil fraction was estimated around 70% of crude oil price [48]. This bio-oil can be further processed to produce bio-combustibles or other chemical compounds [49].

2.3 Overview of current biosolids management methods

Biosolids production is increasing every year due to the ever-increasing urbanisation of the human population and more stringent environmental regulations [21]. This persistent rise of biosolids quantity has created the need to improve and develop new biosolids disposal policies to mitigate the negative environmental impacts and to deal with the increasing amounts. Reducing biosolids disposal costs is also important, it is estimated that sludge disposal costs could be up to 50% of the total expense of wastewater treatment [25]. While biosolids could potentially be used as a basic fill material in construction applications, such as roadway embankments and building pads [32]. The potential value of nutrients, energy and chemicals has gained attention and encouraged the development of new approaches for resource recovery. The resource value will clearly impact on the disposal method choice, with the most common biosolids disposal methods being: land application, incineration and landfilling, while pyrolysis is an emergent approach.

2.3.1 Incineration

Incineration could be a suitable solution for biosolids management, which can reduce up to 90% of volume and 70% of mass [39]. Biosolids incineration consists of the burning of solids at high temperatures in a combustion chamber in the presence of excess oxygen producing carbon dioxide, water and ash. The inert ash could be used as a raw material in construction materials or can be disposed of in landfill [50]. However, a special landfill site could be required due to the possible high concentration of some heavy metals. The heat of the combustion can be used to generate power to offset the cost of incineration. The energy content of biosolids or sewage sludge is around 16-21 MJ/kg of dry biosolids, which is comparable to that of brown coal at 10-20 MJ/kg. For example, in the European Union dried sewage sludge has been used as fuel for coal

fired power stations [51]. The energy efficiency depends significantly on biosolids moisture content, which often requires a dewatering step before combustion. Despite this, replacing coal by biosolids has a huge positive impact in the environment due to the reduction of CO₂ emissions. A tonne of biosolids with 10% of moisture can generate 700 kWh, which means that replacing coal by biosolids can avoid around of 0.7 tonnes of CO₂ emissions to the atmosphere [28].

The incineration of biosolids is compulsory in some countries, particularly in Europe, where landfilling is less common due to population concerns and less land is available [26]. Incineration of biosolids has a significant environmental advantage in comparison with land application in terms of greenhouse gas emissions such as methane (CH₄) and carbon dioxide (CO₂). A life cycle assessment conducted in 2005 showed that biosolids land application produces about 480 kg of CO₂ per dry tonne of biosolids while incineration in a fluidised bed emits 180 kg of CO₂ per dry tonne of biosolids [52].

A combined incineration plant with power generation has been positively established in The United States; although, the yield would be improved with the decrease of biosolids moisture through drying processes [50]. Currently, incineration of biosolids is a very interesting option for biosolids management due to the opportunity of energy recovery, waste volume reduction and thermal destruction of pathogens and toxic organic compounds [53]. However, some researchers considered incineration a way to reduce waste rather than energy production [26]. The final ashes, which contain phosphorus between 5% to 10% could be further processed by wet chemical for phosphorus recovery [54]. One of the biggest disadvantages of incineration is the investment in technology to prevent gases and solid pollutants releasing to the atmosphere.

2.3.2 Land application

Land application is the most common biosolids disposal method [1]. For example, in Australia, more than 60% of biosolids are applied to the land as fertiliser or soil conditioner [28]. Using biosolids in agriculture makes sense from both an environmental and economic perspectives; biosolids contain crucial elements such as phosphorous, nitrogen and potassium for plant growth. Besides nutrient value, the biosolids can be used as soil ameliorant, the organic matter content improves soil

properties, reduce soil erosion and increases moisture retention in soil [1]. Some studies have demonstrated that land application of biosolids improves productivity and saves costs because of the less use of expensive fertilisers [55]. The total gain of biosolids land application could be up to \$34 per dry tonne of biosolids [56], assuming main costs (stabilisation, transport and application) of \$690/dry ton, carbon offset of \$168/dry ton, energy production by anaerobic digestion (\$255/dry tonne) and the CO₂ avoided during inorganic fertiliser production (\$150/dry tonne) [28].

Land application of biosolids is controversial due to high concentration of heavy metals in its composition, such as mercury, cadmium, lead and chromium. Land application of biosolids increases Pb, Ni, Cd, Cr, Cu and Zn concentrations in soil due to its availability in biosolids [57]. The heavy metals accumulation in soil has two main problems: plant contamination because of metals uptake and soil microbial activity reduction [58]. Ultimately, these metals affect human health through the food chain. Another potential risk for humans is the pathogen content in biosolids during its application to land, although this risk can be reduced if the biosolids are composted before being applied [59]. An additional social concern is the releasing of odour related to this final use of biosolids. Also, the organic toxic compounds, pharmaceutical and personal care products content can prevent land application of biosolids [42].

A major challenge in applying biosolids as a fertiliser is determining the rate at which the biosolids should be applied to provide the correct amount of nutrients for plants growth. Usually, biosolids land application is made according to nitrogen needs for plant growth, which means that phosphorus will be applied in higher amounts because of the low ratio of nitrogen/phosphorus [33]. Soil over-fertilisation and leaching of phosphorus to ground waterways may occur, with severe consequences for the environment, such as eutrophication. Yet despite some drawbacks, from an environmental viewpoint, some researchers believe that land application is the most desirable disposal method for biosolids [60].

2.3.3 Landfilling

Landfilling consists of dumping biosolids to a specific area. Landfill disposal is not a very common end use for biosolids because of the amount of land required. Landfill has

also become less popular due to the release of greenhouse gas emissions, which contributes to global warming. Gases such as methane and carbon dioxide are produced and released during the biosolids natural decomposition stage. Landfill gas is a varying mix of gases, usually consisting of between 35-55% CH₄, 30-44% CO₂, 5-25% N₂O and a small amount of other gases (based on estimates from a leading supplier of landfill gas recovery equipment) [61]. These landfill gases can be collected and use for energy production. Besides global warming, another problem of landfill is the soil and groundwater contamination through the leaching of heavy metals [60]. Moreover, the costs associated with landfill disposal are considerably high due to the storage, process for removing moisture and transport. The benefits and simplicity of landfill need to be weighed against the environmental impacts of this method before it is implemented.

2.3.4 Pyrolysis

Pyrolysis is a recent and innovative technology in the biosolids management field. Pyrolysis is the thermal decomposition of carbonaceous material in the absence of oxygen atmosphere, which produces three different products: biochar, bio-oil and biogas [1]. Pyrolysis significantly reduces the total waste volume and can be used for energy and nutrient recovery (nitrogen and phosphorous) from biosolids [25]. The pyrolysis bio-oil could replace fossil fuels in the future with environmental advantages, such as lower SO_x and NO_x emissions than conventional fossil fuels [62]. The biochar resulting from pyrolysis is rich in bioavailable phosphorus and can be applied directly to land as a fertiliser [63]. Pyrolysis could be an alternative to landfilling and land application, not just because of the waste volume reduction, but this process destroys pathogens and toxic organic compounds present in biosolids [36]. The heavy metals present in biochar are less susceptible to leaching compared with incineration ash, which makes biochar a more environmentally friendly solution for land application. Also, no dioxins are produced during pyrolysis due to the absence of oxygen during the heating process [45]. However, a better understanding of this technology has to be developed to increase the level of implementation relative to other biosolids management approaches.

Conventional pyrolysis has been previously studied and recently, microwave assisted pyrolysis (MWAP) has gained attention due to several advantages (listed briefly in

Table 2.2). MWAP has been applied to nutrients and energy recovery from biosolids, particularly because of the time and energy efficiency, yields and properties of the final products. By-products distribution and chemical composition depend on biosolids characteristics and MWAP operating conditions. Temperature, heating rate and residence time have major impacts on product yields and properties, and according to these variables, pyrolysis has been classified in three subclasses: slow, fast and flash (Table 2.3) [64]. In general, high heating rates and temperatures boost gas formation while char yield decreases. The liquid phase production is maximised around 500°C and decreases at a higher temperature due to secondary cracking reactions [65, 66]. The final product distribution can be modified by using catalysts, but variables such as reactor design, sample size and pressure may also affect by-product yields [65].

MWAP has been studied as a process for deriving fuel from biosolids, similar to conventional biomass pyrolysis. In production of synthesis gas (syngas), which consists predominately of hydrogen (H₂) gas with some carbon monoxide (CO), MWAP has demonstrated advantages over conventional pyrolysis (Table 2.2). For instance, Domínguez et al. (2008) found that MWAP had a higher yield of syngas than conventional pyrolysis as well as producing 50-70% less CH₄ and CO₂. This causes the MWAP gas to have a lower gross calorific value than gas produced by conventional pyrolysis (on a molar basis), but produces less greenhouse gases. For liquid bio-fuel production, bio-oil produced via MWAP from sewage sludge has a gross calorific value of 35.7 MJ/kg compared to conventional pyrolysis bio-oil, which has a value of roughly 37 MJ/kg [48]. MWAP bio-oil however, has been reported as having a negligible amount of polycyclic aromatic hydrocarbons (PAHs), whereas conventional pyrolysis bio-oil does contain PAHs, which are mutagenic and carcinogenic hydrocarbons [47]. The solid fraction (biochar) of biosolids MWAP is a carbon-rich material and contains essential nutrients, such as, phosphorus and nitrogen, and may be used as supplement in commercial fertilisers in the future. Besides supplying vital nutrients to soil, biochar can be applied as a soil ameliorant, which improves soil water and carbon retention capacity, and can increase crop yields [67]. Microwave assisted pyrolysis is a potential method for phosphorus recovery from biosolids; however, more research should be conducted in this field.

Table 2.2 – Microwave versus conventional pyrolysis (adapted from [65]).

Process	Advantages	Disadvantages
Microwave Assisted Pyrolysis	<ul style="list-style-type: none"> - Less feedstock pre-treatment is required - Lower theoretical energy consumption than conventional pyrolysis (temperatures 150-300°C). - Volumetric and selective heating. - High heating rates. - No contact between the heating source and biomass. - Good control of reaction parameters (heating stops or starts immediately when the magnetron is turned off or on). - Flexible and transportable technology. 	<ul style="list-style-type: none"> - Temperature measurement. - Scale-up issues (costs, inhomogeneous temperature and inconsistent products). - Limited penetration depth of microwaves, which affects reactor design. - Not well developed.
Conventional Pyrolysis	<ul style="list-style-type: none"> - A wide range of feedstock can be used. - Well established technology. - Easy scale-up. 	<ul style="list-style-type: none"> - High energy and time consuming. - Heating rate is controlled by thermal conductivity of feedstock, which not allowing high heating rates. - Secondary reactions can occur in the hot atmosphere, reducing yield of some desirable products.

Table 2.3 - Classification and main products of pyrolysis (adapted from [64]).

Pyrolysis process	Residence time (s)	Heating rate (K/s)	Temperature (K)	Main Product
Slow	450 – 550	0.1 - 1	550 - 950	Biochar
Fast	0.5 – 10	10 - 200	850 - 1250	Bio-fuel
Flash	<0.5	>1000	1050 - 1300	Bio-fuel

2.4 Microwave Assisted Pyrolysis

Microwaves operate between 0.3 to 300 gigahertz (GHz) with wavelengths between 1 to 0.001 metres, respectively [68]. Domestic and industrial microwaves operate regularly at a frequency 2.45 GHz while some industrial applications use microwaves at a frequency of 900 MHz [69]. Microwave heating is the result of the conversion of electromagnetic energy to thermal energy through two different effects: in polar molecules, such as water, the heating of the sample occurs due to the friction originated by the rotation of the molecules. In solid materials, when electrons cannot align with the changes of the electric field, the energy is subsequently converted into heat [70].

Microwave heating depends on the capacity of a material to absorb electromagnetic energy and to transform it into heat. This ability of the material is defined by the dielectric loss tangent ($\tan\delta$), which is the division between dielectric loss factor and dielectric constant (2.1).

$$\tan \delta = \frac{e''}{e'} \quad (2.1)$$

On the other hand, conventional heating depends especially on the thermal conductivity of the material, consisting of the heat diffusion from the surface to the centre of the material by convection, conduction and radiation mechanisms (Figure 2.3). Microwave heating has several advantages in comparison with conventional heating: non-contact with sample, energy transfers instead of heat transference, and rapid, volumetric and selective heating; because of these reasons, microwave heating is safer and has a higher level of automation [70].

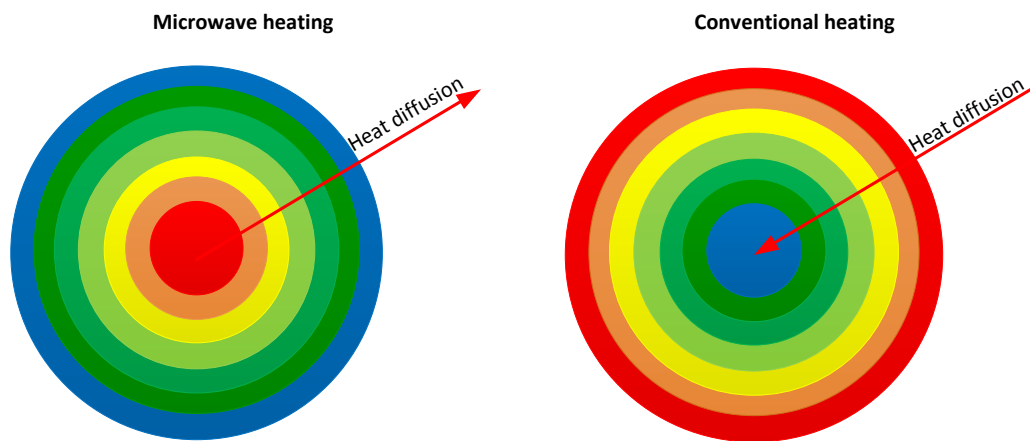


Figure 2.3 – Microwave and conventional heating processes.

Microwave applications have increased significantly in several areas such as food heating and cooking, curing, medical devices sterilisation, chemical synthesis, and drying and biological destruction [71]. Microwaves have also gained attention, especially in the industrial field, because they are energy efficient and are less time consuming. For instance, the microwave heating rate is significantly higher than in conventional heating and also needs fewer steps, such as drying and grinding. In conventional pyrolysis, particles bigger than 2 mm are not suitable for a fast pyrolysis process due to the low thermal conductivity of biomass [49]. Previous studies have shown that MWAP has time savings of around 50% and energy consumption is 20% lower than conventional pyrolysis [72]. In addition, volumetric heating dispersion and selective heating are also advantages of microwave technology [50]. Volumetric heating dispersion consists of the transference of heating from the core of the material to surrounding cooler surfaces [73]. Microwave heating is selective; different molecules (chemical composition and crystal structure) have diverse microwave absorption capacity [74]. Taking advantage of the selective heating, it is possible to induce or

inhibit chemical reactions through monitoring the applied electromagnetic field [75]. Furthermore, rapid heating avoids secondary and undesired reactions, consequently, MWAP produces materials with high purity, higher yields and reproducibility [73].

Microwave assisted pyrolysis (MWAP) is a promising technology for energy and nutrient recovery from waste and biomass, such as biosolids. Biomass MWAP is a clean alternative to replace fossil fuels as well as to produce biochar that has a negligible CO₂ impact in the environment [76]. Microwave assisted pyrolysis has been extensively studied, predominantly for energy recovery from biomass. According to Lehmann's study, one tonne of biomass (dry basis) could produce 1/3 of a tonne of biofuel [77]. Additionally, in the literature, it is possible to find several examples of successful research projects on microwave pyrolysis of biomass, such as oil palm biomass [73, 78], sewage sludge [76], rice straw [79, 80], wheat straw [81], tyres [82] and other kinds of organic waste [83, 84]. Biomass MWAP can produce three different valuable products: biochar (solid phase), liquid fuels and a complex combination of gases, such as H₂, CH₄, CO and others. The final distribution of the end products depends on the biosolids composition and pyrolysis conditions. For example, biochar yield increases with holding time, but decreases with an increase of reaction temperature. Moreover, high liquid and gas yields are associated with higher heating rates [72].

2.4.1 Microwave Pyrolysis of Biosolids

Dry biosolids have a very low tangent loss factor and are almost transparent to microwave irradiation [76]. Consequently, the addition of a microwave absorber (susceptor) is fundamental to reach the high temperatures required for pyrolysis reactions. These microwave absorbers, such as metal oxides, carbon based materials, silicon carbide and sulphur, can play a crucial role in the effective heating of the biomass [78]. Carbon based materials are often selected as microwave absorbers because of the high value of dielectric loss tangent, they are available at relatively low cost and they do not contaminate the final pyrolysis products with an extra inorganic compound [70]. Microwave susceptors work as hot spots, absorbing microwave energy and transferring it as heat from the centre to cooler surroundings by thermal diffusion (Figure 2.4). As the heat transfer from the susceptor to the biosolids via conventional heating mechanisms, a good contact between susceptor and the biosolids is important. If

the susceptor is not well distributed throughout the waste then the temperature will not be uniform across the sample, leading to a less efficient pyrolysis. Biosolids can reach a temperature of 200°C and only drying can occur; however, an addition of just 5% char increases the maximum temperature to 900°C [85]. Further, Salema and Ani (2011) found that yields of pyrolysis by-products (gas, oil and char) depend on the percentage of microwave absorber used in the process. Microwave absorbers must be selected with care because these materials can contaminant the final products or cause greater/lesser secondary heating effects. To solve this problem the susceptor loading required to initiate the pyrolysis can be identified, at this minimal susceptor loading the temperature increases to the point that char begins to form. This char will maintain the heating of biomass, more char will be formed, and the progress of a reaction will be achieved without any external material [73].

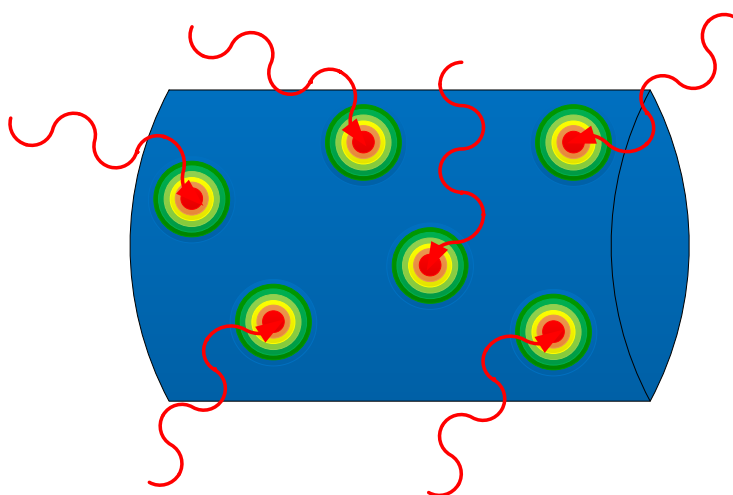


Figure 2.4 – Microwave heating process illustration, transferring energy from microwave susceptors to the cooler surroundings.

2.4.2 Catalyst for MWAP

Catalysts have been studied in MWAP especially to enhance the properties and yields of gas and liquid fractions. In general, catalysts increase gas formation and improve the quality or the organic composition in oils [64]. Some catalysts such as silica, alumina,

zinc oxide, hematite, titania and calcium oxide [25, 78] may affect the biochar formation. Potassium has a positive effect in microwave absorption; it acts as a catalyst by enhancing the transformation of carbon into biochar. Iron oxide is heated very easily and accelerates the heating of the remaining sample, but silica, alumina and calcium oxide are hard oxides to heat and generally, inhibit the biochar formation [25, 78]. Shao et al. (2010) have concluded that alumina and titania can reduce the pyrolysis time, but calcium, zinc and iron oxides could increase the pyrolysis stage. Carbon based materials, which are also very good microwave absorbers, can also act as a catalyst in some gas-phase catalytic reactions [70]. However, the impact of these materials on pyrolysis products is not yet well explored [64].

2.4.3 Temperature measurement inside microwave cavities

Temperature and heating rates are the most important variables to control in MWAP; they affect strongly yields and properties of the final products. However, measuring a sample's temperature in situ could be a challenge in a microwave chamber. Finding a suitable device to measure and control temperature without interferences with the electromagnetic field and minimising errors has been very difficult. A thermocouple probe is probably the most appropriate device because it is in contact with the sample and the response time is fast [72]. This thermocouple must be ungrounded to ensure electrical isolation therefore, it will not absorb microwave irradiation, which makes the thermocouple suitable to work accurately under microwave irradiation [64]. Grounded thermocouples are affected by the electromagnetic field and act as an antenna, causing the temperature around the thermocouple to be higher than that in the rest of sample. Another solution for contact temperature measurement is using an optical fibre thermometer, which is not affected by electromagnetic radiation. The major drawback of this last method is the high price of the optical fibre, and it is more suitable for low temperatures [86]. An infrared optical pyrometer is a non-contact temperature measurement method, which is not affected by microwaves; however, this method can just measure the surface temperature and requires a transparent window to infrared radiation, but opaque to microwaves [65, 76]. All devices have advantages and shortcomings; the most important aspect is to find which one is more appropriate for each study case.

2.4.4 MWAP for nutrient recovery

Nutrient recovery using MWAP is not well explored yet. However, research was developed to release phosphorus from sewage sludge using microwave technology. A few studies in nutrient recovery were carried out using conventional pyrolysis, which is an excellent basis to compare with future results obtained by using microwave technology. MWAP and conventional pyrolysis are utilised to produce biochar, which is gaining attention due to its potential as a soil ameliorant by enhancing soil structure, water retention and fertility [87]. Besides the potential value of nutrients in biochar, converting biosolids in biochar by pyrolysis is also an environmentally appropriate approach to mitigate greenhouse gas emissions due to the higher carbon stability in biochar [40]. Moreover, MWAP destroys pathogens in biosolids, contributing to a safer biochar land application without risks for the population and avoiding land contamination [29]. MWAP relative to conventional pyrolysis also decreases heavy metals availability in biochar, which avoids soil and food contamination [42]. Producing biochar from waste is an encouraging process for the environment, reducing methane emissions usually released during the natural decomposition of waste. Nevertheless, direct application of biochar in agriculture lacks nutrient control, and over fertilisation could occur. Therefore, recovering nutrients from biochar could have several advantages, such as the blending of nutrients in correct concentrations and producing tailor-made fertilisers for each application.

Phosphorus recovery from sewage sludge using pyrolysis is not well explored compared with chemical methods. Recovering phosphorus by wet chemical methods involves a substantial consumption of chemicals and a second step is required to separate the phosphorus from heavy metals [88]. However, the total phosphorus in biosolids was fully recovered in biochar produced and its recovery increased with pyrolysis temperature. Phosphorus concentration in biochar varied between 30 to 51 g/kg [40]. Recovering this element is important, but it is also fundamental to increase its bioavailability to be taken up by plants, consequently decreasing soil and groundwater contamination. Pyrolysis temperature and feedstock composition play a key role on phosphorus bioavailability in biochar. Lu et al. (2013) reported that bioavailable phosphorus was maximised at 300°C [87], but Tao et al. (2012) found that phosphorus bioavailability in biochar depends strongly on biosolids composition for temperatures

below 450°C, particularly on the concentration of coordinated cations. Results showed that Ca/Mg-P precipitates revealed higher bioavailability than Al/Ca-P precipitates [40], but nutrient bioavailability in biochar is not well discussed in the literature [89].

Phosphorus could be released from sewage sludge through microwave digestion. Researchers from The University of British Columbia have developed a new process for phosphorus releasing and sewage sludge disintegration: microwave enhanced advanced oxidation process [90-92]. This process consists of the combination of microwave heating with simultaneous addition of hydrogen peroxide, causing carbon and other nutrients solubilisation [93]. For example, microwave heating can release up to 76% of total phosphate in the solution by heating the sludge over just five minutes at 100°C [94]. A combination of hydrogen peroxide with high temperature (170°C) increased the phosphorus released amount by 10.5%; more than 84% of the total phosphorus was released in the solution [91]. Heating time was studied, but its impact was negligible for nutrient solubilisation. The addition of sulphuric acid increased the solubilisation of phosphate from sewage sludge, with more than 95.5% of total phosphorus in the solution, with 2 ml of hydrogen peroxide and 0.5 ml of sulphuric acid at 200°C [95]. These conditions also maximised the solubility of ammonia, with 78.4% of the total nitrogen in the solution [95]. However, the addition of sulphuric acid had the smallest effect on ammonia and phosphate solubilisation. Microwave heating had the biggest impact on phosphate solubilisation, and hydrogen peroxide addition was the most significant variable on ammonia solubilisation [95]. This microwave enhanced advanced oxidation process was also applied for releasing phosphorus from dairy manure with an efficiency around 92% of total phosphorus [96].

Nitrogen recovery from biosolids using MWAP can be an interesting alternative to conventional pyrolysis and land application. However, according to our best knowledge, nitrogen recovery using MWAP is not yet developed; just a few studies have been carried out using conventional pyrolysis to recover nitrogen [40]. Nitrogen content in biochar decreases with rise of pyrolysis temperature due to the loss of volatile organic matter [89]. Pyrolysis temperature impacts on chemical structure of nitrogen in biochar, biochar produced at higher temperatures contains less available nitrogen [40, 89]. In contrast, Galinato et al. (2011) stated that nitrogen in biochar is not available for plants; availability of nitrogen in biochar is still unclear, which requires further studies.

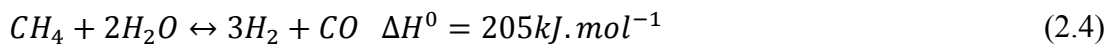
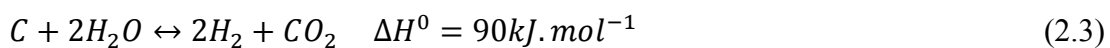
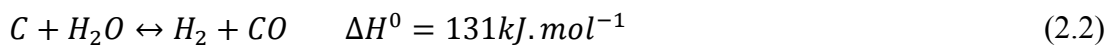
Small amounts of a few heavy metals (Zn, Cu, Ni, Fe, Mn and Mo) are important micronutrients for plant growth. However, land application of large amounts of heavy metals impacts on the environment and could pose a significant risk to human health [97]. Sewage sludge pyrolysis could be an encouraging approach to solve the heavy metals issues. Heavy metals are concentrated in the final char residue and they are less susceptible to leach due to the high pyrolysis temperature, which also improves the pH buffering capacity of the char, contributing to a better stabilisation of the heavy metals. Another potential factor to reduce the metal leaching is the high specific surface area of char, which enhances metals retention [98]. Jamali et al. (2009) studied the efficiency of using microwave pyrolysis to recover heavy metals: Cd, Cr, Cu, Ni, Pb and Zn, finding that maximum recovery for Cd, Cr, Ni and Zn was obtained with 60 s of microwave heating while Cu and Pb needed 90 s at 900 W. Recovering these elements is important from an economic and environmental point of view, but more research is required for a better understanding of the potential of microwave pyrolysis benefits and profits on heavy metals recovery from sewage sludge.

Biochar is a carbon-based material produced from biomass by pyrolysis [87]. The composition of biochar is influenced by biomass composition and pyrolysis operating conditions. This material can be used for energy production by combustion; however, it is becoming more attractive due to the potential of new applications such as, soil ameliorant, fertiliser, nutrient retention and carbon sequestration [49, 65, 99]. Biochar land application improves soils fertility, agronomic productivity, water and nutrient holding capacity, air permeability while mitigates greenhouse gas emissions from soil [87, 99]. Recent research work has demonstrated that biochar can increase soil pH, which may replace agricultural lime applications in the future [100]. Further, biochar can be used as contaminant remediation due to the strong sorption capacity of heavy metals, pesticides and other organic pollutants [99]. All of these advantages make biochar a brilliant product; however, some researchers have found a negative impact on crop production when biochar is applied to soil [100]. Therefore, more research is needed to better understand the conditions and processes responsible for the aforementioned benefits.

2.4.5 MWAP for energy recovery

Microwave pyrolysis of biosolids is used to produce both gaseous and liquid fuels [44]. A gaseous fuel that has been successfully produced using MWAP of biosolids and other biomass such as coffee hulls was synthesis gas (syngas) [101, 102]. Syngas is a mixture of hydrogen (H₂) and carbon monoxide (CO) gas with small amounts of other gases such as methane (CH₄) and carbon dioxide (CO₂); it is commonly used as a clean burning fuel or for chemical synthesis in various industries [44]. MWAP of sewage waste has been found to produce a gas yield of up to 60% (dry basis) comprised of 29%-52% H₂ and 18-27% CO depending on sewage waste composition, with the balance being mostly carbon dioxide [101, 103]. The calorific value of this gas was between 7400-9500 MJ/m³, which is comparable to gas produced from coal gasification [47]. Syngas is produced from biosolids by heating the feedstock and the susceptor (usually carbon based) to 800°C or more. At these temperatures the carbon in the char and the sample undergoes cracking into syngas.

The reactions that have been found to be significant are [104]:



The rapid heating of the entire sample in MWAP allows the moisture to come into contact with the produced volatiles, increasing the rate of these reactions [105]. The likely reason for syngas produced via MWAP having a lower hydrocarbon content but a higher H₂ content than conventional pyrolysis (CP) produced syngas reported in other studies are the reactions (2.3) and (2.4). The rapid heating of MWAP allows the solid portion of the sewage waste to reach a high temperature while the water is still being removed. This contact between the water vapour and hot organic waste increases the reaction rate of reactions (2.1) and (2.2). The increased rate of reactions (2.1) and (2.2) causes the higher moisture content sewage waste to produce more hydrogen gas at the start of the process while the water is still being removed. Once the moisture has been removed, reaction (2.5) is favoured under MWAP conditions where the feedstock is at a uniform and high temperature [76].

When compared to syngas produced from biosolids using gasification [106] and conventional pyrolysis [47], MWAP produced syngas richer in H₂. Gasification and conventional pyrolysis are producing H₂ yields of approximately 28%. The syngas produced via MWAP also contains a lower concentration of hydrocarbons such as methane, and lower amounts of hazardous polycyclic aromatic hydrocarbons (PAHs) [47].

The oil portion of MWAP products is also a potential source of energy. Studies on MWAP for fuel oil production have found that sewage waste derived oil has a gross calorific value of between 28 to 37 MJ/kg, which is comparable to the 43 MJ/kg of No.2 Diesel [47, 66]. In addition to favourable energy content, the composition of MWAP derived bio-oils is superior in some aspects to bio-oil derived from other thermal treatments such as conventional pyrolysis. MWAP oil is more aliphatic, more oxygenated, contains a lower amount of PAHs and is less viscous when compared to pyrolysis oil produced under similar conditions from conventional pyrolysis [47, 66]. Bio-oil is produced from MWAP of biosolids at temperatures generally below 600°C as the maximum oil yield is reported as being between 450-550°C [53]. Above the peak oil yield the oil produced undergoes cracking into gases, down to a minimum oil yield at 800°C [66]. The susceptor used in the MWAP process plays an important role in determining the composition of the produced oil, some susceptors that have been observed to have a positive impact on bio-oil composition are: graphite, activated

carbon and char. Graphite favours the cracking of heavy aliphatic hydrocarbons into lighter aliphatic hydrocarbons [107]. Activated carbon increases the yield of aliphatic hydrocarbons and decreases the SO_x and NO_x content of the oil hydrocarbons [70, 101]. Char has similar effects as activated carbon, but the heating rate is lower (at same microwave power) than activated carbon due to its lower tangent loss factor. This can be compensated by char being a by-product of the MWAP process, and could be recycled back into the reactor, eliminating the need to use a susceptor [70].

2.4.6 MWAP for chemicals recovery

Bio-oils produced from biosolids MWAP are not only a potential source of energy, they have also been investigated as a potential source of petrochemicals [108]. Petrochemicals are hydrocarbons that are used extensively in the plastics industry, construction industry and other industries that supply products crucial to modern life. Petrochemicals are produced from biosolids due to the thermal depolymerization of the organic carbon present, the organic carbon in the biomass volatilises in the heat of the pyrolysis and can be recovered via condensing [108]. As previously mentioned the oil yield is maximised at temperatures between 450-550°C. A MWAP tends to preserve functional groups, a wide range of hydrocarbons can be found in this oil [109]. Some hydrocarbons of interest are described below.

The low molecular mass aromatics produced in MWAP are very high relative to the amount produced in conventional pyrolysis, this is advantageous as higher weight aromatic compounds include harmful PAHs [50, 110]. Monoaromatic hydrocarbon contents of 25-30 wt% or greater have been produced from sewage sludge MWAP [66, 107], larger concentrations of around 40% have been reported with the use of a catalyst [109].

Alkenes in MWAP bio-oil: aliphatic alkenes in the size range of 10-22 carbons are present in the bio-oil produced from the MWAP of sewage sludge [111], with other authors reporting a wider size range of alkenes using different biomasses [110]. The amount of alkenes present in the oil is usually presented as a percentage of the GC-MS chromatogram area or incorporated into the measurement of the amount of aliphatic

hydrocarbons present but MWAP has been reported to favour the production of alkenes over other aliphatic hydrocarbons [111].

Alkanes in MWAP bio-oil: lighter alkanes are not present in the oil product portion but in the gas portion, this is due to lighter alkanes being non-reactive and having boiling points lower than room temperature. In general, alkanes with a chain less than 5 carbons are gases at room temperature [112]. It has been reported that the majority of alkanes in MWAP bio-oil are between 10-18 carbons long and comprise 17 wt% of the oil on a dry basis [47, 113]. Alkanes of this chain length are mostly useful as fuels.

Aromatics, alkanes and alkenes are the most desirable organic volatile products of MWAP as they are the most widely used petrochemicals, with the majority of other petrochemicals derived from them. Other organic volatile groups are present in MWAP oil, such as, ketones [111], aldehydes [108], carboxylic acids [108], alkynes [47] and alcohols [113].

2.5 Biochar

Biochar is an important product fraction resulting from biosolids pyrolysis, varying between 35 to 80% depending on biosolids composition and pyrolysis conditions [53]. The number of applications of biochar has increased in the last decade; biochar can be used for soil amelioration, soil remediation, as a fertiliser, for activated carbon production, as a microwave susceptor and as a low-cost adsorbent [3]. The soil applications of biochar have a clearly demonstrated benefit on plant growth, microbial activity, soil organic composition and water retention [2]. Using biochar as an adsorbent is the most promising application where the biochar removal capacity of contaminants from aqueous solution is often higher than the activated carbon removal capacity [13]. Biochar is usually produced from biomass waste, which significantly decreases the production costs and environmental impact compared to activated carbon production.

Biochar has been used for removing heavy metals, dyes, phenols, antibiotics, phosphorus and many other compounds from aqueous solution [2]. The removal capacity of biochar depends on the biochar properties, contaminant solution characteristics and adsorption conditions. Pyrolysis conditions of biochar production

and activation parameters impact heavily on biochar performance as an adsorbent [3]. Pyrolysis temperature is the pyrolysis condition that most affect biochar adsorption, higher pyrolysis conditions produces biochar with higher surface area and porosity, increasing its adsorption capacity. Pyrolysis time and heating rate also impacted on biochar surface area and porosity, longer pyrolysis time increases porosity while heating rate impacts on the pore diameter consequently affecting biochar surface area [114].

The characteristics of contaminant solution play a key role in contaminant adsorption by biochar. Initial concentration of contaminant solution, pH and temperature of solution are the characteristics that most affect the adsorption. Usually, higher initial concentration of contaminant in the solution increases adsorption capacity. The effect of pH and temperature of solution depends on the contaminant type, and there are no trends. The adsorption conditions that affect adsorption process are: contact time between the contaminant solution and biochar, adsorbent quantity and agitation speed. The adsorption capacity of biochar (mg of contaminant/g of biochar) increases with contact time until reaching the equilibrium and decreases with increase of the amount of biochar. The agitation speed impacts on adsorption capacity, but the increase of adsorption capacity is only observed within certain ranges of agitation speeds, outside of these ranges, the adsorption capacity tends to decrease.

Heavy metals and dyes adsorption by biochar are very well reported in the literature [2]. However, biochar produced from sewage sludge or biosolids is less used in these studies, as there are other biomass feedstocks available for producing biochar with higher removal capacity. The three tables below compile only the adsorption capacity of biochar produced from sewage sludge or biosolids for heavy metals (Table 2.4), dyes (Table 2.5) and other compounds (Table 2.6). As can be observed in these tables, the adsorption capacity is significantly different from study to study, mainly due the number of combinations of contaminant solution characteristics, pyrolysis conditions, biochar activation and adsorption conditions.

Heavy metal adsorption by biochar is well reported in the literature due to the serious threat these metals represent to all types of organisms. Finding effective approaches to minimise the impact of these metals in environment and society is urgent as these metals can cause physiological disorders in tissues. Using biochar produced from

biomass waste has been proven to be a potential solution to mitigate heavy metal contamination. The adsorption capacity of biochar is much higher than activated carbon while the production costs are much lower [2]. As can be observed in Table 2.4 the adsorption capacity of heavy metals by biochar can be up to 80 mg/g of biochar. The adsorption capacity of metals by biochar depends on many variables and can be very different from one study case to another case.

Figure 2.5 and Figure 2.6 show a difference in the adsorption capacity of copper and lead by biochar. The reasons for this big disparity in copper adsorption capacity are mainly due to the biochar production conditions and activation. In the adsorption experiments, pH, initial concentration of metal, biochar dose and temperature also impacted significantly. For these reasons, results cannot be directly compared. Copper adsorption varies between 4 and 79 mg/g with an average of 28 mg/g while the difference between lead adsorption is lower, it varies between 30 and 66 mg/g with an average of 46 mg/g. In general, adsorbents with higher surface area have a higher adsorption capacity, but the selection of the activation agent may vary with the heavy metal type. For Cu and Pb adsorption, it was reported that biochar activated with H_3PO_4 exhibited a higher removal capacity than using KOH and $ZnCl_2$ [115].

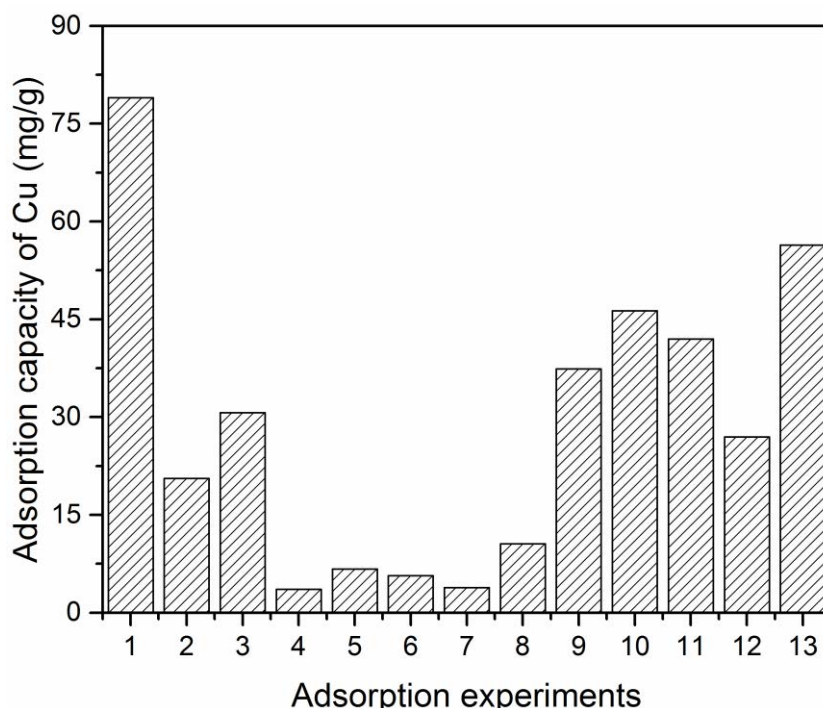


Figure 2.5 – Adsorption capacity of Cu(II) by sewage sludge adsorbents.

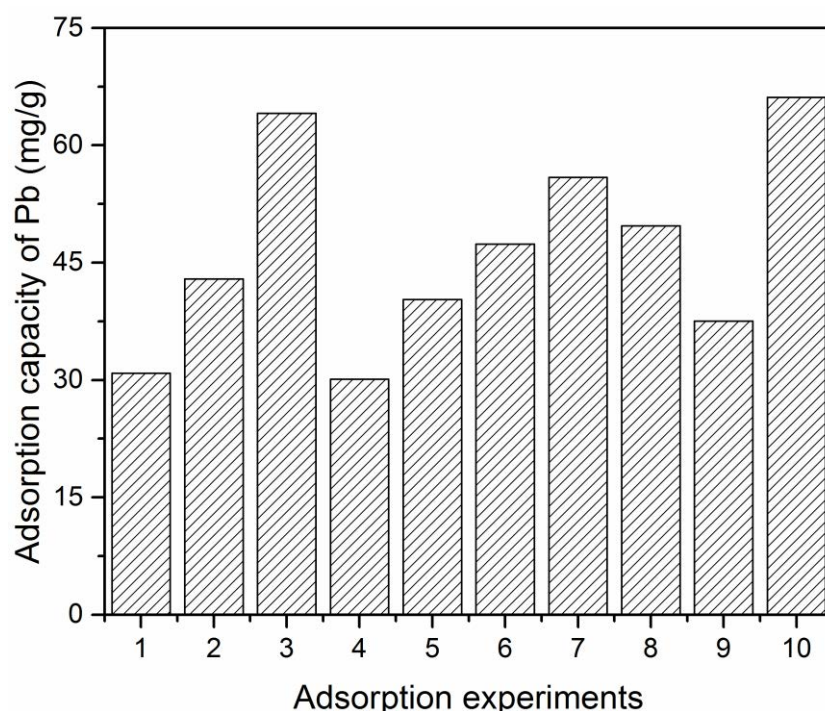


Figure 2.6 – Adsorption capacity of Pb(II) by sewage sludge adsorbents.

The adsorption of heavy metals by biochar is mainly described by the Langmuir model (Table 2.4), demonstrating that is a simple adsorption process. The adsorption of heavy metals can be explained mainly by five mechanisms: (1) metal precipitation as insoluble compounds, (2) electrostatic interactions between metals and biochar surface, (3) ion exchange, (4) ion complexation with the surface functional groups of biochar, and (5) metal reduction followed by physical adsorption [116]. The specific surface area of biochar plays a key role on the adsorption process, the increase of surface area enhances heavy metal adsorption since there is more surface available for complexation with metal ions, more surface for physical adsorption and as the surface area increases biochar becomes reactive favouring ion exchange [117]. In case of physical adsorption, pore volume and size are also important and define the adsorption rate. The pH of metal solution considerably affects the metal adsorption of biochar as metal speciation depends on pH [116]. Recent studies have shown that chemical activation changes surface functional groups of biochar and creates more sites for heavy metal interaction and connection. This process can be optimised to target the adsorption of certain metal species [118].

The contamination of water streams with dyes from textile industry or other type of dyeing industry represents a serious problem to the environment. These dyes contain very toxic compounds that are hazardous at only a few mg/L for aquatic organisms. Besides the hazardous properties, dyes also represent an aesthetic problem due to the colouring potential of the receiving water bodies. Adsorption is a potential economically viable solution to control these dyeing industry problems [119].

Table 2.5 summarizes the adsorption capacity of different dyes by sewage sludge based adsorbents prepared in different conditions. The adsorption capacity varies from 1 mg/g to 560 mg/g, which is due to the impact of preparation conditions of the biochar on adsorption capacity. Surface area of biochar has a great impact on adsorption capacity, biochar with higher surface area have higher adsorption capacity. The adsorption capacity of acid yellow 49 increased 62% when the surface area of biochar increases from 34.3 to 60.7 m²/g. The activation of biochar with chemicals has also affecting the adsorption capacity as a consequence of the surface area increase and porosity structure. In general, the biochar activated with zinc chloride performs better than with sulphuric acid.

Dye adsorption by biochar depends on the molecular size of the dye and pore size of biochar. Biochar with mesopores has a greater dye adsorption capacity [118]. The chemical activation process of biochar is fundamental to improving dye adsorption capacity because of the pore structure development, but the activation chemical will also change the biochar pH, which may decrease the dye adsorption. For example, the methylene blue adsorption by non-activated biochar was 21.7 mg/g, increased to 31.45 and to 168.81 mg/g with H₂SO₄ and ZnCl₂ activation, respectively. The activation with H₂SO₄ increased significantly the surface area of biochar, but only slightly enhanced the adsorption capacity compared with the biochar activated with ZnCl₂, which can be explained by the low pH of the activated biochar.

The adsorption of dyes by biochar is usually described by both the Langmuir and Freundlich models. The description by the Freundlich model demonstrates that dye adsorption can be also controlled by the chemical surface of biochar, chemisorption. Organic dye adsorption can be explained by two mechanisms: electrostatic interaction and ion exchange [120]. The adsorption of anionic dyes increases with char basicity

indicating an electrostatic interaction while the adsorption of cationic dyes is mainly explained by ion exchange between dye cations and surface functional groups of biochar [120]. In general, biochar with high surface basicity exhibits high dye adsorption from an aqueous solution [118].

Biochar has been used for the removal of other compounds, such as phenols, phosphorus, toluene and other pollutants that represent a threat to life. Biochar for phenol removal has been well studied with adsorption capacities between 25 to 96 mg/g (Table 2.6). Phenol adsorption by biochar is often described by the Langmuir model demonstrating that physical adsorption is one of the main mechanisms; however, the biochar surface modified with NaOH has the highest phenol uptake indicating that chemisorption should also be considered. Surface biochar modification with NaOH or HCl changes biochar pH, which may change the pH of phenol solution impacting on phenol adsorption. The mechanism of phenol adsorption by biochar is not well understood yet.

Phosphorus and phosphates removal by biochar is well reported in the literature; however, there are just a few examples of using sludge biochar. The main mechanisms of phosphorus and phosphate removal from an aqueous solution are ligand exchange and surface complexation with metals such as Fe, Al, Mg and Ca [121]. The modification of the surface area of biochar with these metal salts improved significantly the phosphorus removal capacity. Also, the pH of the phosphate solution plays a key role on removal capacity due to the impact on phosphate species in the solution. The biochar surface pH is also important as it can change the pH of mixture during adsorption.

Contaminant removal from an aqueous solution using biochar has been well explored compared with gas adsorption. Table 2.6 shows six examples of toluene adsorption by biochar, indicating that the activation process of biochar has a great impact on the adsorption capacity. The chemical activation process develops microporosity in the biochar enhancing toluene adsorption capacity [122].

Table 2.4 - Heavy metals removal by biochar produced from sewage sludge or biosolids.

Biochar activation / Modification	Metal	Surface area (m²/g)	Concentration solution (mg/L)	Contact time (h)	Model	Adsorption capacity (mg/g)	Reference
	Ag(I)	78.51	100 - 1000	24	Langmuir	43.9	[114]
ZnCl ₂	Cd(II)	550	40	1	Langmuir	16.7	[123]
	Cd(II)	67.60	200	-	-	42.8	[124]
	Cd(II)	100	100 – 300	72	Langmuir	15.0	[125]
ZnCl ₂ / H ₂ SO ₄	Cd(II)	327.67	50	6	Langmuir	1.42	[126]
ZnCl ₂ / H ₂ SO ₄ /Pyrolusite	Cd(II)	364.71	50	6	Langmuir	7.55	[126]
	Cr(III)	67.60	50 - 200	-	-	20	[127]
ZnCl ₂	Cr(III)	472	10 – 1000	24	Langmuir	13.7	[128]
ZnCl ₂	Cr(III)	472	10 – 2000	48	Langmuir	15.4	[129]
	Cr(III)	60	10 – 1000	24	Langmuir	1.5	[128]
	Cr(III)	60	10 – 2000	48	Langmuir	3.0	[129]
H ₂ SO ₄	Cu(II)	217	100	-	-	79	[130]
ZnCl ₂	Cu(II)	472	10 – 1000	24	Langmuir	20.6	[128]
ZnCl ₂	Cu(II)	472	10 – 2000	48	Langmuir	30.7	[129]
	Cu(II)	60	10 – 1000	24	Langmuir	3.6	[128]

	Cu(II)	60	10 – 2000	48	Langmuir	6.7	[129]
	Cu(II)	51	500	1	Langmuir	5.71	[131]
	Cu(II)	48.3	50	1	Langmuir	3.88	[9]
ZnCl ₂	Cu(II)	377.1	50	1	Langmuir	10.56	[9]
ZnCl ₂	Cu(II)	118.3	10 – 160	1	Langmuir	37.4	[132]
H ₃ PO ₄	Cu(II)	124.8	10 – 160	1	Langmuir	46.3	[132]
KOH	Cu(II)	130.7	10 – 160	1	Langmuir	42.0	[132]
ZnCl ₂ / H ₂ SO ₄	Cu(II)	327.67	200	4	Langmuir	26.96	[126]
ZnCl ₂ / H ₂ SO ₄ /Pyrolusite	Cu(II)	364.71	200	4	Langmuir	56.41	[126]
ZnCl ₂	Hg(II)	472	10 – 1000	24	Langmuir	106.4	[128]
ZnCl ₂	Hg(II)	472	10 – 2000	48	Langmuir	175.4	[129]
	Hg(II)	60	10 – 1000	24	Langmuir	64.9	[128]
	Hg(II)	60	10 – 2000	48	Langmuir	64.9	[129]
ZnCl ₂	Ni(II)	550	30	1	Langmuir	9.09	[123]
	Pb(II)	24.73	10 - 1000	4	Freundlich	30.88	[133]
ZnCl ₂	Pb(II)	472	10 – 1000	24	Langmuir	42.9	[128]
ZnCl ₂	Pb(II)	472	10 – 1000	24	Langmuir	64.1	[128]
	Pb(II)	60	10 – 1000	24	Langmuir	30.1	[128]
	Pb(II)	60	10 – 1000	24	Langmuir	40.3	[128]
ZnCl ₂	Pb(II)	118.3	10 – 160	1	Langmuir	47.39	[132]

H ₃ PO ₄	Pb(II)	124.8	10 – 160	1	Langmuir	55.9	[132]
KOH	Pb(II)	130.7	10 – 160	1	Langmuir	49.7	[132]
ZnCl ₂ / H ₂ SO ₄	Pb(II)	327.97	200	4	Langmuir	37.53	[126]
ZnCl ₂ / H ₂ SO ₄ /Pyrolusite	Pb(II)	364.71	200	4	Langmuir	66.14	[126]

Table 2.5 – Dyes removal by biochar produced from sewage sludge or biosolids.

Biochar activation / modification	Dye	Surface area (m²/g)	Concentration solution (mg/L)	Contact time (h)	Model	Adsorption capacity (mg/g)	Reference
	Acid brown 283	253	100	2	Langmuir	20.5	[134]
H ₂ SO ₄	Acid Red 18	217	30	-	-	58	[130]
KOH	Acid Brilliant Scarlet GR	381.62	300	0.25	Langmuir	14.95	[135]
	Acid yellow 49	34.3	10 – 750	48	Langmuir	71.43	[120]
CO ₂	Acid yellow 49	60.7	10 – 750	48	Langmuir	116.28	[120]
	Basic Blue 41	34.3	10 – 750	48	Langmuir	416.67	[120]
CO ₂	Basic Blue 41	60.7	10 – 750	48	Langmuir	558.24	[120]
	Basic red 46	253	100	2	Langmuir	188	[134]
H ₂ SO ₄	Basic Violet 4	217	30	-	-	58	[130]
	Direct red 89	253	100	2	Langmuir	49.2	[134]
	Direct red 89	253	100	2	Langmuir	0.29	[134]
	Indigo carmine	100	2000	40	Langmuir	92.83	[136]
Ethanol	Malachite green	12	10 - 120	1	-	34.2	[137]
Acetone	Malachite green	17	10 - 120	1	-	49.2	[137]

Methanol	Malachite green	16	10 - 120	1	-	27.3	[137]
	Methylene blue	60	10 – 4000	48	Freundlich	21.7	[138]
H ₂ SO ₄	Methylene blue	216	10 – 4000	48	Freundlich	31.45	[138]
ZnCl ₂	Methylene blue	472	10 – 4000	48	Freundlich	168.81	[138]
	Reactive red 198	34.3	10 – 750	48	Langmuir	18.93	[120]
CO ₂	Reactive red 198	60.7	10 – 750	48	Langmuir	25.06	[120]
	Reactive brilliant red K-2BP	298	50	1	Langmuir	37.31	[139]
	Reactive Brilliant Red X-3B	88.9	-	-	Langmuir	92.6	[140]
	Reactive Brilliant Red X-3B	120.6	-	-	Langmuir	144.9	[140]
	Sandolan brilliant red N-BG 125	60	10 – 4000	48	Freundlich	29.16	[138]
H ₂ SO ₄	Sandolan brilliant red N-BG 125	216	10 – 4000	48	Freundlich	75.92	[138]
ZnCl ₂	Sandolan brilliant red N-BG 125	472	10 – 4000	48	Freundlich	273.64	[138]

Table 2.6 – Contaminant removal by biochar produced from sewage sludge or biosolids.

Biochar activation / modification	Contaminant	Surface area (m²/g)	Concentration solution (mg/L)	Contact time (h)	Model	Adsorption capacity (mg/g)	Reference
ZnCl ₂	CCl ₄	674.4	5 - 80	4	Langmuir	7.73	[141]
H ₂ SO ₄	2-clorophenol	162.2	20 - 2000	6	Langmuir	47.98	[142]
NaOH	Phenol	346.5	20 - 150	1	Langmuir	96.15	[143]
ZnCl ₂	Phenol	674.4	100 - 2000	4	Langmuir	46.95	[141]
Steam	Phenol	226	100	24	-	44.0	[130]
Steam	Phenol	217	100	24	-	43.0	[130]
H ₂ SO ₄	Phenol	390	100 - 1000	-	Langmuir	42.04	[144]
H ₂ SO ₄	Phenol	253	5 - 100	-	-	25.0	[145]
H ₂ SO ₄ /ZnCl ₂	Phosphate	144.47	19.7	11	-	41.2	[146]
ZnSO ₄ /H ₂ SO ₄	Phosphate	-	90 - 330	24	Langmuir	123.46	[147]
	Phosphorus	64.67	1500	24	-	16.4	[13]
	Phosphorus	51.89	1500	24	-	13.7	[13]
ZnCl ₂	Toluene	517.4	70	-	-	490	[148]
Citric Acid	Toluene	117.6	70	-	-	320	[148]
Citric Acid/ ZnCl ₂	Toluene	867.6	70	-	-	830	[148]

H ₃ PO ₄	Toluene	240	-	-	Langmuir	224	[122]
H ₃ PO ₄	Toluene	278	-	-	Langmuir	250	[122]
H ₃ PO ₄	Toluene	230	-	-	Langmuir	284	[122]

3 DIELECTRIC PROPERTIES OF BIOSOLIDS

Abstract

Microwave assisted pyrolysis (MWAP) is an alternative heating approach to convert biosolids into value-added products, such as biochar, biogas and bio-oil. Studying the dielectric properties of biosolids is fundamental to understand the behaviour of this material under microwave irradiation and to design microwave assisted pyrolysis systems. This study examined the dielectric properties of biosolids with changes in moisture content and applied microwave frequency. Results demonstrated that the dielectric constant decreases with decreasing moisture content and with increasing microwave frequency. The penetration depth increases with decreasing moisture content, while the dielectric loss factor of dry biosolids is almost zero. Because of the poor dielectric properties of dry biosolids, a microwave susceptor must be added to the biosolids to attract microwave energy so that the materials can reach temperatures required for pyrolysis. Therefore, this study also investigated the impact of four microwave susceptors (activated carbon, charcoal, biochar and glycerol) on biosolids pyrolysis and on biochar properties produced from biosolids via microwave assisted pyrolysis at 600°C. The choice of microwave susceptor influences the heating rate of biosolids and the specific surface area of the resultant biochar. Results show that activated carbon favours the heating process, increases surface area, and the biochar produced with activated carbon has the highest carbon stability and energy value.

Keywords: biosolids; biochar; carbon stability; dielectric properties; pyrolysis; microwave susceptor.

Highlights

- Dielectric properties of biosolids depend on moisture content and frequency.
- Sample size impacts on distribution and intensity of microwave field.
- Microwave susceptor impacts significantly on pyrolysis heating rate.
- Microwave susceptor affects specific surface area of resultant biochar.
- Biochar produced with activated carbon has the highest carbon stability.

As submitted in: Antunes, E., Brodie, G., Jacob, M. V., Schneider P. A., “Microwave pyrolysis of sewage biosolids: dielectric properties, microwave susceptor role and its impact on biochar properties”, *Journal of Analytical and Applied Pyrolysis* 2017.

3.1 Introduction

The recovery and recycling of resources is a highly important issue currently facing the world. The global population and non-renewable resource consumption per capita are increasing at a greater rate. Peak oil and peak phosphorus are probably the major concerns in the near future; while oil can be replaced by other forms of energy, for example hydrogen, phosphorus has no substitute. Peak phosphorus will occur in the next 20 years, consequently a problem of food security may arise because this element is fundamental for plant growth and cannot be chemically synthesised or produced [149]. Biosolids could be a sustainable source of energy and nutrients, such as nitrogen and phosphorus. Further, biosolids production rate is increasing rapidly due more restricted environmental regulations, urbanisation and population standards [150], increasing the availability of this feedstock. Recovering nutrients, energy and chemicals from biosolids could be a viable solution to manage the ever-increasing amounts of biosolids and to replace vital nutrients for plant growth.

Microwave pyrolysis heats biomass via dielectric heating, which occurs through one of two mechanisms. The first, dipole polarization, occurs when the poles of polar molecules attempt to align with the microwave field, which oscillates at 2.45GHz, releasing heat due to the intramolecular resistance to this motion [108]. The second is Maxwell-Wagner depolarization, which occurs at the boundary between two materials with different dielectric properties or in materials where electrons can freely move, most notably in some carbon materials with delocalized π electrons [64]. The efficiency of a material to convert the electromagnetic radiation to thermal energy depends upon the dielectric properties, including the dielectric loss tangent ($\tan\delta$). The $\tan\delta$ is the ratio between the efficiency with which microwave energy is converted into thermal energy (dielectric loss factor - ϵ'') and the ability of the materials molecules to be polarized (dielectric constant - ϵ') [70]. Some materials do not have the dielectric properties necessary to be heated in a microwave field – this selective heating is considered an advantage in MWAP as the microwave energy only heats the biomass and not the chamber or pyrolysis atmosphere, unlike with conventional heating [64].

Most biomass do not heat in a microwave field and hence need to be mixed with high $\tan\delta$ materials, termed microwave absorbers or susceptors. A microwave susceptor acts

as a hot spot, undergoing dielectric heating and transforming this into thermal heating. A material with $\tan\delta > 0.2$ is considered an efficient absorber [85]. By homogeneously distributing a susceptor through the biomass, the sample can be uniformly heated by the penetrating microwave field, causing the centre of the sample to be hotter than the outside, due to the surface losing heat to the pyrolysis atmosphere via conventional heat transfer mechanisms [50]. Microwave susceptor particles are hotter than biosolids and transfer heat to the cooler surroundings by conduction. Different susceptors have been used in MWAP studies, the most common being carbon susceptors, such as activated carbon, MWAP-derived biochar, graphite and silicon carbide [102, 109, 151]. The choice of susceptor is an important consideration when designing a MWAP process as the susceptor influences the distribution of the products between char, oil and gas, and the properties of the final products, in addition to affecting the heating rate and maximum temperature [107].

Microwave assisted pyrolysis of sewage sludge and/or biosolids has been studied by several researchers, but little attention has been given to dielectric properties of biosolids [45, 84, 109, 152]. The dielectric properties of materials are fundamental to the design of microwave systems as well as understanding the behaviour of materials under microwave irradiation during heating and pyrolysis. Therefore, the first objective of this study was to understand the variation of dielectric properties of biosolids with moisture content and microwave frequency. The second objective was to assess the impact of different microwave absorber materials (activated carbon, charcoal, biochar and glycerol) on the microwave pyrolysis process of biosolids and biochar properties. MWAP of glycerol has been explored [153], but glycerol has not been studied as a microwave susceptor for biomass MWAP. Finding new applications for glycerol is fundamental, since this product is produced in large quantities as a waste product from biodiesel production [69].

3.2 Materials and methods

Stockpiled biosolids from Euroa Wastewater Treatment facility in Victoria, Australia with approximately 40% moisture content were used as a feedstock material in this study. Biosolids were mixed with 20 wt% (dry mass of biosolids) of a microwave susceptor material to obtain a homogenous mixture, then pyrolysed at 600°C for 10 minutes. Four different microwave susceptors were tested in this work: activated carbon, charcoal, biochar and glycerol. The activated carbon, charcoal and glycerol were supplied by Sigma Aldrich while the biochar was previously produced from biosolids via MWAP.

A 1.2 kW customised single-mode microwave with 2.45 GHz magnetron source was used for pyrolysis tests. A detailed description of this microwave system is outlined elsewhere [13]. The applied microwave power was 600 W during the heating process and, once at the desired temperature, the microwave power was adjusted to maintain sample temperature at $600 \pm 10^\circ\text{C}$. The pyrolysis chamber was purged with nitrogen (99.9% purity) before and during pyrolysis to keep an oxygen-free atmosphere. The pyrolysis gases were pumped through a condenser and a water trap to protect the vacuum pump. The gas and oil fractions were not collected and not analysed in this study.

The dielectric properties of the biosolids and the four microwave susceptor materials were measured using an Agilent network analyser (PNA 8357B) equipped with a dielectric probe (Agilent 85070E Dielectric Probe kit). Dielectric loss and dielectric constant were measured between 1 to 10 GHz at intervals of 100 MHz at room temperature ($23^\circ\text{C} \pm 2^\circ\text{C}$) for all biosolids with variable moisture content.

Biochar specific surface area characterisation was carried out with a Micromeritics TriStar 3000 gas adsorption analyser. Prior to analysis, samples were degassed at room temperature for 10 hours and then 1 hour at 250°C. Morphology and surface porosity assessment was carried out by using a scanning electron microscopy Jeol JSM5410LV. The carbon, hydrogen, nitrogen and sulphur were determined by a CHNS elemental analyser (FLASH 2000 CHNS/O Analyser) whereas the oxygen content was calculated by difference. The biochar yield was calculated according to (3.1):

$$\text{Biochar Yield} = \frac{A - C}{B} \quad (3.1)$$

where A is the weight of dry biochar, B is the weight of dry biosolids, and C is the weight of the microwave absorber mixed within the biosolids. For the biochar samples produced with glycerol, C is the weight of carbon plus final solid residue of glycerol, which was considered to be 4% of the glycerol initial mass [154].

The stability of biochar in the natural environment was simulated by placing a certain amount of biochar (equivalent to 0.1 g of carbon) in 7 ml of hydrogen peroxide (5%) for 48 hours at 80°C [155]. Elemental analysis was carried out on the biochar before and after oxidation and the concentration of carbon was used to estimate the biochar stability using equation (3.2).

$$\text{Biochar stability (\%)} = \frac{B_o \times C_o}{B_i \times C_i} \times 100 \quad (3.2)$$

where B_o is the biochar mass after oxidation, C_o is the carbon concentration after oxidation, B_i is the initial mass of biochar and C_i is the initial concentration of carbon in biochar.

To understand the impact of different biosolids composition and load on microwave field intensity and distribution, numerical simulations were carried out using Inventor Professional 2015 software (AutoDesk Co., USA) and XFDTD software, version 7.5.1.3.r43518 (Remcom Co., USA). The materials and microwave feed ports were defined in XFDTD software and the Maxwell's electromagnetic equations in three dimensions were solved using finite-difference time-domain (FDTD) method using Inventor Professional 2015 software.

3.3 Results and discussion

3.3.1 Dielectric properties of biosolids and microwave susceptors

The dielectric constant and dielectric loss of dry biosolids and of biosolids with different moisture content measured between 1 to 10 GHz at room temperature are presented in Figure 3.1. Both the dielectric constant and the dielectric loss factor decrease as the moisture content of the biosolids decreases due to the reduction of water dipoles, and biosolids with no water are almost transparent to microwave irradiation. The dielectric constant decreases with an increase of microwave frequency while the dielectric loss factor decreases as the microwave frequency increases until around 2 GHz, after which it increases with microwave frequency. Biosolids with high moisture content (above 80%) exhibit similar dielectric properties to water. Water is a good microwave absorber, and its dielectric loss factor increases with microwave frequency, which means that the capacity of water to absorb and convert microwave energy into heat increases with microwave frequency. However, after biosolids are exposed to sufficient microwave irradiation/intensity, the water will boil off, and the dry biosolids will not absorb the electromagnetic radiation.

At 2.45GHz (the most used microwave frequency), the dry biosolids are almost transparent to microwaves mainly due to the high silica content, which is considered as an inactive material under microwave heating [156]. At this frequency the dielectric properties of biosolids are very poor. The dielectric constant is 1.39, the dielectric loss factor is 0.06 and the dielectric loss tangent is only 0.04. These results show that biosolids can absorb some microwave energy, but the conversion of electromagnetic energy into heat is very low, making it impossible to reach high temperatures under microwave irradiation. Therefore, a microwave susceptor is required to heat this sample with electromagnetic heating. The microwave susceptor absorbs dielectric heating and transforms into thermal heating, then heat is transferred to the cooler surroundings by conduction. A good distribution of this material in biosolids is fundamental to achieve uniform heating of the entire sample.

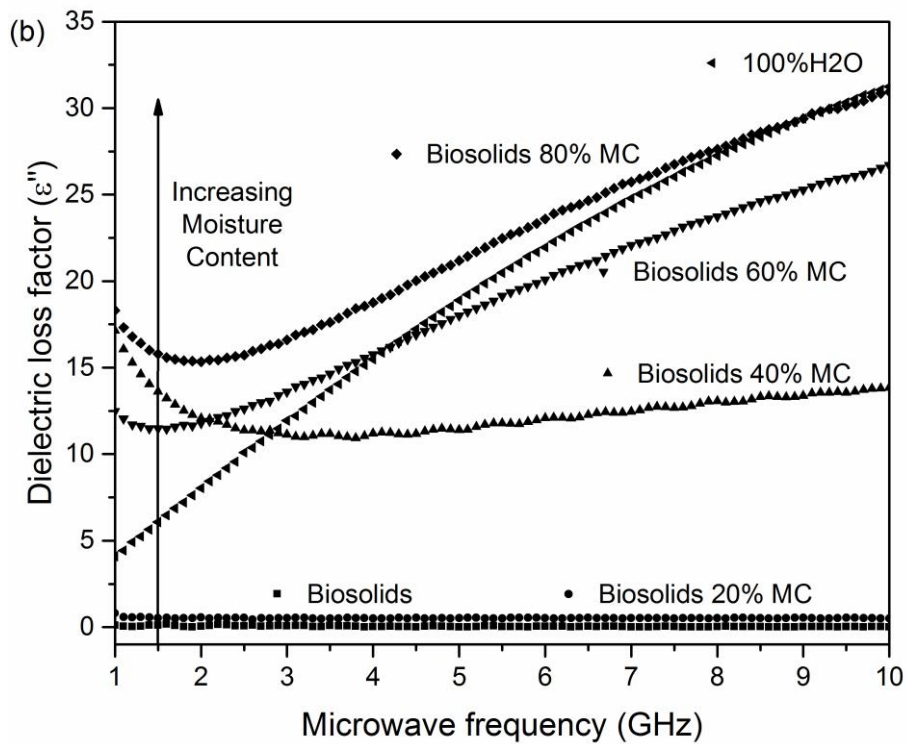
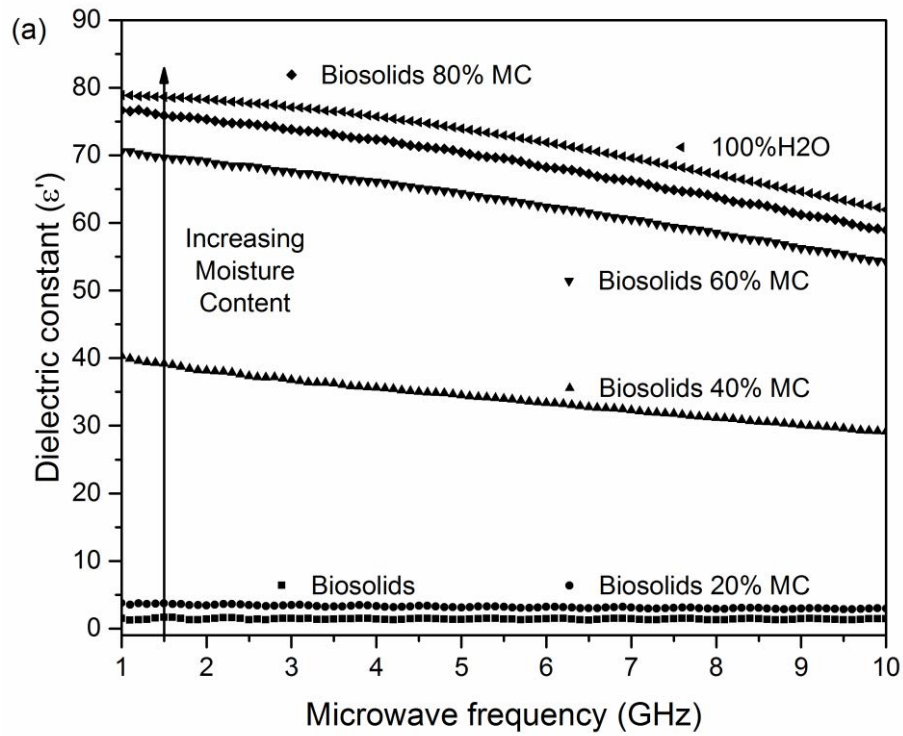


Figure 3.1 - Dielectric constant (a) and dielectric loss factor (b) of biosolids with varying moisture content measured at room temperature (23°C) between 1 to 10GHz.

The power conversion (p) of electromagnetic energy into thermal energy can be calculated using equation (3.3) [157]:

$$p = 5.56 \times 10^{-4} f k'' E^2 \quad (3.3)$$

where, p is the power conversion per unit of volume (W/cm^3), f is the microwave frequency (GHz), k'' is the relative dielectric loss factor ($k'' = \varepsilon''/\varepsilon_0$) where ε_0 is the dielectric permittivity of free space ($8.85 \times 10^{-12} F/m$), and E is the dielectric field strength (V/cm). As shown in Figure 3.1, the dielectric loss factor decreases with moisture content, so the power conversion will also decrease. For example at 2.45GHz, the dielectric loss factor of biosolids with 40% of moisture content was 11.44 while with no moisture content was only 0.06.

The moisture content in biosolids also affects the electromagnetic field distribution, as can be observed in Figure 3.2. The electromagnetic field in the cavity with 25 g of dry biosolids (1159.53 V/m) decreases when the cavity is loaded with the same quantity of biosolids with 40% moisture content (960.11 V/m). Therefore, the power conversion energy of the biosolids with 40% moisture content is $1.52 \times 10^{12} W/cm^3$, but when the water boils off from the sample, the conversion of electromagnetic into to thermal energy is more than a thousand times lower ($p = 9.63 \times 10^9 W/cm^3$). These results show that the impact of moisture content on biosolids microwave pyrolysis is beyond the impact on dielectric properties of materials; it is important to consider the influence on microwave field intensity and consequently on the capacity of power conversion.

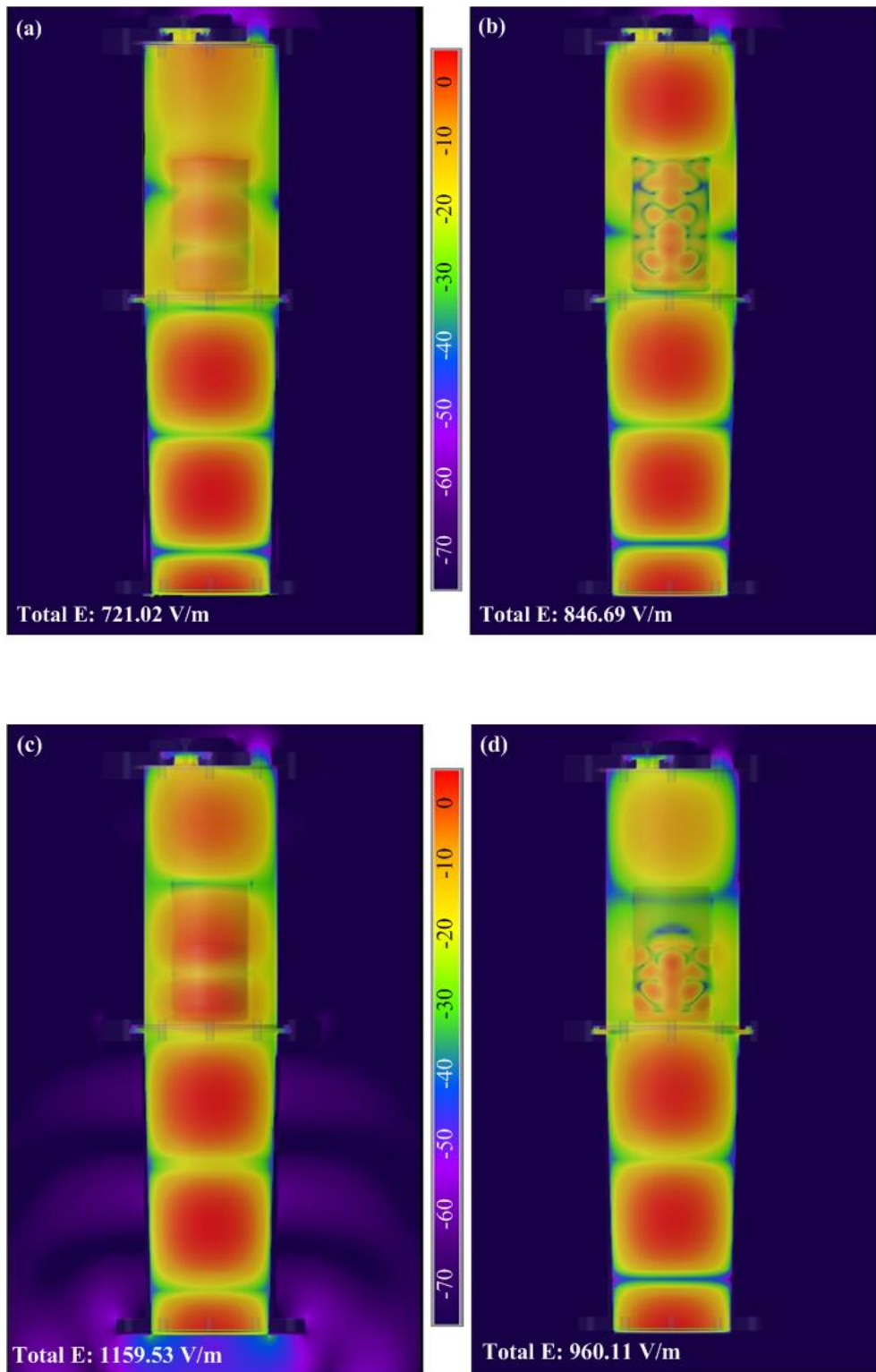


Figure 3.2 – Electromagnetic field distribution and intensity in microwave cavity with 50 g of dry biosolids (a), 50 g of biosolids with 40% moisture content (b), 25 g of dry biosolids (c) and 25 g of biosolids with 40% moisture content (d).

Besides moisture content, other variables impact on microwave heating, such as temperature and sample size. The impact of temperature on dielectric properties of biosolids is very complex; it depends on moisture content, free water, bound water and ionic conduction. The dielectric properties are changing during the biosolids heating and eventual microwave pyrolysis due to temperature and composition changes. As the biosolids are converted to biochar, it is expected that the dielectric constant increases due to a higher concentration of carbon. The impact of sample size and moisture content on microwave assisted pyrolysis process was analysed based on simulations. However, the temperature effect was not analysed in this study as the biosolids composition changes with temperature and dielectric properties depends on both temperature and sample composition.

The sample size impacts on electromagnetic field strength intensity and distribution as seen in Figure 3.2. As the sample size increases the electromagnetic field intensity decreases and this decrease is higher with the sample with lower loss tangent (dry biosolids). This is due to de-tuning of the resonant conditions inside the single-mode microwave chamber used in this experiment [158]. A perfect empty cavity would support a potentially infinite field; however, chamber walls and the load in the chamber absorb some of the field and convert it into heat. In spite of this, the size of the load will affect how much the field strength will build up. Larger load sizes result in more damping of the field and therefore a lower field strength [158].

Increasing the wet biosolids (40% moisture content) sample size from 25 g to 50 g decreases the intensity of electromagnetic field due to the absorption of microwave energy by the sample. However, this decrease was much lower compared with the dry biosolids sample; samples, which are almost transparent, disturb more of the microwave field than samples that can absorb microwave energy. These results were confirmed with the experimental microwave pyrolysis test, where the reflected energy was much higher with a dry biosolids sample than with a wet sample, but the reflected energy decreased as the char formation increased due to an increase in the absorption. Further, assuming that the microwave field peak is always in the centre of a microwave cavity is not valid for all situations, as shown in Figure 3.2; it depends on mass and characteristics of the sample. In the case of wet biosolids, as the sample size increases the microwave field is more intense in the top of the cavity; however, with dry biosolids

the microwave field intensity narrow as the sample size increase, but it is concentric for both cases. For better field coupling, the sample should be placed in the hot spot which may vary, so it is important to predict the characteristics of the microwave field before starting experiments.

When a material is exposed to microwave irradiation, microwave energy converts into thermal energy. Therefore the intensity of microwave irradiation decreases from the surface to the core of the sample, and this decay can be measured by the penetration depth (D_p). The penetration depth in meters (m) of biosolids with different moisture content was calculated using equation (3.4) [159]:

$$D_p = \frac{c}{2\pi f \sqrt{2\varepsilon' \left[\sqrt{1 + \left(\frac{\varepsilon''}{\varepsilon'}\right)^2} - 1 \right]}} \quad (3.4)$$

where c is the speed of light in free space (3×10^8 m/s), f is the microwave frequency (Hz), ε' and ε'' are the dielectric constant and dielectric loss respectively. Figure 3.3 shows that the penetration depth of biosolids decreases as the microwave frequency increases and with the increase of moisture content. At 2.45 GHz, the penetration depth of biosolids with moisture content above 40% is less than 0.5 cm, 0.78 cm and 1.44 cm corresponding to biosolids with 20% moisture content and dry biosolids, respectively. Biosolids with higher moisture content have lower penetration depth because of the higher dielectric constant of these samples, which in case of 60% and 80% moisture content the dielectric constant is similar to the water dielectric constant value. These results show that as the biosolids sample is drying during microwave pyrolysis the penetration depth is increasing which is desirable. However, the dielectric loss factor (Figure 3.1 (b)) decreases with the decrease of moisture content and in the case of biosolids with no water is almost zero, indicating that a microwave absorber is necessary to reach the temperature required for pyrolysis.

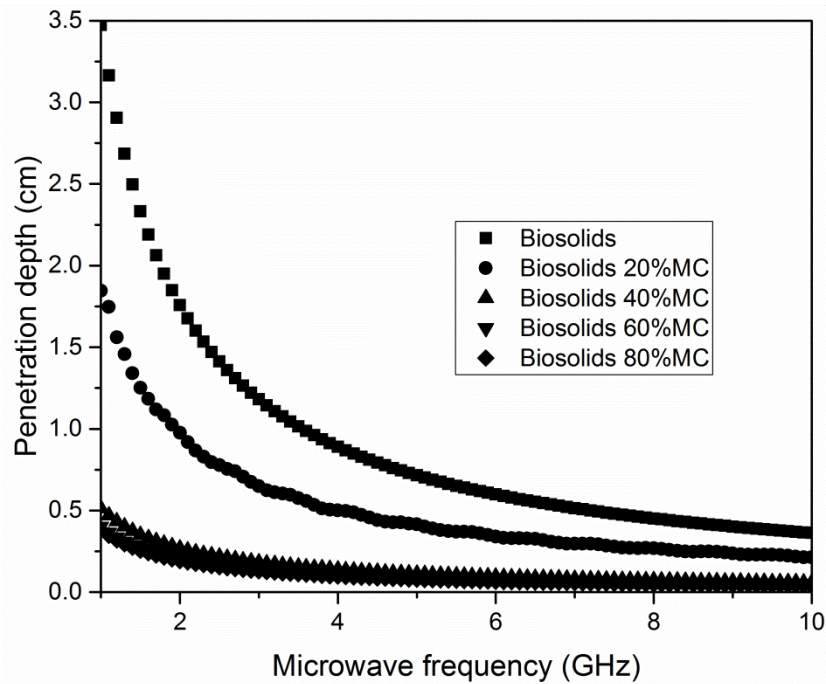


Figure 3.3 – Penetration depth of dry biosolids and biosolids with varying moisture content at different microwave frequency.

3.3.2 Microwave susceptor selection

The microwave absorber material should not contaminate the final pyrolysis by-products and not increase significantly the overall costs. Several materials can be used as a microwave absorber, in particular carbon rich materials, such as, activated carbon, coal, carbon nanotubes, and also some metal compounds like magnetite, pyrite and silicon carbide [70, 156, 160].

Table 3.1 contains the measured dielectric properties of the four microwave susceptors considered in this study. The activated carbon has the highest ability to absorb microwave energy and to re-emit it as heat. The charcoal is a carbon-rich material, but its dielectric properties are poor compared to activated carbon. Dielectric loss of charcoal has the largest contribution for the lower loss tangent, which is only 40% of the activated carbon. The biochar has poor dielectric properties due to the high silica content, which is transparent to microwaves. The $\tan\delta$ and dielectric loss factor of glycerol are much lower than the other microwave susceptors, but the use of this material as a microwave susceptor makes sense because it is abundant and cheap. These

measured dielectric properties are in agreement with other values found in the literature [70, 161].

Table 3.1 - Dielectric properties of microwave susceptors at 2.45 GHz.

Microwave susceptor	ϵ'	ϵ''	$\tan\delta$
Activated carbon	16.12	27.50	1.71
Charcoal	9.67	11.13	1.15
Biochar	9.60	9.95	1.04
Glycerol	7.84	5.58	0.71

Using glycerol as a microwave susceptor requires much more microwave power (1100 W) input to reach the final pyrolysis temperature. To use similar energy input (600 W) for glycerol and other microwave susceptors, a mixture (named as glycerol) of 90 wt% of glycerol and 10 wt% activated carbon was prepared, then mixed with the biosolids. With this small amount of carbon (1% of dry sample) it was possible to understand the impact of glycerol on biosolids microwave pyrolysis and how this material affects the final properties of biochar. Besides the poor dielectric properties of glycerol, using a liquid microwave susceptor increases contact through the entire sample and the distribution of temperature should be more homogenous in comparison with solid, discretely distributed, materials. However, the slow heating rate represents a higher power consumption, which increases the overall costs of the pyrolysis process since the overall power consumption is mainly attributed to the power consumption until reaching the temperature set-point. After reaching the temperature set-point, the power consumption decreases significantly and, in this study, less than 120 W was enough to maintain pyrolysis temperature at 600°C.

Producing biochar as a microwave susceptor has advantages; it does not introduce any contamination in the final products and has similar physicochemical properties to the final solid fraction (biochar). However, the dielectric loss tangent of this material is very low and results were not consistent because of the difficulty of heating the sample using

dielectric heating. Moreover, the thermocouple in this sample seemed to work as an antenna which is not desirable. This occurred as the thermocouple is made with conducting wires and when the surrounding sample has very low dielectric properties, power reflection is very high creating higher order modes, consequently microwave absorption by thermocouple can occur in these circumstances. The measured temperature was not representative and not consistent. As a result biochar as susceptor was not further investigated as part of this research. Biochar produced from other types of carbon-rich biomasses may have better dielectric properties due to the higher carbon content and should work well as a microwave susceptor.

3.3.3 Impact of microwave susceptors on pyrolysis heating rate and biochar properties

The temperature profile of biosolids mixed with 20 wt% of the three microwave susceptors is exhibited in Figure 3.4. The heating rate until approximately 100°C was similar for all samples because of the water content in the biosolids, which is the main contribution for the heating process at this stage. The chamber was kept at a slight vacuum (-10 KPa) to rapidly remove moisture and volatiles; therefore, the moisture boiled at slightly less than 100°C in some experiments. After approximately 200°C, the heating rate of the sample blending with activated carbon is much faster than the other two samples. This difference in the heating rate can be attributed to the higher dielectric loss tangent of activated carbon compared with the glycerol mixture.

In contrast, the sample with glycerol presented a much slower heating rate in comparison with the other two treatments. The biosolids with glycerol showed a longer plateau closer to 100°C corresponding to water evaporation and glycerol degradation [154]. The slow temperature rise between 100°C and 400°C corresponded to the degradation phase of glycerol and bound water evaporation [154]. However, after 400°C the heating rate of this sample was much faster than in the previous stage due to the formation of biochar, which accelerates the heating rate due to its dielectric properties. At this stage the dielectric properties of the sample were changing rapidly due to char formation and the whole sample was absorbing microwave energy consequently the heating rate was much faster.

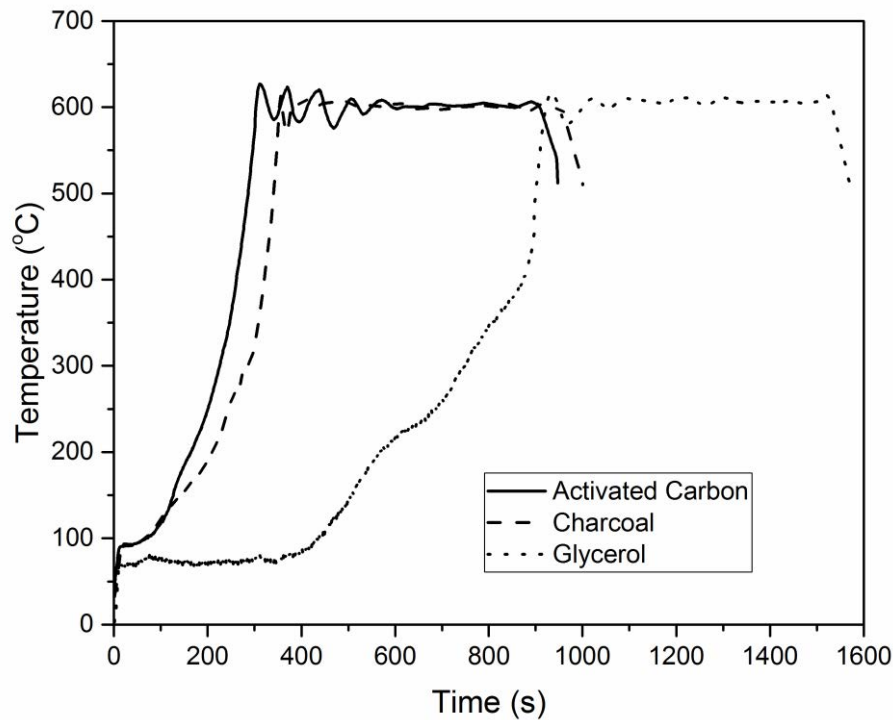


Figure 3.4 – Temperature profile of microwave pyrolysis of biosolids mixed with 20% of a microwave susceptor.

Microwave susceptors affect heating rate and consequently impact on power consumption. While activated carbon and charcoal had similar energy consumption until reaching 600°C (51 Wh and 59 Wh respectively), the energy required to reach the same set-point when using glycerol is three times higher than activated carbon (153 Wh). The energy consumption for the ten minutes of pyrolysis holding time was very low (average of 80 Wh) and similar for all microwave susceptors used. The total value of energy consumption per kg of dry biosolids is \$0.25, \$0.29 and \$0.77 for activated carbon, charcoal and glycerol, respectively.

The price of activated carbon (\$2.5/kg) is much higher than charcoal (\$0.5/kg) and glycerol (\$0.1/kg), but considering the energy cost of \$0.25/kWh, the total cost for the pyrolysis of 1kg of dry biosolids is much lower using charcoal (\$0.39/kg of dry biosolids) than with glycerol and activated carbon (\$0.83 and \$0.75 per kg of dry biosolids, respectively). The price of glycerol is much lower than the activated carbon, but the power consumption during the heating stage was much higher than activated carbon, consequently changing the total microwave pyrolysis costs. This results show

the importance of an economic analysis of this process and how a small amount of a microwave susceptor can change the overall costs. Pyrolysis costs (\$390/dry tonne) are much lower than land application even when just stabilisation, transport and land application costs are considered (\$690/dry tonne) [28].

The biochar yield, biochar stability and the elemental analysis of each biochar sample is presented in Table 3.2. The yield of biochar produced with glycerol was lower than the other two samples, which can be explained by the slower heating rate and consequently the total pyrolysis time was much higher increasing volatile organic compound release. It was expected that the sample produced with activated carbon had a lower biochar yield than the sample produced with charcoal due to the high surface area of the microwave susceptor, which improves heat transfer, but the small particles of activated carbon could block the biochar surface pores and prevent volatile organic compounds release. Higher pyrolysis time increases the volatile organic compound release, consequently decreases biochar yield.

The elemental analyses show a greater increase on carbon percentage in biochar compared with the concentration of carbon in biosolids (19.9%). However, the percentage of carbon in the biochar produced with glycerol is just slightly higher than the initial percentage in biosolids due to the combination of carbon with the oxygen from glycerol during pyrolysis, which increased the percentage of the gas fraction. The biochar sample produced with activated carbon has the highest carbon concentration which can be explained by the carbon added as a microwave susceptor and the better carbonisation of this sample as the microwave susceptor has the smaller particle size and the highest surface area promoting a faster and more uniform heat transfer to the biosolids particles.

The biochar stability depends significantly on the microwave susceptor used for pyrolysis (Table 3.2). Microwave susceptors impact on heating rate, which affects pyrolysis gas formation and carbonisation of biochar. The biochar sample produced with glycerol has the lowest carbon stability, which can be attributed to the poor carbonisation of the biosolids due to the oxygen content in glycerol; however, the sample produced with activated carbon exhibits the highest carbon stability due to an efficient carbonisation of the whole sample. These results show the impact of

microwave susceptors, which had a great impact on the heating rate and carbon stability. Samples produced with carbon-rich materials are much more stable due the better carbonisation and because these microwave susceptor (part of the final biochar) also have greater stability [155].

Table 3.2 – Biochar yield and properties of the three samples produced with different microwave susceptors (20 wt% based on dry mass of biosolids).

Biochar	BC-AC	BC-Charcoal	BC-Glycerol
Yield	0.85	0.85	0.74
BET (m ² /g)	134.7	54.4	63.7
C (%)	52.32	39.42	23.4
H (%)	1.25	1.72	1.38
N (%)	1.62	1.77	1.34
S (%)	0.4	0.51	0.33
O* (%)	44.41	56.57	73.55
Ash (%)	55.3	57.7	66.1
Biochar stability (%)	83.08	71.02	52.78

* Calculated by difference

Carbon stability, porosity and surface area of biochar are important properties for land application. Biochar can improve soil properties by increasing carbon content, pH, and water retention capacity [100]. Therefore, it is fundamental to predict how long these benefits will last after biochar soil application. The results demonstrated that biochar produced with activated carbon is much more stable than other biochar produced with charcoal or glycerol, indicating a better longevity when applied to land and similar to humic acid [155]. The biochar produced with activated carbon has the highest surface area. Surface area and porosity of biochar impact on soil microbial activity, soil

aeration, and nutrient and water holding capacity [162]. These biochar samples contain mainly micropores (< 2 nm) and mesopores (2 – 50 nm), which are responsible for the increase of surface area. Micropores of biochar are fundamental for microbial activity and for the sorption capacity of water, nutrients, heavy metals and gases [163]. However, the benefits from biochar land application are beyond biochar characteristics, are also affected by the soil type, pH, texture and composition, crop type and ecosystem [164].

The biochar can be also used for energy production. The energy value (Q in MJ/kg) of biochar can be calculated by equation (3.5) [165]:

$$Q = 0.3417 C + 1.3221 H + 0.1232 S - 0.1198 (O + N) - 0.0153 A \quad (3.5)$$

where, C, H, S, N and O are the percentages of carbon, hydrogen, sulphur, nitrogen and oxygen obtained by elemental analysis and A is the percentage of ash in biochar. The energy value of biochar produced with activated carbon is 13.2 MJ/kg, which almost double energy from biochar-charcoal (7.9 MJ/kg). Conversely, the energy value of biochar-glycerol is negative (-0.1 MJ/kg) mainly due to the oxygen and nitrogen content in biochar. For energy production, just the biochar produced with activated carbon is viable, which has the closest caloric value of charcoal. These results combined with carbon stability and pyrolysis costs demonstrated that using activated carbon as a microwave susceptor is the best option for biochar production and its applications.

The SEM images of biochar (Figure 3.5) show the impact of different microwave susceptors on the biochar surface. The biochar produced with activated carbon (Figure 3.5 (a)) has more pores on the surface, which enhances the surface area of this biochar. The higher porosity of the biochar surface can be explained by the increase in the pressure inside the biosolids particles due to the rapid heating. As the gases escape from the interior of the particles, it enhances surface porosity on biochar particles.

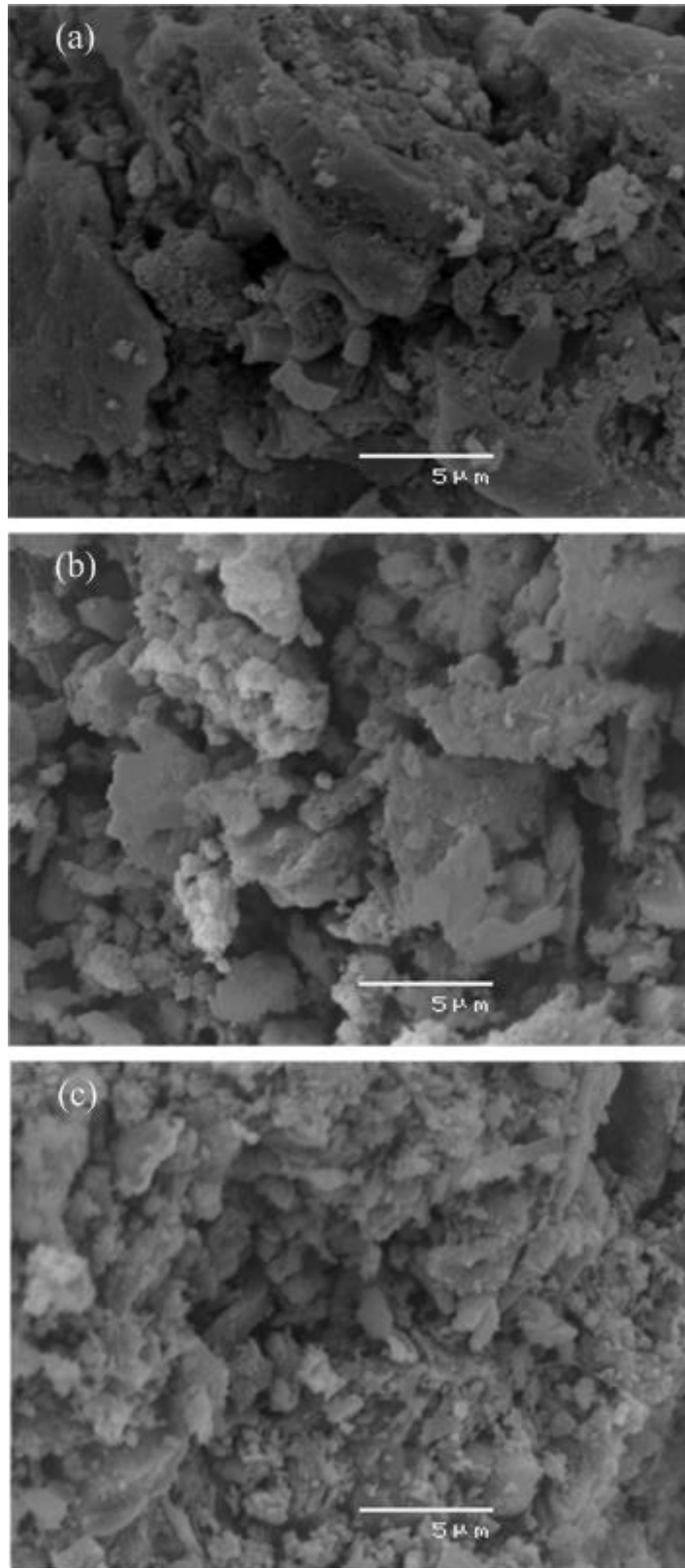


Figure 3.5 – SEM of biochar produced from biosolids with different microwave absorbers: activated carbon (a), charcoal (b) and glycerol (c).

Interestingly, the surface of biochar produced with charcoal (Figure 3.5 (b)) shows a graphitised surface very likely due to the heat concentration on the charcoal particles due to its better dielectric properties compared with biochar. Also, the charcoal particles were bigger than the activated carbon, leading to a higher concentration of heat in the charcoal particles. The biochar produced with glycerol (Figure 3.5 (c)) has big agglomerates and the hardest surface, which was very brittle. The glycerol worked as a bonding agent, keeping the biosolids together and even after pyrolysis the biochar was just one big piece.

3.4 Conclusions

This research investigated the dielectric properties of biosolids with different moisture content, and the role that microwave susceptors play in microwave pyrolysis of these materials. The moisture content of biosolids significantly affects the dielectric properties of biosolids. Also, the sample size impacts on microwave field intensity and distribution affecting the power absorbing by each sample. The penetration depth of microwaves on biosolids depends on moisture content; dry biosolids has the highest penetration depth, which is desirable. Dry biosolids are almost transparent to microwaves; therefore, microwave susceptors play a fundamental role in microwave assisted pyrolysis of this feedstock. Microwave susceptors have a great impact on pyrolysis conditions, particularly on the heating rate. Samples prepared with glycerol exhibited a significantly lower heating rate compared to the activated carbon and charcoal materials, which impacted on biochar yield and properties. This study demonstrated that microwave susceptors play a crucial role on biochar properties, particular on specific surface area and biochar stability. The biochar produced with activated carbon has the highest energy value, the best carbon stability and the lowest microwave power consumption, making this susceptor the best choice due to its economic analysis and properties of biochar.

4 IMPACT OF PYROLYSIS TEMPERATURE ON BIOCHAR

Abstract

The amount of biosolids increases every year, and social and environmental concerns are also rising due to heavy metals and pathogen contamination. Even though biosolids are considered as a waste material, they could be used as a precursor in several applications, especially in agriculture due to the presence of essential nutrients. Microwave assisted pyrolysis (MWAP) is a promising technology to safely manage biosolids, while producing value-added products, such as biochar, that can be used to improve soil fertility. This study examined the impact of pyrolysis temperature between 300°C and 800°C on the chemical and physical properties of biochar obtained from biosolids via MWAP. Preliminary phosphorus adsorption tests were carried out with the biochar produced from biosolids. This research demonstrated that pyrolysis temperature affects biochar specific surface area, ash and volatiles content, but does not impact heavily on the pH, chemical composition and crystalline phases of the resultant biochar. Biochar yield decreases as the pyrolysis temperature increases. Phosphorus adsorption capacity of biochar was approximately around 15 mg/g of biochar. Biochar resulting from MWAP is a potential candidate for land application with an important role in water and nutrient retention, due to the high surface area.

Keywords: biosolids, biochar, microwave assisted pyrolysis, surface area, pyrolysis temperature, phosphorus removal.

Highlights

- Biochar yield decreases 15% when the pyrolysis temperature increases from 300°C to 800°C.
- Pyrolysis temperature affects significantly biochar surface area.
- The inorganic elements are concentrated in biochar, no volatilisation was observed with the increase of pyrolysis temperature.
- Phosphorus removal capacity of biochar was approximately 15 mg/g of biochar.

As published in: Antunes, E., Schumann, J., Brodie, G., Jacob, M. V., Schneider P. A., “*Biochar produced from biosolids using a single-mode microwave: characterisation and its potential for phosphorus removal*”, *Journal of Environmental Management* 2017, 196: 119-126.

4.1 Introduction

Biosolids are the partially or totally stabilised solids from the municipal wastewater treatment process [1]. Global population and the proportion of the population that have access to sewage treatment have both been increasing, implying that the production rates of biosolids will continuously increase [31]. For example, in Asia the amount of biosolids is increasing 6.25% per annum, and it is estimated to reach 1 billion tons by 2030 [166]. As the amount of biosolids grows, so too does the pressure to safely and efficiently dispose of these materials. Current methods for biosolids disposal are land application, incineration and landfill [67]. Land application is applying the biosolids to land to utilise its nutrient content as a fertiliser substitute [56], which is a commonly used method, particularly in less developed countries where human waste has historically been applied to crops [31]. Application of these wastes to land potentially exposes the community to pathogens and other contaminants, and biosolids are also a potential source of greenhouse gas emissions [167]. Incineration is commonly used in countries with a shortage of land and is effective at sterilising and reducing the volume and mass of waste [168]. However, this volume reduction concentrates heavy metal contaminants into the leftover ash, and the energy efficiency of this method is heavily dependent upon moisture content [169]. Landfill involves simply storing the waste at a particular location and is simple and easy to implement. This method is not efficient, though, as it does not utilise either the energy or nutrient content of the waste, and with increasing amounts of sludge being produced, the cost to landfill will only increase.

In Australia, as an example, there is no ubiquitous solution to biosolids management, partly due to the differing regulations that govern biosolids disposal in each state. There has, however, been a general trend to more beneficial use of biosolids, rather than disposal. Beneficial use includes disposal methods, such as land application as a fertiliser, forestry, composting, and land rehabilitation, while non-beneficial use includes landfilling, stockpiling and ocean discharge. In the five year period 2008-2013, the annual production of biosolids in Australia increased from approximately 300,000 dry tonnes to 330,000 dry tonnes [170], and during this time, the proportion of biosolids disposed with beneficial use increased from 59% to 69%. The majority of this increase was due to the diversion of biosolids from landfill to land application, particularly in the states of Queensland and New South Wales [170]. Of the 102,000 tonnes of dry

biosolids that were not beneficially used in 2013, 62% was produced by the state of Victoria, with the majority being placed into stockpiles [31]. The current size of the Victorian stockpiles, which have been in use for more than two decades, is estimated at 3.2 million dry tonnes. Environmental regulations and local logistical challenges in developing alternative disposal methods contributed to the need to store the majority of Victorian biosolids, and these same factors inhibit the transition to beneficial biosolids use. For this reason it is necessary to explore alternative management approaches of biosolids, such as microwave assisted pyrolysis (MWAP), so that biosolids can be utilised as a resource in places like Victoria where traditional beneficial use methods, such as land application, are not feasible due to heavy metals and pathogen contaminants.

MWAP is a potential technology for biosolids management. Compared with conventional heating, MWAP uses a microwave field to provide energy for the pyrolysis process. The use of microwave heating has several advantages over conventional heating. In particular, microwave heating is selective, since the microwave field only heats materials that have sufficiently high loss tangent ($\tan \delta > 0.2$), high capacity to absorb microwave energy and transform into heat, and does not heat the pyrolysis atmosphere. At sufficiently small scale, the entire biomass volume is also exposed to the microwave field at once, producing uniform heating throughout the mass for a biomass of homogenous composition. These microwave heating properties are collectively termed “volumetric heating”. Due to these properties of microwave heating, MWAP provides faster heating, better overall efficiency, and a faster and more controllable process compared to conventional pyrolysis [50, 64, 108]. However, biosolids are essentially transparent to microwave irradiation [171]; therefore the addition of a microwave absorber (also known as a susceptor) plays an important role in achieving the temperatures required for pyrolysis [78]. These microwave absorbers work as hot spots, absorbing microwave energy and transferring it as heat to the cooler surrounding material by thermal conduction. Carbon-based materials, including biochar, are often selected as microwave absorbers because of the high value of their loss tangent, and their relatively low cost [70].

Pyrolysis of biosolids offers many advantages, such as: significant reduction in biosolids volume, destruction of pathogens, decreased availability of organic pollutants

and heavy metals, and increased carbon stability of biochar [22]. Biochar is an important fraction of the biosolids pyrolysis by-products, which are biochar, biogas and bio-oil. Biochar produced from biosolids can be used as fertiliser; it contains important nutrients for plant growth, such as phosphorus, nitrogen, potassium and trace amounts of micronutrients. The properties of biochar depend on feedstock characteristics and pyrolysis conditions [22, 36]. Pyrolysis temperature is a key variable with a great impact on biochar properties; for example, specific surface area increases with temperature while lower temperatures can produce hydrophobic biochar [172]. Pyrolysis temperature influences molecular structure, carbonisation and porosity of biochar since these characteristics are strongly linked to temperature of the process. Depending upon its physical and chemical properties, biochar can be applied as a soil ameliorant, improving water retention capacity, pH and carbon sequestration [4]. For example, biochar with macropores of around one micron possess a good water retention capacity; however, micropores do not play a relevant role in the soil or plant growth [172]. More research is needed to completely understand the chemical and physical mechanisms of biochar to take advantage of it in the future [173].

Biosolids management is an environmental problem due to the amount of biosolids produced and the costs associated with its disposal. Recently, research has been developed to use alum sludge as an inexpensive phosphorus adsorbent in wastewater treatment plants [174, 175]. Some researchers claimed that alum biosolids applications can prevent phosphorus run-off from soil; however, heavy metals in the biosolids can leach through the soil and groundwater, which is another environmental problem. Finding a solution with the advantages of phosphorus removal capacity and without heavy metal leaching is ideal. Using biochar for contaminant removal has been studied, particularly metals removal from aqueous solutions [2, 4, 176]. To this point biochar from biosolids for phosphorus removal has not been studied. This study aims to use the biochar produced via MWAP biosolids for phosphorus removal, which is a new approach to beneficial reuse biosolids.

Therefore this study has three main objectives: explore the impact of pyrolysis temperature on biochar properties, examine the MWAP process with focus on the challenges and peculiarities of single-mode microwave fields, and perform tests on

phosphorus adsorption with biochar produced at different temperatures, compared against untreated biosolids phosphorus removal capacity.

4.2 Materials and Methods

4.2.1 Materials

Biosolids were extracted from clay settling ponds at a sewage treatment facility (Euroa Wastewater Treatment facility in Victoria, Australia), stored for one month and used in the laboratory experiments. To minimise inconsistencies, a 10 kg lot of biosolids was blended to obtain a homogenous sample. The homogeneous lot was stored in a sealed container in a refrigerator at 4°C to minimise bacterial activity. Using the cone and quarter method, three random samples were taken for characterisation. The main properties of the biosolids are presented in Table 4.1 and Table 4.2. Activated carbon, obtained from Sigma Aldrich (Ref. 242276), was used as a microwave susceptor in all experiments.

4.3 Methods

4.3.1 Pyrolysis experiments

The microwave assisted pyrolysis tests were carried out in a customised single-mode microwave chamber connected to a 1.2 kW microwave source (Figure 4.1). The microwaves produced by the magnetron travel through the flanged wave guide to a circulator, which diverts any reflected (*i.e.* returning) microwave power into an electromagnetically matched water load. A microwave directional coupler, which allows forward and reflected power to be measured, and a three stub tuner, which matches the impedance of the wave guide segments to the load, directs the microwaves into the single-mode chamber. The microwave coupler segment allows a small portion of the forward and reflected power to be diverted to a power meter where it is amplified and measured; the ratio of the diverted power to the actual power is 1:10^{7.8} for this coupler, which represents an insignificant loss. During the experiment, a thermocouple was positioned in the centre of the sample, within the single-mode chamber, to measure the sample temperature. Pyrolysis temperature was monitored by a shielded type K

thermocouple connected to an Arduino board, and recorded every 500 milliseconds. The pressure in the microwave chamber was manually controlled by an inline needle valve between the cold water trap and the vacuum pump.

The microwaves enter the pyrolysis chamber from below through a quartz disc that also acts as a process seal for the pyrolysis chamber. The pyrolysis chamber is a cylindrical section of mild steel pipe with a volume of 1.17 L; the chamber is sealed at the top with a flanged lid that has connections to allow nitrogen in-flow, an insertion thermocouple to sense the sample temperature, and a connection for pyrolysis product gas removal. The pyrolysis gases are removed using a vacuum pump, and the pressure inside the vessel is monitored with a pressure gauge. The gases were contacted with dichloromethane in a glass column, where the soluble gases dissolve and gases with higher boiling points condense. Dichloromethane was selected as it can dissolve a wide range of polar and nonpolar organic compounds. Gases that do not dissolve or condense are condensed in a cold water trap, preventing damage to the vacuum pump and reducing environmental impact. The amount of condensed oils in the cold water trap was typically very low and the analysis of these oils was not considered in this study.

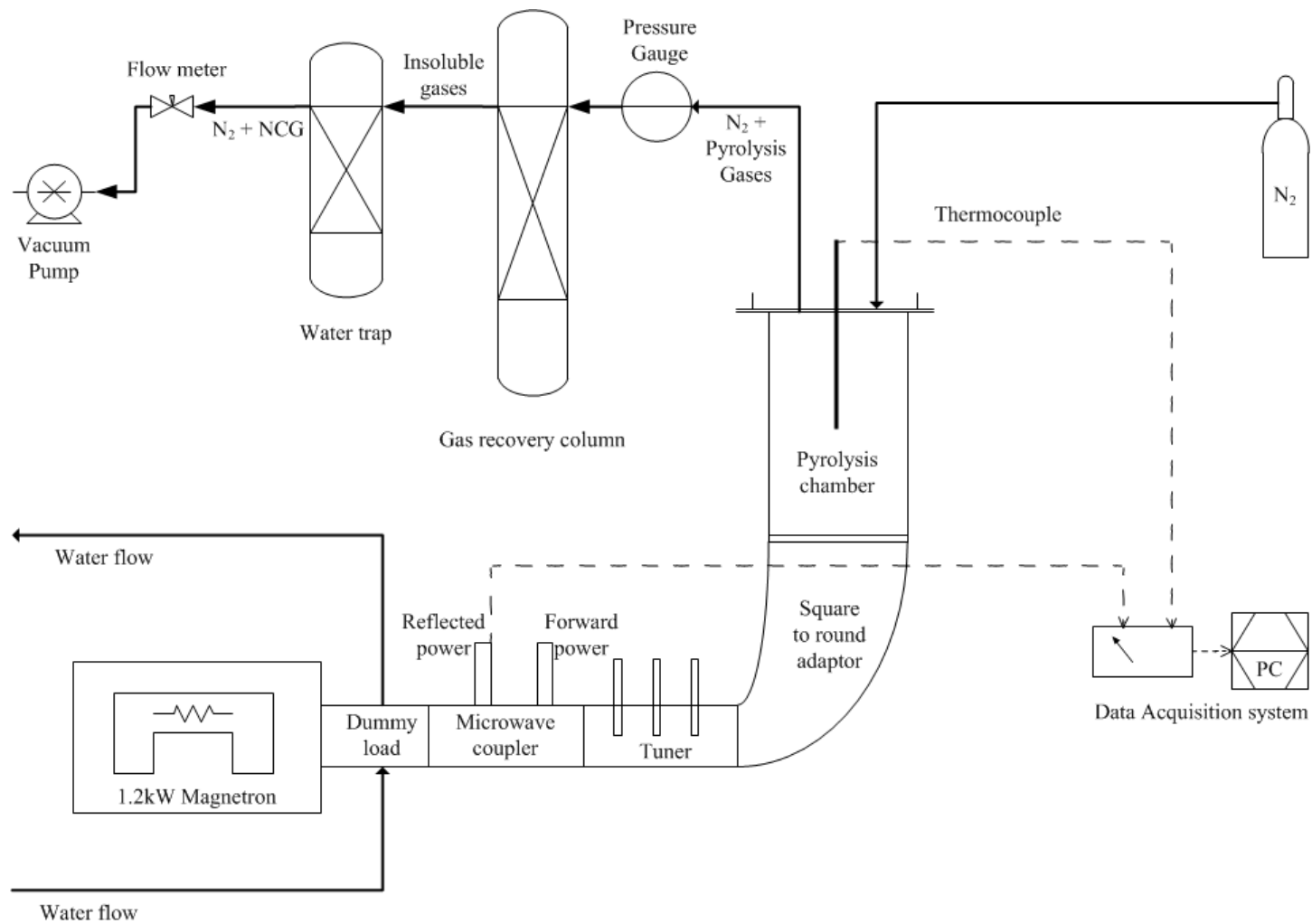


Figure 4.1 – Schematic of the single-mode microwave system used in this research.

Two series of samples (nominal mass of 63.0 ± 1 g (wet basis)) were prepared. Each sample was loaded with activated carbon at 10 wt% of the dry weight of biosolids. The biosolids and the activated carbon were blended in a coffee grinder for 20 seconds to obtain a uniform distribution of the activated carbon. These samples were placed into a quartz beaker (volume: 150 ml) inside the MWAP chamber. The chamber was purged with 11 L/min of nitrogen (99.9% purity) for 40 seconds before the needle valve was opened and the pressure lowered to -15 kPa gauge pressure. The nitrogen flow rate of 11 L/min corresponds to a mean residence time of 6.38 seconds for the nitrogen in the pyrolysis chamber, so a purge time of 40 seconds was sufficient. At the start of the pyrolysis, the magnetron output power was set to 600 W to allow for rapid, but controlled heating of the sample and eventual removal of sample moisture. Once the target temperature was reached, the output power of the magnetron was manually adjusted to keep the sample temperature as close as possible to set point ($\pm 15^\circ\text{C}$). The control valve was manually adjusted to maintain the pressure within the chamber around -15 kPa gauge pressure.

Biosolids samples were pyrolysed at different temperatures between 300°C and 800°C for approximately 10 minutes. After the magnetron was turned off, the pyrolysed sample was immediately removed and placed into a desiccator. The biochar samples were characterised according to the methodology described in the following sections. Each experiment was repeated twice, and the results presented are the average of these two experiments.

4.3.2 Proximate analysis

Proximate analysis was carried out using a conventional oven and a balance with a resolution of 0.1 mg. To assure the reproducibility of the measurements, each sample was checked at least twice and final values presented are the average. Before the moisture determination, crucibles were placed in the oven at 105°C for one hour. These crucibles were cooled in a desiccator for one hour. The cooled crucibles were weighed and approximately one gram of material was placed in the crucible. Samples were then initially weighed, heated at 105°C for two hours and cooled in a desiccator for 1 hour. The samples were re-weighed and the moisture content was determined according to equation (4.1):

$$\text{Moisture (\%)} = \frac{A - B}{A - C} \times 100\% \quad (4.1)$$

The ash mass percentage was determined by heating the dry sample at 600°C in a conventional oven. Approximately one gram of dry sample was weighed and placed in a ceramic crucible, weighed, and heated at 10°C/min to a final temperature of 600°C for six hours. After the furnace cooled, samples were removed and placed in a desiccator. Samples were weighed after cooling in a desiccator for one hour, and ash content was calculated according to the equation (4.2):

$$\text{Ash(\%)} = \frac{B - C}{A - C} \times 100\% \quad (4.2)$$

The determination of volatile matter consists of thermal treatment of a dry sample at 500°C for one hour, after which the sample was cooled in a desiccator for one hour then weighed. The volatile matter mass percentage was calculated according to equation (4.3):

$$\text{Volatile matter(\%)} = \frac{A - B}{A - C} \times 100\% \quad (4.3)$$

where B is the weight of crucible plus mass of material after thermal treatment, A is the mass of crucible plus mass of initial material, and C is the mass of crucible.

4.3.3 Biochar yield

Biochar yield was determined according to equation (4.4):

$$\text{Biochar yield} = \frac{BC - AC}{F} \quad (4.4)$$

where F is the weight of dry biosolids, BC is the weight of dry biochar, and AC is the weight of the carbon used as a microwave absorber.

4.3.4 pH

A solution, consisting of one gram of dry material in 20 ml of deionised water, was prepared and shaken in an ultrasonic bath for 90 minutes to ensure contact between the material and water. Then pH measurements were carried out with an Orion 5-Star Plus pH meter by using a pH 8175 BNWP probe. All measurements were done in triplicate after the instrument calibration.

4.3.5 Specific surface area

Biochar specific surface area was determined using a Micromeritics TriStar 3000 gas adsorption analyser. Around 0.2 g of material was used for each run and all samples were analysed at least two times. Prior to the analysis, all samples were degassed under vacuum overnight at room temperature, followed by one hour at 250°C.

4.3.6 Thermogravimetric analysis

Thermogravimetric analyses were conducted to understand thermal decomposition and mass loss at different temperatures of the biosolids and biochar. A Mettler Toledo TGA/SDTA851e thermogravimetric analyser was used for thermal analyses. All the thermal experiments were carried out under nitrogen atmosphere (nitrogen flow rate was 30 mL/min) between 25 to 1000°C with a heating rate of 10°C/min.

4.3.7 Chemical analyses

Biosolids and biochar samples were dried in a conventional oven at 100°C, and then were ground to obtain powder with particle size lower than 75 microns to perform the chemical analyses. Fourier transform infrared (FTIR) analysis was conducted to identify the chemical functional groups present in biosolids and in biochar obtained at different processing temperatures. A Perkin Elmer Spectrum 2000 FTIR Spectrometer was used to carry out the analyses for wavenumbers between 650 and 4000 cm^{-1} .

The concentration of heavy metals was determined by inductively coupled plasma - mass spectrometry (ICP-MS), using a Varian 820-MS Mass Spectrometer. Before analysis by ICP-MS, the samples were digested using microwave digestion, using nitric acid and hydrogen peroxide.

Crystalline structures present in biosolids and biochar were identified using the X-ray diffraction technique (Bruker Phaser D2 X-ray Powder Diffractometer, Cu radiation). The XRD spectrum was obtained from 5 to 65 degrees with a scan step size of 0.02 degrees and time step of 1 second.

4.3.8 Phosphorus adsorption capacity

Phosphorus adsorption capacity of biochar and biosolids was tested using batch tests at room temperature ($22^\circ\text{C} \pm 2^\circ\text{C}$). Phosphorus stock solution was prepared by dissolving potassium dihydrogen phosphate (KH_2PO_4) in distilled water. One gram of dry material was added to 100 ml of phosphate solution with a concentration of 1500 mg-P/L, this mixture was continuously agitated at 350 RPM. After 24 hours of reaction time, the mixture was filtered using a 0.45- μm membrane and the phosphorus in the supernatant was analysed by inductively coupled plasma atomic emission spectroscopy (ICP-AES). The phosphorus adsorbed by biochar and biosolids, Q_e in mg/g, was calculated by using equation (4.5):

$$Q_e = \frac{(C_0 - C_e) V}{m} \quad (4.5)$$

where, C_0 and C_e are the initial and equilibrium phosphate concentrations respectively (mg/L), V is the volume of P-stock solution (L) and m is the mass of adsorbent (g).

4.4 Results and discussion

4.4.1 Biosolids chemical composition

The chemical composition of the biosolids is presented in Table 4.1, indicating that cadmium and mercury were lower than 1 mg/kg. A more comprehensive chemical analysis of biosolids can be found in Appendix (Table A2). This biosolids sample was classified contaminant grade C2, according to the Guidelines for Environmental Management of the State of Victoria, Australia, because of the higher concentrations of copper, selenium and zinc [177]. The phosphorus amount in this biosolids sample is lower than the global average (1.5 – 3.0%) and is considerably lower when compared with the national average in Australia (2.5%) [28, 164]. However, phosphorus content depends on various factors, such as food habits and previous wastewater treatment steps. Extended ageing times may decrease the phosphorus content, due to the leaching susceptibility of phosphorus. The biosolids sample contains around 1.5% (dry basis) of micronutrients, which can be beneficial for land application as a fertiliser. The amount of aluminium (62,300 mg/kg) is high due to the use of aluminium salts in the wastewater treatment process to induce precipitation of phosphorus and due to the use of a clay lined settling lagoon. This aluminium content may prevent biosolids land application due to the toxic effects on plant growth in acid soil and also because aluminium can inactivate phosphorus through its precipitation in plant roots. This precipitation makes phosphorus unavailable for the plant metabolic process, decreasing plant growth and development [178, 179].

Table 4.1 – Chemical composition of biosolids determined by ICP.

Classification	Nutrients					Heavy metals				
Element	Ca	Fe	Mg	P	K	Cr	Cu	Ni	Pb	Zn
(mg/kg)*	6142	18995	1895	13300	1910	52.9	236	24.7	24.3	548

* Values on dry weight basis

4.4.2 Biosolids proximate and ultimate analyses

The non-mineral composition and proximate analysis of biosolids are presented in Table 4.2. The percentage of ash is slightly higher than the values found in the literature while the amount of fixed carbon is six times lower [180]. These differences can be due to the use of different wastewater treatment methodologies, as well as the ageing process of biosolids. The percentage of non-minerals in biosolids agrees with values found in the literature [180]. Biosolids from this source could be an interesting feedstock for biochar production using microwave pyrolysis, as a high yield of biochar is expected due to the lower amount of volatile organic compounds.

Table 4.2 – Proximate and ultimate analyses of the biosolids.

Proximate analysis (%)				Ultimate analysis (%)*				
Moisture	Volatiles*	Ash*	Fixed Carbon*	C	H	N	S	O**
50.0	43.5	55.5	1.0	19.9	3.5	2.2	1.0	17.8

* Values on dry weight basis; ** Calculated by mass difference.

4.4.3 Thermogravimetric analysis

To understand the thermal decomposition of biosolids, thermogravimetric analysis (TGA) was conducted and is represented in Figure 4.2. Thermal decomposition of

biosolids exhibits two main peaks with maximum mass loss rates of around 330°C and 420°C. The simultaneous TGA/FTIR analyses suggest that the first peak corresponds to water and carbon dioxide release and the second peak corresponds to carbonisation involving C-H stretching, methane and ammonia release. Further, the maximum mass loss occurs between 280°C and 500°C, which corresponds to approximately 60% of total mass loss.

Figure 4.3 is an example of the temperature profile obtained from experiments, showing five different stages of pyrolysis. The first stage has a high heating rate of 3.2°C/s due to the presence of water, which is a very good microwave absorber. The second stage is a plateau and corresponds to the water evaporation. In the third stage, the material is heating up very slowly (0.8°C/s) due to the poor dielectric properties of the dry material. The heating rate of the fourth step, between 240°C and 280°C, is also very slow (0.6°C/s) and corresponds to the evaporation of bound water, which was confirmed by the simultaneous thermal analysis. The fifth step has the second highest heating rate (2.4°C/s) due to the formation of char, which acts as a microwave absorber and increases the heating rate of the sample.

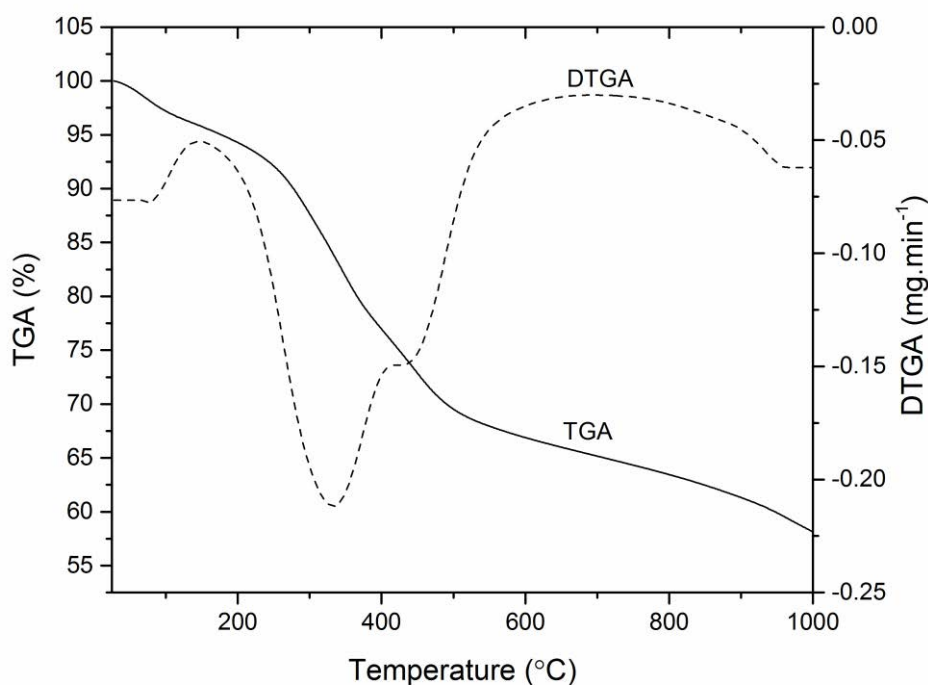


Figure 4.2 – Thermogravimetric analysis of biosolids.

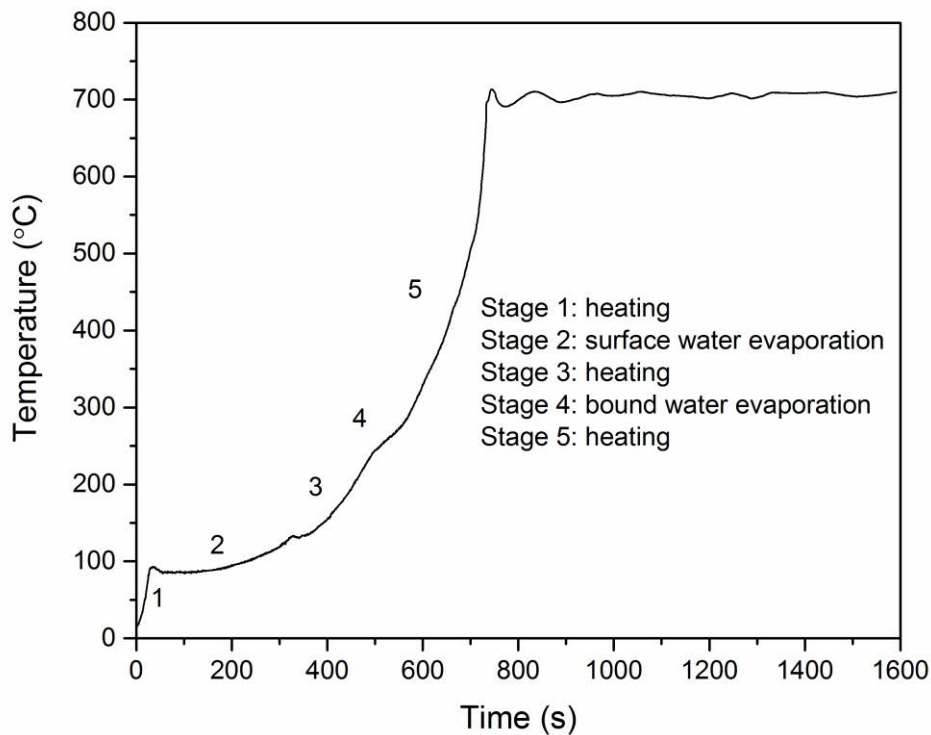


Figure 4.3 – Temperature profile of biosolids MWAP.

Measuring and controlling temperature in a microwave field are key challenges in MWAP. A shielded type K thermocouple was selected to measure the temperature in the sample. This device can deliver measurements that are representative of the sample bulk temperature [65]. Since a thermocouple can act as an antenna in a microwave field, leading to self-heating, experiments were carried out to find the position where microwave irradiation had the least impact on thermocouple self-heating. Manual control of input microwave power combined with thermal inertia of the pyrolysis process, meant that the temperature had a maximum deviation of $\pm 15^{\circ}\text{C}$ from the set-point for all experiments. Moreover, during the heating process, the dielectric properties of the samples were very likely changing, since they are functions of temperature and material properties, making control rather difficult. For example, the char formation above 300°C enhances microwave absorption; consequently leading to higher heating rates and commensurately faster reaction rates.

4.4.4 Biochar yield

The biochar yield was assessed in samples pyrolysed at different temperatures. These yield values are the mean of two experiments and were calculated on the dry basis of feedstock and biochar. The data represented in Table 4.3 show that biochar yield decreases with increasing pyrolysis temperatures. Higher temperatures lead to lower biochar yields due to higher decomposition rates of volatile organic matter and reactions between carbon, CO₂ and H₂O. The biochar yield obtained in this work was more than three times higher than biochar yield from sewage sludge due to the higher concentration of inorganic compounds and lower volatile organic content in biosolids [67]. The char yield ranges between 35 and 80 % (dry basis), it depends significantly on biosolids composition [53]. The volatile organic content in biosolids is the variable that more affects the pyrolysis by-product yields. Volatile organic matter varies between 35 (biosolids) and 85% (primary sludge), as the sewage sludge is processed the organic matter is decreasing and biosolids is the material with less organic content [181]. The biosolids used in this study contains lower volatile organic matter because of the loss of organic matter during pre-treatment stages and stabilisation, and also because this sample was stockpiled for more than 2 years. The high concentration of inorganic compounds changes the bond dissociation energy between organic and inorganic matter, and decreases the release of volatile organic matter, consequently increasing biochar yield [4]. A comparison between biochar yield from biosolids and biochar yield from sewage sludge was made in this research because there is limited data in the literature about yield of biochar obtained via microwave pyrolysis of biosolids.

However, the biochar yield obtained from microwave pyrolysis tests is higher than expected from the TGA analysis. The main reason for this difference is because TGA only requires a small sample (mg) while our pyrolysis tests were carried out with a larger sample (approximately 63 g), which makes volatile organic matter transport more difficult from the core to the surface of the sample. For example, the biochar yield from 50 g of biosolids, pyrolysed at 600°C, was 0.74, which is much lower than the yield of the 63 g of biosolids sample (0.85) and closer to the TGA analysis. As the sample mass increases, surface heating is more significant compared to the core heating of the sample, therefore the rest of the sample is heated by conduction, which requires more

time than by microwave heating [182]. These results showed how important is to identify the area where the microwave field strength is high to optimise the interaction between microwaves and samples.

Table 4.3 – Summary of biochar yield and properties.

Pyrolysis temperature (°C)	Biochar Yield	Volatiles (%)	Ash (%)	pH	BET (m ² /g)
Biosolids	-	43.5	55.5	6.13	16.64
300	0.91	37.7	55.8	6.42	50.06
400	0.90	37.2	57.2	6.44	51.57
500	0.88	37.4	58.3	6.34	51.89
600	0.85	35.2	59.1	6.40	51.39
700	0.82	33.5	62.4	6.50	60.86
800	0.77	25.0	63.3	6.60	64.67

In a single-mode microwave chamber, the sample position plays a crucial role in the dielectric heating process. Single-mode microwave chambers have one electromagnetic field concentrated in one region [183]. Therefore, locating the sample in this “hot spot” is critical. Also the sample size and the dielectric properties of the sample can significantly change the microwave field strength and its distribution [184]. Numerical simulations were performed to assess the impact of biosolids sample on microwave field strength and distribution, by solving the Maxwell’s electromagnetic equations in three dimensions using finite-difference time-domain (FDTD) method using Inventor Professional 2015 software (AutoDesk Co., USA). The model was exported into XFDTD software, version 7.5.1.3.r43518 (Remcom Co., USA). The materials and microwave feed ports were defined in XFDTD and the simulations for the chamber, in both empty and loaded conditions, were run for 10,000 iterations. The biosolids sample changes the microwave field strength, but impacts only slightly on the electric field distribution, due

to the poor dielectric properties (Figure 4.4). These results show that samples were placed in the main peak of the electric field distribution, which is ideal for processing of the samples and for minimising the variance between experiments. Also to minimise the variance between experiments, mass and volume of sample were kept constant as much as possible and the same quartz vessel was used in all experiments.

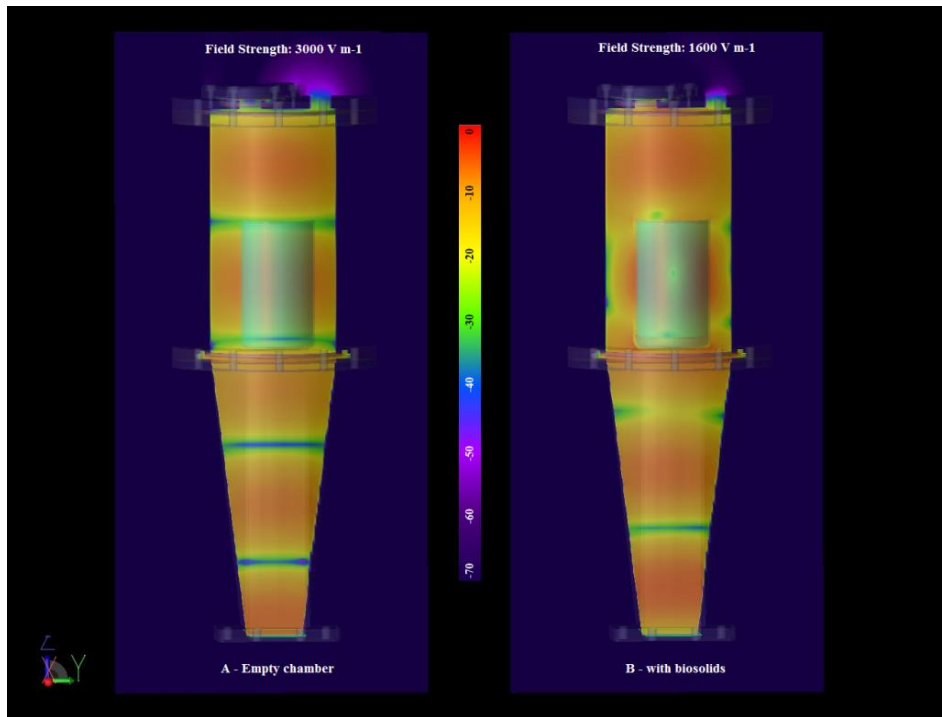


Figure 4.4 – Microwave field intensity and distribution in empty chamber and with biosolids.

4.4.5 Volatiles, ash content, pH of biochar

The percentage of volatile organic compounds, ash content and pH of biosolids (feedstock) and biochar obtained at different pyrolysis temperatures are shown in Table 4.3. In general the ash content in biochar increased slightly with increase of pyrolysis temperature due to the better carbonisation achieved at higher temperatures. The volatile organic content was approximately constant for a pyrolysis temperature lower than 500°C; however, it decreased with a temperature rise above 500°C. This is a logical relationship, as a greater amount of the biosolids sample is volatilised at the higher

temperature, therefore the volatiles percentage decreases while the ash content increases.

The pH of biochar is slightly higher than the pH of biosolids. For pyrolysis temperatures lower than 600°C, the pH is around 6.40, but it increased slightly with of pyrolysis temperatures above 700°C. Recent research on biochar production from sewage sludge has demonstrated that the pH of biochar increases significantly with the rise of pyrolysis temperature, producing alkaline biochar above 500°C [4]. This pH behaviour was not observed in this study since the stabilisation of sewage sludge to biosolids may induce chemical changes in the feedstock, and the lower volatile organic content in biosolids is an explanation for the slight increase of pH with rise of pyrolysis temperature. This was confirmed by FTIR of biosolids and biochar (Figure 4.5), which demonstrated a significant difference between biosolids and biochar functional groups, while as the temperature increased, no significant changes in biochar were observed with FTIR.

4.4.6 Biochar specific surface area

Surface area of biochar is an important characteristic particularly for adsorption and land application. Biochar surface area affects the interaction of biochar with soil, higher surface area and porosity are associated with higher water and cations retention [164]. In terms of adsorption, biochar with high surface area exhibits higher adsorption capacity due to higher surface for chemical and physical adsorption. The specific surface area values of biochar samples pyrolysed at different temperatures are presented in Table 4.3. The results show that surface area of biochar is significantly higher than the original biosolids. Specific surface area of biochar is roughly constant (around 51 m²/g) for pyrolysis temperatures between 300°C and 600°C; however, between 600°C and 800°C, it increases 26%. Previous studies demonstrated that BET increased with pyrolysis temperature due to volatile organic matter releasing under 500°C, which was recognized as the main reason for porosity and BET rise [185]. The main reasons for difference between this study results and others findings were the high biochar yield and the low volatile organic content in biosolids. The increase in surface area with pyrolysis temperature is due to chemical and physical changes occurring during pyrolysis, for example, the release of volatile organic compounds creates more micro and mesopores, which increases the surface area of the biochar material [67, 180]. In

addition, volumetric heating, a characteristic of microwave heating, favours the decomposition of volatile organic matter due to the increase of the pressure inside of particles, increasing the number of small pores, and consequently increasing the specific surface area of biochar [4, 185]. The heating rate is also an important variable affecting surface area, which impacts on the rate of volatile organic formation. Due to decomposition rate of volatile organic and pore formation, the initial chemical and physical properties of the biosolids feedstock also impact upon the biochar surface area.

4.4.7 Chemical analysis of biosolids and biochar

The results of the FTIR analyses of the original biosolids and the biochar pyrolysed at different temperatures are represented in Figure 4.5. These results show that the majority of the functional groups present in biosolids are not present in the biochar samples, especially at pyrolysis temperatures above 600°C. The hydroxyl groups (3302 cm^{-1}) present in biosolids were not identified in the biochar samples, suggesting that these groups are very unstable and decompose during pyrolysis [87]. The peaks at 2920 cm^{-1} and 2853 cm^{-1} correspond to aliphatic bonds and are present in biosolids and only in the biochar sample prepared at 300°C. These aliphatic bonds decompose into gases such as methane, ethane and carbon dioxide, and consequently, the mass loss of the material will increase while the gas fraction yield increases [36]. These results align with the TGA/FTIR analysis, which indicated that carbon dioxide and methane are releasing around 300°C and 450°C, respectively. The peaks around 1644 cm^{-1} correspond to amide bonds; these bonds are unstable and break down at elevated temperatures, so are only present in biosolids and biochar samples produced below 400°C [87]. The strongest peak approximately at 1037 cm^{-1} in biosolids and biochar is attributed to the stretching of C-O functional group [186]. The intensity of this peak is much higher in biosolids than in biochar, and its intensity decreases significantly in biochar produced at temperatures higher than 400°C due to the carbonisation of the biochar.

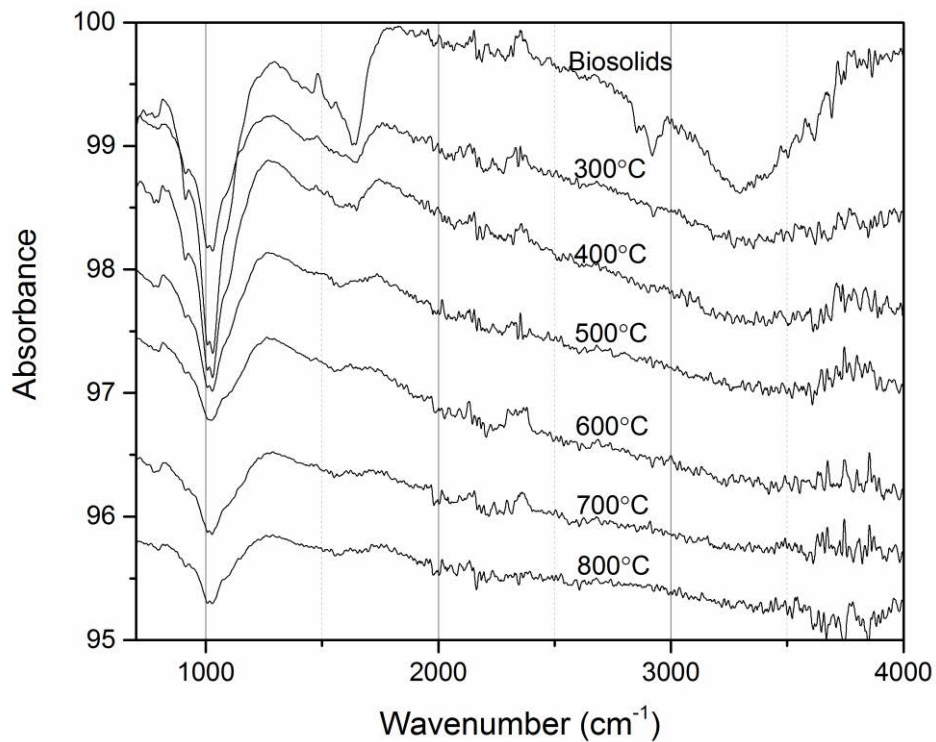


Figure 4.5 – FTIR spectrum of biosolids and biochar obtained at different temperatures.

While the FTIR analyses indicated changes in organic composition of biosolids and biochar, the inorganic structure did not change with pyrolysis temperature, as demonstrated in XRD represented in Figure 4.6. These results demonstrated that the crystalline structure of biochar is very similar to biosolids, where quartz is the main crystalline phase, which likely came from the clay ponds used in the wastewater treatment. Increasing pyrolysis temperature does not impact significantly on the phase structure of biochar; 800°C is not enough to rearrange and form new inorganic products. The XRD spectrum has some background noise due the presence of organic matter in the samples, but this tends to decrease with a pyrolysis temperature rise.

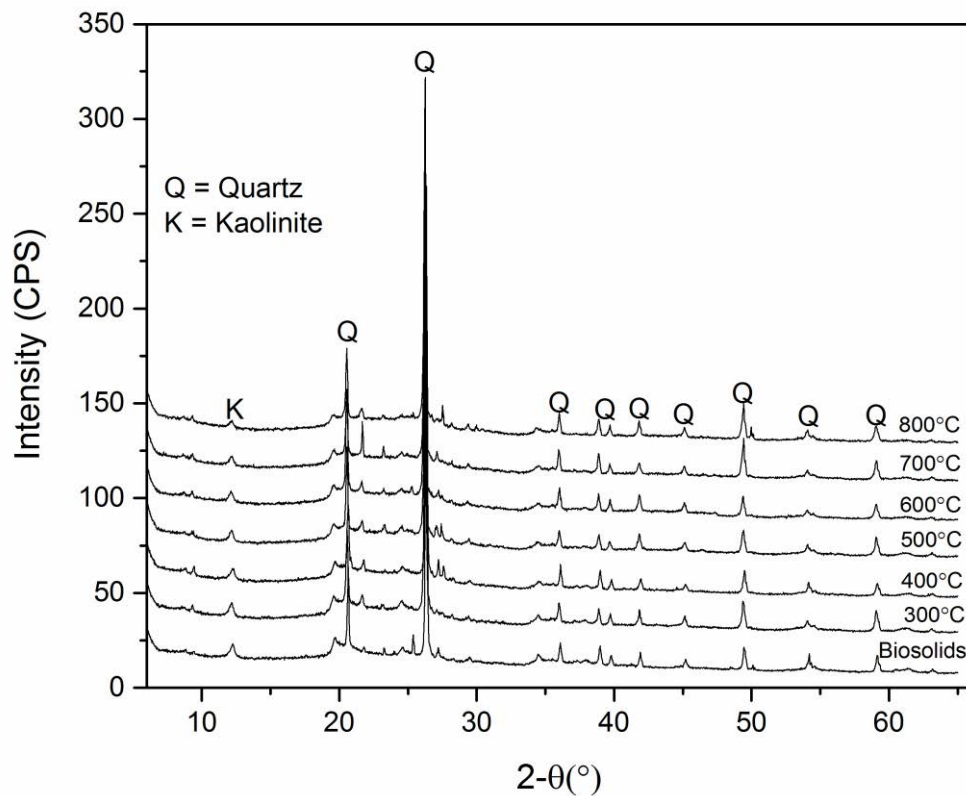


Figure 4.6 – XRD spectrum of biosolids and biochar obtained at different temperatures.

Chemical composition (Table A1) was assessed by ICP-MS for different pyrolysis temperatures and results showed that all nutrients, heavy metals and other elements were fully recovered in the biochar. These final values are in line with the mass balance calculations based on initial feedstock composition and mass loss during pyrolysis. The heavy metal content in biochar is below the maximum allowed thresholds indicated by the international biochar standards, which would make this product acceptable for land application [187].

4.4.8 Phosphorus adsorption by biochar and biosolids

Activated carbon was tested using the same conditions of biochar and the phosphorus adsorption capacity of activated carbon was around 2.2 mg/g while with biochar varied between 13.7 to 16.4 mg/g. The phosphorus adsorption capacity was affected by the pyrolysis temperature, it decreased from 16.4 mg/g (300°C) to a minimum of 13.7 mg/g with biochar produced at 500°C, then it increased up to 16.4 mg/g (800°C). The increase after 500°C can be explained by the increase of the specific surface area of the

biochar, which is a key variable in adsorption mechanisms. The decrease on phosphorus removal capacity by biochar observed from 300°C to 500°C may have resulted from the decrease of the electrical conductivity of biochar. The main process of phosphorus removal by biochar is complexation of phosphate species with divalent cations such Al, Ca, Fe and K. As the pyrolysis temperature increases the availability of these divalent cations is decreasing, which was reflected on the measurements of electrical conductivity (EC). The electrical conductivity of biochar depends on cations exchange and carbonisation, but in this temperature range (300 to 500°C) the carbonisation did not contribute to the increase of EC due to the lower carbon content in this biosolids. However, the phosphorus adsorption capacity of this biochar is higher than results reported in the literature of unmodified biochar [99]. The phosphorus adsorption capacity can be explained by the presence of Al, Fe and Ca ions, which favour phosphorus removal by precipitation. When these elements were removed by an HCl solution, the treated biochar did not remove any phosphorus from aqueous solution, which demonstrated that the key mechanism of phosphorus adsorption by biochar is mainly precipitation.

Phosphorus removal capacity of biochar is similar to biosolids (17.1 mg/g); however, using biochar for phosphorus removal from an aqueous solution has many advantages over biosolids. Heavy metals within the biosolids can leach through soil, which can represent a serious threat to human health through food chain. As demonstrated by previous studies, the heavy metals present in biochar are not bioavailable [188]. Therefore, using biochar for phosphorus removal and then use this final material for land application can be a sustainable solution for biosolids management and phosphorus recycling. Also, biochar land application has many benefits: improving soil structure, soil fertility and water retention, which increases crop production [2].

4.5 Conclusions

This study showed that MWAP is a potential solution for biosolids management, since the biochar produced from biosolids meet the requirements of biochar guidelines, therefore can be used for land application. The results from this research showed that as the pyrolysis temperature increases, the biochar yield and volatile organic content decrease, while the ash content increases with temperature. Specific surface area was

the property most affected by pyrolysis temperature. In contrast, pyrolysis temperature does not have a significant impact on pH and crystalline phases of biochar. Pyrolysis temperature affected the organic composition of materials while the inorganic elements were concentrated in biochar, and no volatilisation was observed in the elements analysed in this project. In terms of phosphorus adsorption, the biochar exhibited a similar phosphorus adsorption capacity of biosolids, approximately 15 mg/g, which is almost seven times higher than the activated carbon. This study also demonstrated that MWAP scale-up should be done with care due to the difficulties on heat and mass transport within larger samples.

5 PHOSPHORUS RECOVERY FROM AQUEOUS SOLUTION BY Ca-DOPED BIOCHAR

Abstract

Phosphorus (P) scarcity and eutrophication have triggered the development of new approaches for phosphorus recovery. This study investigated the impact of calcium-doped biochar, produced via microwave assisted pyrolysis at 700°C for 20 minutes, on phosphorus recovery. The phosphorus removal isotherms, removal kinetics and the impact of initial pH of phosphorus stock solution on phosphorus recovery were studied. The phosphorus recovery was proportional to the calcium content in biochar, leading predominantly to the production of brushite. Precipitation was the main mechanism of phosphorus removal by calcium-doped biochar. Phosphorus removal capacity of biochar reached equilibrium after 8 hours of contact time and was described by a pseudo-second-order kinetic model. The Langmuir isotherm model fitted the experimental data well with a maximum adsorption capacity of 147 mg-P/g for biochar BC20 (20 wt% Ca(OH)₂). Using Ca-doped biochar for P-removal is a promising alternative for phosphorus recovery from contaminated streams as well as for biosolids management.

Keywords: biosolids; brushite; Ca-doped biochar; phosphorus recovery; precipitation.

Highlights

- Initial pH of phosphorus stock solution played a key role on phosphorus recovery.
- Phosphorus removal capacity was proportional to the calcium content in biochar.
- Precipitation was the main mechanism for phosphorus removal by biochar.
- Brushite was the main compound formed during the phosphorus removal process.

As submitted in: Antunes, E., J., Brodie, G., Jacob, M. V., Schneider P. A., “*Phosphorus recovery from aqueous solution using Ca-doped biochar: removal mechanisms and the potential for a slow release fertiliser*”, Korean Journal of Chemical Engineering.

5.1 Introduction

Phosphorus (P) is a fundamental element for all living organisms, and one of the three main elements (phosphorus, nitrogen and potassium) in fertilisers. Currently, the phosphorus incorporated in industrial fertilisers is extracted from phosphate mines, which are a finite source of phosphorus. Economic phosphate reserves may be exhausted in the next 50 to 100 years, and just a few countries, such as Morocco, China and the US, control the majority of these phosphate reserves [41]. However, the near monopoly of the phosphate reserves by Morocco and the political instability in this region may affect international trade of phosphorus and could negatively impact on food production in phosphorus importing countries. On the other hand, phosphorus can be a pollutant in water streams because it triggers algae growth, consequently causing eutrophication. Currently, eutrophication reduction has been achieved through the use of massive amounts of Al, Ca, and Fe salts in wastewater treatments plants, which increase the amount of sludge production [189]. These two drivers - phosphorus scarcity and pollution - have created the necessity of developing new methods for phosphorus recovery. Phosphorus recycling is a potential solution for meeting the increased global need for phosphorus, while stemming flows that would otherwise cause eutrophication. Several approaches have been tested for phosphorus removal/recovery: crystallisation, ionic exchange, precipitation, adsorption, and biological phosphorus removal [190, 191].

In the last two decades, the number of technologies for phosphorus recovery from wastewater streams has increased significantly. For example, in Europe the number of phosphorus recovery processes from wastewater was only 2 in 1998 while in 2014 it was 22 [192]. Chemical precipitation is a well-established method, but it is expensive due to the chemical consumption and it produces a large amount of sludge, which creates a new environmental problem of sludge disposal due to pathogens, heavy metals, micro-pollutants and other hazardous materials in the sludge [193]. The biological phosphorus removal method uses microorganisms for phosphorus removal from the liquid, which has lower operational costs compared with chemical precipitation, and there is no need for chemicals [194]. Crystallisation, using hydroxyapatite ($\text{Ca}_5(\text{PO}_4)_3\text{OH}$) and struvite (MgNH_4PO_4), has many advantages over precipitation, including: lower overall costs and reduced sludge production [24, 195].

Both products, hydroxyapatite and struvite, are slow release fertilisers, which are potential substitutes for industrial fertilizer produced from phosphate rock [196]. Also, hydroxyapatite and struvite have low solubility in water, thereby contributing to a better and efficient use of phosphorus and reducing eutrophication of water streams [196].

Phosphorus removal using a low cost adsorbent, such as biochar, has been gaining attention as a potential method for phosphorus recovery/recycling because of its adsorption capacity. Biochar is able to reduce phosphorus content in water streams to levels that are lower than the environmental requirements for phosphorus discharge. Biochar is a porous carbon-based material produced from biomass waste via the pyrolysis process [4]. Recently, biochar produced from numerous biomass wastes, such as corn straw, pinewood, rice husk and sugarcane bagasse, has been studied for organic and inorganic contaminant removal from aqueous solutions [2]. Phosphorus removal from aqueous solutions using biochar has been successfully explored by several researchers [15, 99, 197]. In general, unmodified biochars have low phosphorus removal capacity due to its negatively charged surfaces [99, 198]; however, the adsorption capacity of this low-cost adsorbent can be enhanced by several surface modification methods: chemical activation with metal chloride salts and potassium hydroxide, physical activation with steam and carbon dioxide, and surface activation with hydrogen peroxide [199]. Recent studies have demonstrated that modifying biochar with MgO, AlOOH, Fe and KOH enhanced significantly the phosphorus removal capacity of biochar [15, 17, 176, 197, 200]. Biochar for pollutants removal/recovery from aqueous solutions has been studied, but the subsequent valorisation of this material, such as fertilisers, catalysts, metal and biologically activated composites, is not yet well explored [201].

The use of biochar for phosphorus removal and subsequent land application of the final material has several advantages. First the biochar works as a carrier for phosphorus compounds. Second, biochar is well-known as a soil ameliorant, enhancing water retention and sequestering carbon, while improving plant growth [100, 202]. Third, biochar increases soil pH avoiding the application of agricultural lime, usually as calcite or dolomite. Agricultural lime has severe impacts on the environment, such as contamination of groundwater with Ca^{2+} due to its leaching through the soil, and CO_2

emissions to the atmosphere from the decomposition of carbonates and production process [203].

In this study, calcium hydroxide was selected as a dopant for biochar production because there is a need to obtain an alkaline biochar that will avoid the addition of agricultural lime to neutralise soil acidity, and to increase the phosphorus removal capacity of biochar [100]. The approach of this study may also hold favour, since wastewater treatment plants use lime to precipitate phosphorus and to improve sludge filterability. Therefore, this work had three main objectives: first, examine the impact of calcium content in biochar on phosphorus removal kinetics and isotherms; second study the effect of initial pH of P-stock solution on phosphorus removal capacity by biochar; and third investigate the mechanism of phosphorus removal by biochar.

5.2 Materials and Methods

5.2.1 Biochar preparation

Biosolids with approximately 40% moisture content were collected from clay settling ponds at a sewage treatment facility (Euroa Wastewater Treatment facility in Victoria, Australia). These biosolids were blended in a grinder with varying amounts of calcium hydroxide ($\text{Ca}(\text{OH})_2$) and 10 wt% (dry basis of biosolids) of activated carbon. To obtain mixtures with comparable pyrolysis behaviour, water was added to the calcium hydroxide mixtures to maintain the same water content across all samples. Subsequently, these mixtures ($80.0 \pm 0.5\text{g}$) were pyrolysed at 700°C for 20 minutes. The microwave assisted pyrolysis (MWAP) experiments were carried out in a custom made single-mode microwave chamber fed from a 2.45 GHz microwave generator [13]. The applied microwave power was 720 W until the temperature set-point (700°C) was reached and then manually adjusted to keep the temperature constant for 20 minutes. The temperature was measured by a shielded type K thermocouple placed in the middle of the sample. Nitrogen (99.9% purity) with a flow rate of 11 L/min was used to keep an inert atmosphere during the pyrolysis process.

To examine the impact of calcium content in biochar on phosphorus removal, four samples of biochar doped with differing amounts of calcium hydroxide (0, 7, 11 and

20 wt%) undergoing microwave assisted pyrolysis as described above. Biochar samples were named according to the initial calcium hydroxide content, for example BC20 means that this biochar contains 20 wt% of $\text{Ca}(\text{OH})_2$.

5.2.2 Biochar characterisation

The chemical composition of the biochar samples was determined by inductively coupled plasma - mass spectrometry (ICP-MS), using a Varian 820-MS Mass Spectrometer. Prior to ICP-MS measurements, biochar samples were microwave digested using hydrogen peroxide and nitric acid. The electrical conductivity (EC) and pH of the biochar samples were measured using an Orion model 5 Star pH plus conductivity meter. These measurements were carried out in the supernatant after 90 minutes of contact between 1 g of biochar and 20 ml of deionised water. Specific surface area and pore size were determined by nitrogen sorption isotherms using a Micromeritics TriStar 3000 gas adsorption analyser. Morphology and qualitative analysis of chemical composition of biochar samples were performed by a scanning electron microscopy connected to energy dispersive spectrometer (SEM-EDS) model Jeol JXA8200. Also, X-ray diffraction (XRD) was carried out to identify crystalline phases in the biochar before and after phosphorus removal using a Bruker Phaser D2 X-ray Powder Diffractometer (Cu radiation).

5.2.3 Phosphorus removal capacity

Synthetic phosphate solutions (or P-stock solutions) with concentrations between 100 to 1500 mg-P/L were prepared by dissolving potassium dihydrogen phosphate (KH_2PO_4) in single distilled water. Phosphorus concentration tested in this research is higher than the phosphorus content in wastewater stream, but the idea is to study the feasibility of adsorption process for higher phosphorus concentrations. The phosphate removal experiments were carried out in batch at room temperature ($22^\circ\text{C} \pm 2^\circ\text{C}$). One gram of biochar (particle size less than $450\ \mu\text{m}$) was added to 100 ml of phosphate stock solution and the mixture was stirred continuously using a magnetic stirrer at 350 RPM for different contact times (1 to 30 hours). The solution was then filtered using a $0.2\text{-}\mu\text{m}$ membrane, and the elemental phosphorus and calcium concentrations of the supernatant were analysed by inductively coupled plasma atomic emission spectrometer (ICP-AES).

The pH of the supernatant was also measured while the solid portion was dried at 100°C then analysed by XRD.

Two replicates of each experiment were carried out. When the deviation of these two experiments was higher than 5%, new experimental replicates were performed. The final results presented are the average of these values. A mass balance was performed to calculate the phosphorus removal capacity of each biochar sample. The specific phosphorus removal capacity (Q_e in mg-P/g of biochar) was calculated according to equation (5.1):

$$Q_e = \frac{(C_0 - C_e) V}{m} \quad (5.1)$$

The phosphorus removal percentage (%) was calculated with equation (5.2):

$$\% \text{ Phosphorus removal} = \frac{(C_0 - C_f)}{C_0} \times 100 \quad (5.2)$$

where, C_0 (mg/L) is the concentration of the P-stock solution, C_e (mg/L) is the equilibrium concentration of the supernatant after phosphorus removal, C_f (mg/L) is the final concentration of the supernatant after phosphorus removal, V (L) is the volume of P-stock solution and m (g) is the mass of biochar.

Statistical analyses were conducted with Excel 2010. The impact of calcium concentration in biochar and the initial pH of the P-stock solution on phosphorus removal by biochar were analysed by two-way analysis of variance (ANOVA). In this study, differences were considered statistically significant when $p < 0.05$.

5.3 Results and Discussion

5.3.1 Biochar characterisation

The main characteristics of biochar are presented in Table 5.1. The calcium content measured by ICP-MS is in line with the mass balance, where the difference between calcium calculated and measured was less than 4%. This agreement between the values suggests that no calcium hydroxide or other calcium compounds were volatilised during experiments. The percentages of Mg (less than 0.24%), Al and Fe (Table 5.1) were also measured since these elements can affect the phosphorus removal capacity of biochar. The XRD (Figure 5.5) of biochar samples revealed that quartz (SiO_2) is the main crystalline phase of biochar, which is also the main crystalline compound in biosolids. The XRD of BC0 biochar only exhibited quartz; no calcium was added before pyrolysis. The BC7 and BC11 biochar samples contained quartz and calcite (CaCO_3) while the BC20 contained three phases: quartz, calcite and small amounts of calcium hydroxide (Ca(OH)_2). The formation of calcite was due to the inert pyrolytic atmosphere, where calcium hydroxide reacts with carbon dioxide produced from biosolids during the pyrolysis process.

The BET of biochar was in line with the literature and did not vary significantly across the four samples with differing calcium content, which allowed us to quantify the impact of calcium concentration on phosphorus removal [4]. Also, the pore size (around 8 nm) and the total volume of pores are similar across biochar samples. The four biochar samples exhibited an alkaline tendency, with pH ranging between 7.6 and 10.2. The pH and EC increased with the percentage of calcium in the biochar likely due the dissolution of calcium in deionised water, which increased with the calcium percentage as presented in Table 5.1.

SEM-EDS was performed to observe the particle morphology of biochar, and to understand the calcium distribution in the biochar particles. The SEM observation showed biochar particles of irregular shape and with a porous surface, which may enhance P-removal. Several SEM-EDS analyses were carried out on different particles of each sample, demonstrating that the calcium was uniformly distributed in biochar particles in all samples produced.

Table 5.1 – Biochar composition, specific surface area, pore size and volume.

	BC0	BC7	BC11	BC20
Ca(OH) ₂ load (wt%)*	0	7	11	20
Ca (%)	0.65	4.06	6.99	11.52
SD	±0.01	±0.03	±0.01	±0.05
Al (%)	6.18	6.83	6.54	5.94
SD	±0.03	±0.03	±0.03	±0.02
Fe (%)	1.76	1.87	1.78	1.63
SD	±0.01	±0.01	±0.01	±0.01
pH	7.54	7.98	9.22	10.22
SD	±0.03	±0.02	±0.01	±0.02
EC (µS/cm)	888	1304	1555	1718
SD	±10	±5	±8	±17
BET (m ² /g)	53.55	48.63	50.73	54.40
SD	±2.59	±1.42	±0.22	±0.75
TVP (cm ³ /g)	0.135	0.125	0.132	0.142
SD	±0.012	±0.008	±0.009	±0.003
Mean pore size (nm)	8.074	7.885	7.872	8.161
SD	±0.437	±0.319	±0.475	±0.073

*Dry basis of biosolids; SD – Standard deviation.

5.3.2 Phosphorus removal kinetics

The impact of contact time (1 to 30 hours) on phosphorus adsorption was examined in this study, with the results showing that the phosphorus adsorption increased rapidly until 8 hours and after this it was almost constant (Figure 5.1 – Phosphorus removal kinetics of biochar. and Table 5.2). The adsorption rate of these biochar samples was similar to other modified biochars [15, 193]. The results show that adsorption rate increased with the percentage of calcium in biochar, which was expected due to increase of phosphorus precipitation with calcium.

To understand the phosphorus removal kinetic mechanism, the three most common models used to describe phosphorus adsorption from an aqueous solution were used to analyse the experimental data: pseudo-first-order, pseudo-second-order and intra-particle diffusion which are described by the linear equations (5.3), (5.4) and (5.5) respectively.

$$\ln(Q_e - Q_t) = \ln Q_e - k_1 t \quad (5.3)$$

$$\frac{t}{Q_t} = \frac{1}{k_2 Q_e^2} + \frac{t}{Q_e} \quad (5.4)$$

$$Q_t = k_{id} t^{1/2} + C \quad (5.5)$$

where Q_e (mg/g) is the phosphorus removal capacity at equilibrium, Q_t (mg/g) represents the phosphorus uptake at time t , k_1 (h^{-1}), k_2 (g/mg h) and k_{id} (g/(mg.h^{1/2})) are the rate constants. The results (Table 5.2 and Figure 5.1) show that the pseudo-second-order kinetic model ($R^2 > 0.96$) fits the experimental data better than the pseudo-first-order kinetic model ($0.62 < R^2 < 0.96$) and intra-particle diffusion kinetic model ($R^2 < 0.83$), which indicates that the phosphorus removal process is likely controlled by multiple mechanisms. However, until reaching the equilibrium (time = 8 hours), the phosphorus removal capacity had a linear dependency on the square root of time, which

is a typical behaviour of intra-particle diffusion mechanism ($R^2 > 0.92$). This mechanism is commonly observed in solid-liquid systems, where the intra-particle diffusion is the rate-limiting mechanism. After 8 hours of contact time, the equilibrium stage takes place and the phosphorus removal rate slows down due to the lower concentration of Ca^{2+} in the solution.

The phosphorus removal process by biochar was mainly due to chemical bonding or chemisorption involving sharing electrons between phosphate ionic species and calcium-doped biochar as described by the equation (5.6):

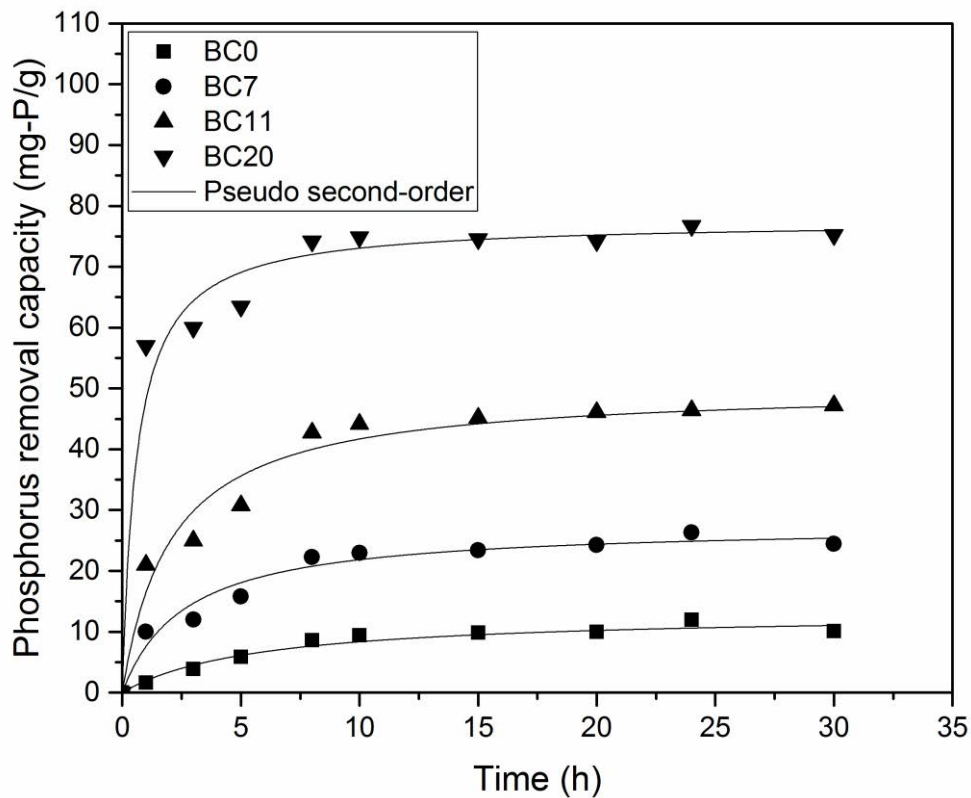
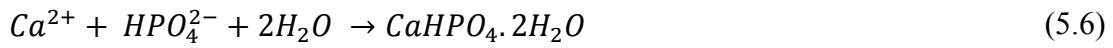


Figure 5.1 – Phosphorus removal kinetics of biochar.

Table 5.2 – Phosphorus removal kinetic parameters for the four biochar samples.

	BC0	BC7	BC11	BC20
Pseudo-first-order				
Q_e (mg/g)	7.3390	12.3246	28.2869	12.3839
k_1 (1/h)	0.1379	0.1808	0.4756	0.2020
R^2	0.7347	0.7780	0.9638	0.6223
Pseudo-second-order				
Q_e (mg/g)	13.1406	27.6243	50.2513	77.5194
k_2 (g/mg h)	0.0133	0.0137	0.0097	0.0211
R^2	0.9614	0.9899	0.9951	0.9990
Intra-particle diffusion				
C (mg/g)	1.1393	8.2873	18.7660	55.5360
k_{id} (g/mg h ^{1/2})	2.0547	3.6050	6.0226	4.33960
R^2	0.7548	0.7988	0.8253	0.8324

The chemical reaction between calcium and phosphorus species was the main chemical reaction as demonstrated by XRD spectrum after phosphorus removal (Figure 5.5), but other ionic elements, such as aluminium, iron and magnesium may react with phosphates, particularly in the case of biochar BC0. The phosphorus removal capacity of the biochar BC0 is around 10 mg-P/L, but when the aluminium, iron and magnesium were removed with an HCl solution the adsorption capacity was nearly zero.

5.3.3 Phosphate adsorption isotherms

Phosphate adsorption isotherm experiments were carried out working with P-stock solution with concentrations between 100 mg-P/L and 1500 mg-P/L. The reaction time

was 24 hours for all the tests. Two isotherm models were fitted to the experimental results: Langmuir and Freundlich (equations (5.7) and (5.8) respectively).

$$Q_e = \frac{Q_m K_L C_e}{1 + K_L C_e} \quad (5.7)$$

$$Q_e = K_F C_e^{1/n} \quad (5.8)$$

The model constants (K_F (L/g)^{1/n} and K_L (L/g)) represent the adsorption capacity, the Freundlich exponent (n) characterises the adsorption intensity and Q_m (mg/g) represents the monolayer adsorption capacity. The model parameters for both Langmuir and Freundlich models are presented in Table 5.3, which show that the Langmuir model fits better the experimental data ($R^2 > 0.98$) than the Freundlich model ($R^2 > 0.94$). For this reason, only the Langmuir fitting curves and the experimental data are shown in Figure 5.2. The Langmuir maximum adsorption capacity of phosphorus adsorption increased with increasing calcium content in biochar, reaching a maximum of 147 mg-P/g with biochar BC20, which was ten times higher than undoped biochar (BC0).

To confirm that the Langmuir isotherm was favourable, a dimensionless constant called the equilibrium parameter (R_L) was calculated according to equation (5.9):

$$R_L = \frac{1}{1 + K_L C_0} \quad (5.9)$$

where K_L (L/mg) is the Langmuir constant and C_0 is the initial highest (1500 mg-P/L) concentration of P-stock solution. When $0 < R_L < 1$ means favourable adsorption while $R_L > 1$ shows unfavourable adsorption, and $R_L = 1$ indicates linear adsorption [204]. The values of R_L obtained in this study were between 0.18 and 0.47 (Table 5.3), which indicates that the Langmuir isotherm was favourable for phosphorus adsorption by biochar. Moreover, all the values for $1/n$ were below one, which confirmed a normal Langmuir isotherm [119]. In general, the Freundlich constant (K_F) increased with the calcium content, which confirms the increase of the adsorption intensity of the biochar due to the chemical reaction between phosphate ions and Ca^{2+} .

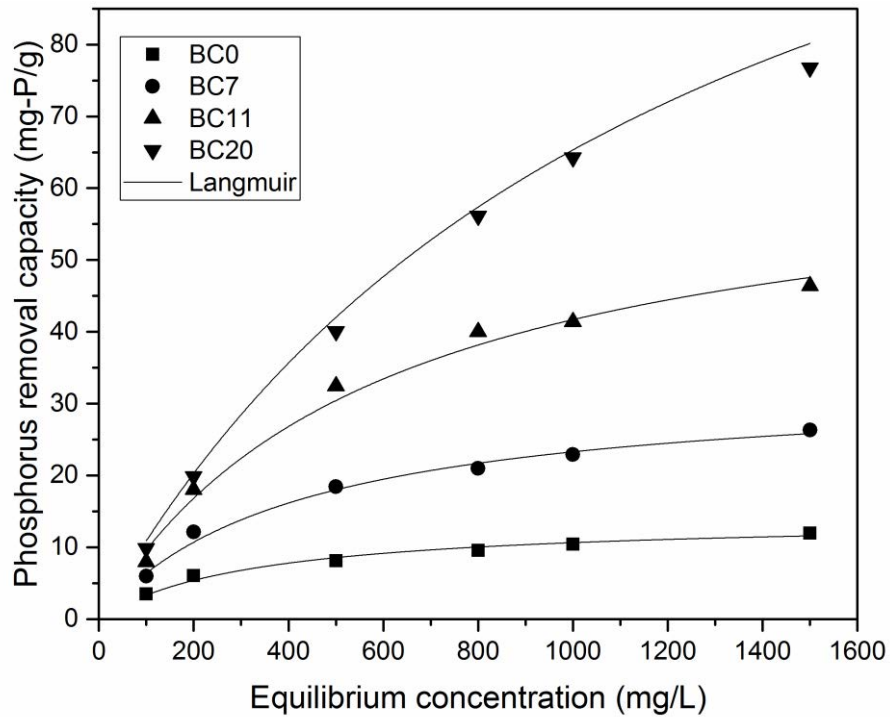


Figure 5.2 – Phosphorus adsorption isotherm of biochar samples with Langmuir model superimposed.

Table 5.3 – Phosphorus removal isotherm parameters for the four biochar samples.

	BC0	BC7	BC11	BC20
Langmuir model				
Q_m (mg/g)	14.0845	33.0033	66.2252	147.0588
K_L (L/mg)	0.0031	0.0024	0.0017	0.0008
R^2	0.9909	0.9928	0.9755	0.9921
R_L	0.1765	0.2150	0.2835	0.4690
Freundlich model				
K_F (mg/g)	1.8384	1.5238	1.9340	3.1037
$1/n$	0.4290	0.5179	0.6390	0.7642
R^2	0.9654	0.9456	0.9408	0.9883

5.3.4 Impact of initial pH of P-stock solution on phosphorus removal

To assess the impact of the initial pH of P-stock solution on phosphorus removal, the four biochar samples were studied in a pH range between 2 and 12 (starting pH). The results of phosphorus removal and final pH of the supernatant are shown in Figure 5.3 and Figure 5.4. The results suggest that the initial pH of the P-stock solution has a strong effect on phosphorus removal by biochar, with a maximum phosphate removal capacity at pH 4 of 29 and 36 mg-P/g of biochar for BC0 and BC7, respectively. While BC0 and BC7 samples had a phosphorus removal capacity peak at pH 4, the samples BC11 and BC20, which have a higher alkaline property, can be used in a large range of pH with similar phosphorus removal capacity, as seen in Figure 5.3. The maximum phosphate removal capacity of BC11 and BC20 biochar was approximately 50 and 79 mg-P/g of biochar (at initial pH 3), respectively. The BC20 biochar demonstrated a higher phosphate removal capacity, which represented a rise of more than 270% compared with the BC0 biochar. This difference in phosphate removal capacity can be explained because this sample contained a higher calcium concentration, which is soluble in acid pH conditions, and the alkaline property of this biochar increased the final pH of the mixture, which is fundamental for calcium phosphate precipitation [205]. As the calcium content increases in the biochar samples, the pH range of high phosphate removal capacity increases. For example, biochar BC0 had the highest phosphorus removal at pH 4 and this P-removal capacity declined significantly above or under this pH, whereas biochar BC20 could be used in a broad pH range (from pH 2 to 6) with similar P-removal efficiency.

The calcium compounds also have an impact on phosphorus removal. Calcium hydroxide (solubility product: 5.5×10^{-6}) exhibits high solubility compared with calcium carbonate (solubility product: 2.9×10^{-9}) [205]. Higher calcium hydroxide percentages increase the concentration of calcium ions in the solution, which contributes to calcium phosphate precipitation increasing the phosphate removal capacity. Acidic conditions are the best for this process as the solubility of the calcium compounds is high and the Ca^{2+} ions are released into the solution where they complex with the HPO_4^{2-} ions before the alkaline biochar increases the pH, precipitating them as salts [206]. For these reasons, the highest phosphate removal capacity was obtained by the BC20 biochar, which contained calcium hydroxide and was the most alkaline biochar.

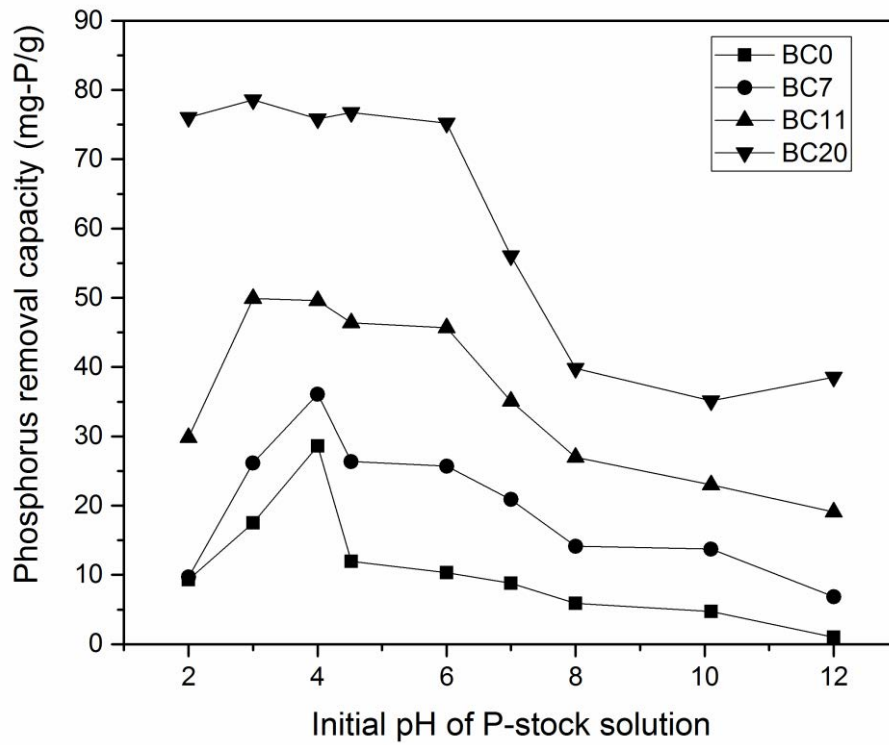


Figure 5.3 – Effect of pH on phosphorus removal by Ca-doped biochar.

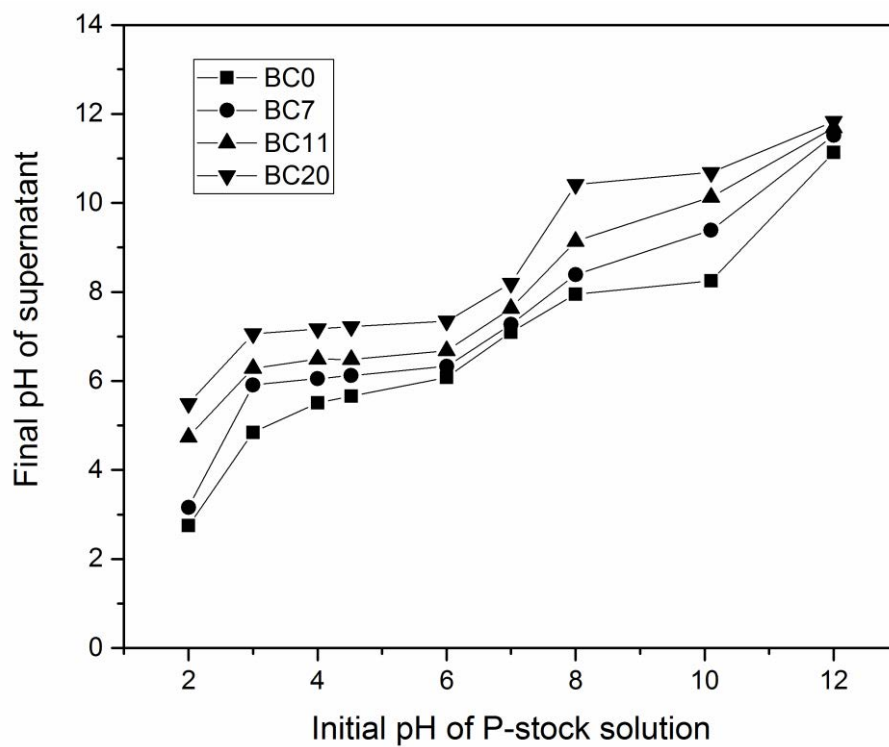


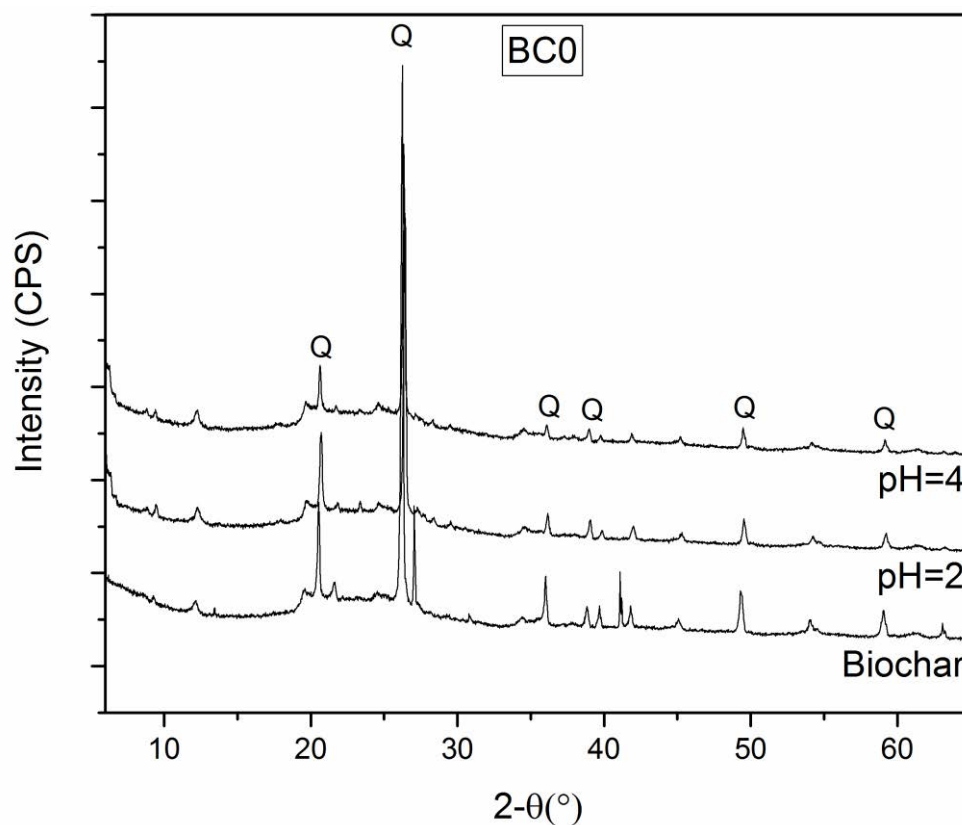
Figure 5.4 – Final pH of supernatant after 24 hours of reaction time of biochar with P-stock solution with different pH.

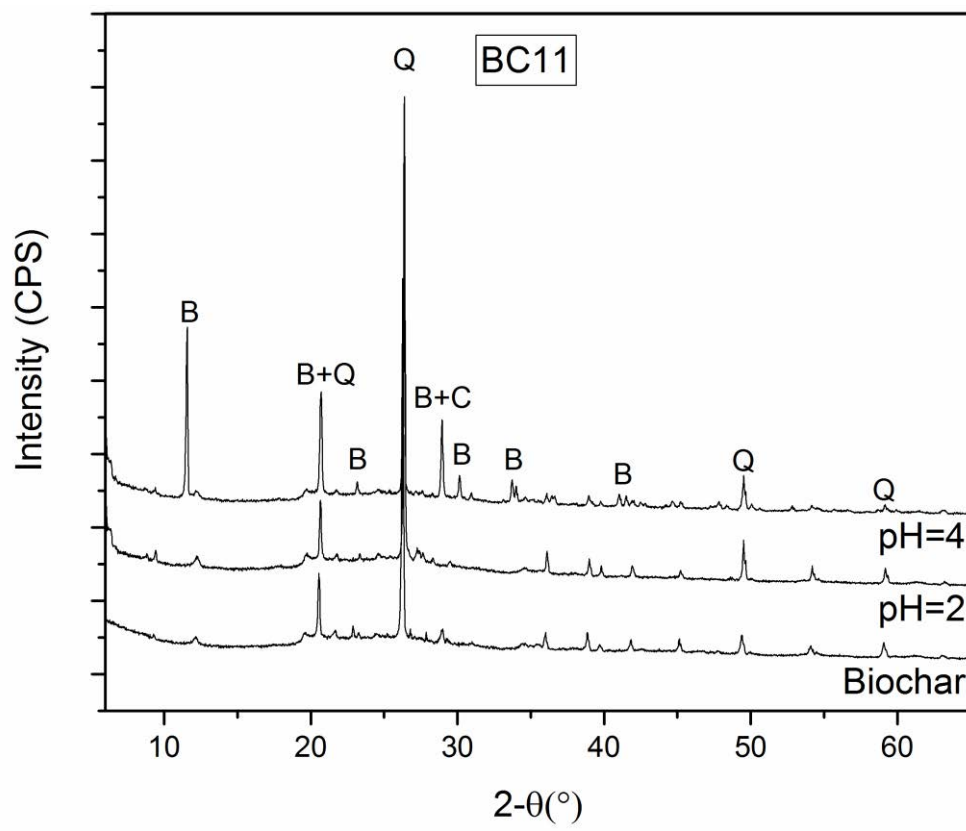
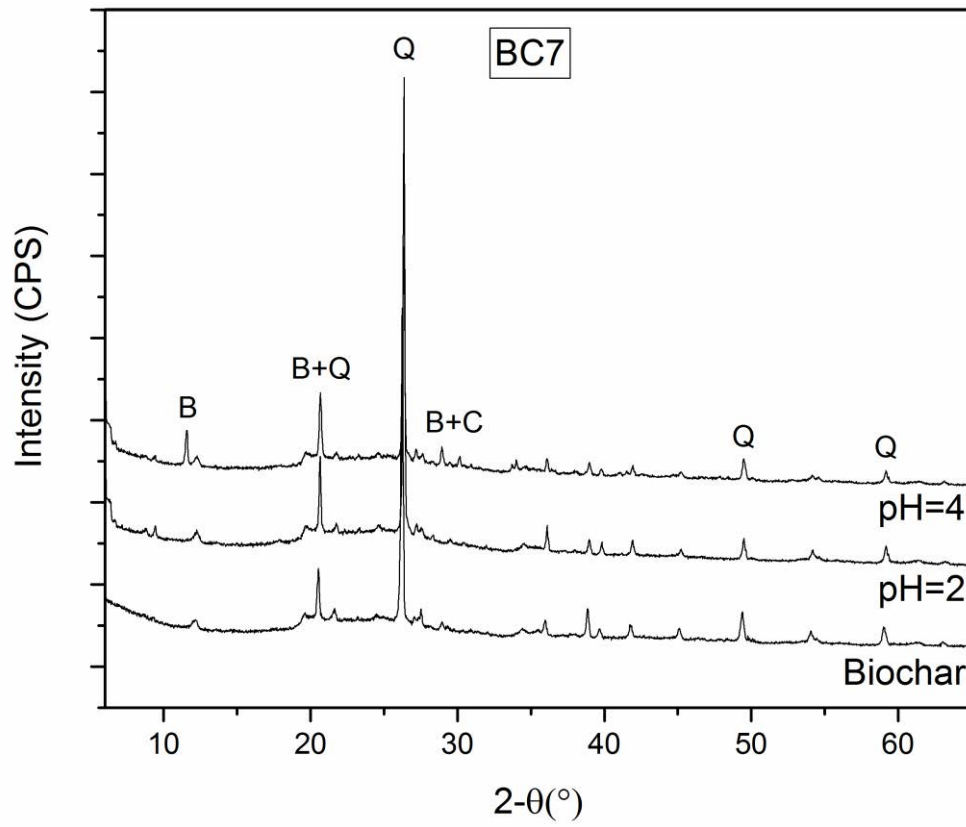
XRD analysis was carried out before and after phosphorus removal to identify the crystalline phases in the biochar. These results are represented in Figure 5.5, where each graph comprises a spectrum of biochar before phosphorus removal tests and two spectrums after phosphorus adsorption, which correspond to the conditions of minimum and maximum phosphorus removal capacity. The main phase presented in all biochar samples before phosphorus removal was quartz (SiO_2), which is also the main crystalline compound in biosolids. However, after phosphorus removal brushite was the predominant phase for BC11 and BC20 samples.

After the phosphorus removal tests, new peaks appeared in the XRD spectrum, which correspond to brushite, also known as calcium hydrogen phosphate dihydrate ($\text{CaHPO}_4 \cdot 2\text{H}_2\text{O}$). Besides this calcium orthophosphate compound, other amorphous calcium salts that are not identified by XRD, such as hydroxyapatite (HAP – $\text{Ca}_5\text{OH}(\text{PO})_4$) and octacalcium phosphate (OCP – $\text{Ca}_8\text{H}_2(\text{PO}_4)_6 \cdot 5\text{H}_2\text{O}$) may precipitate in small amounts depending on the pH of the solution, concentration of H_2PO_4^- and HPO_4^{2-} species and the ratio Ca/P [206, 207]. However, brushite is the most thermodynamically stable phase relative to other calcium compounds at room temperature and in lower pH region, where Ca^{2+} reacts with H_2PO_4^- producing brushite as demonstrated by XRD [208].

To quantify the phosphate adsorption percentage by biochar, the biochar BC0 was treated with HCl (1M) to remove Al, Fe, Ca and Mg. The treated biochar was tested with a P-stock solution, and the phosphorus removal capacity was nearly zero. These results and the brushite presence in biochar after phosphorus removal tests confirm that precipitation is a key mechanism for phosphorus removal by Ca-doped biochar. The XRD spectrums of BC0, BC7 and BC11 after phosphorus removal at pH = 2 do not indicate brushite, so low pH appears crucial to the release of Ca^{2+} , but a higher Ca^{2+} concentration and high final pH are required for brushite precipitation. The BC20 biochar after P-removal contained a substantial amount of brushite, which can be explained by the higher Ca^{2+} concentration in solution and the higher final pH of the solution, which represent the necessary conditions for brushite precipitation. These XRD results are in line with the mass balance. At lower pH, the phosphorus removal capacity was very low for 3 samples (BC0, BC7, BC11) of biochar and no brushite was identified in XRD spectrums. At pH 4, the phosphorus removal capacity was 29, 36, 50

and 79 mg-P/g of biochar for BC0, BC7, BC11 and BC20 respectively, with all four samples containing brushite after phosphorus removal tests. The sample BC20 was less affected by acid pH due to its alkaline property (see Figure 5.3), and because of the high calcium concentration, which favours precipitation. At pH 12, the XRD spectrum of BC20 did not exhibit any brushite, since Ca^{2+} at this pH was not released from calcium compounds into the solution. This shows the importance of calcium dissolution on the phosphorus removal process.





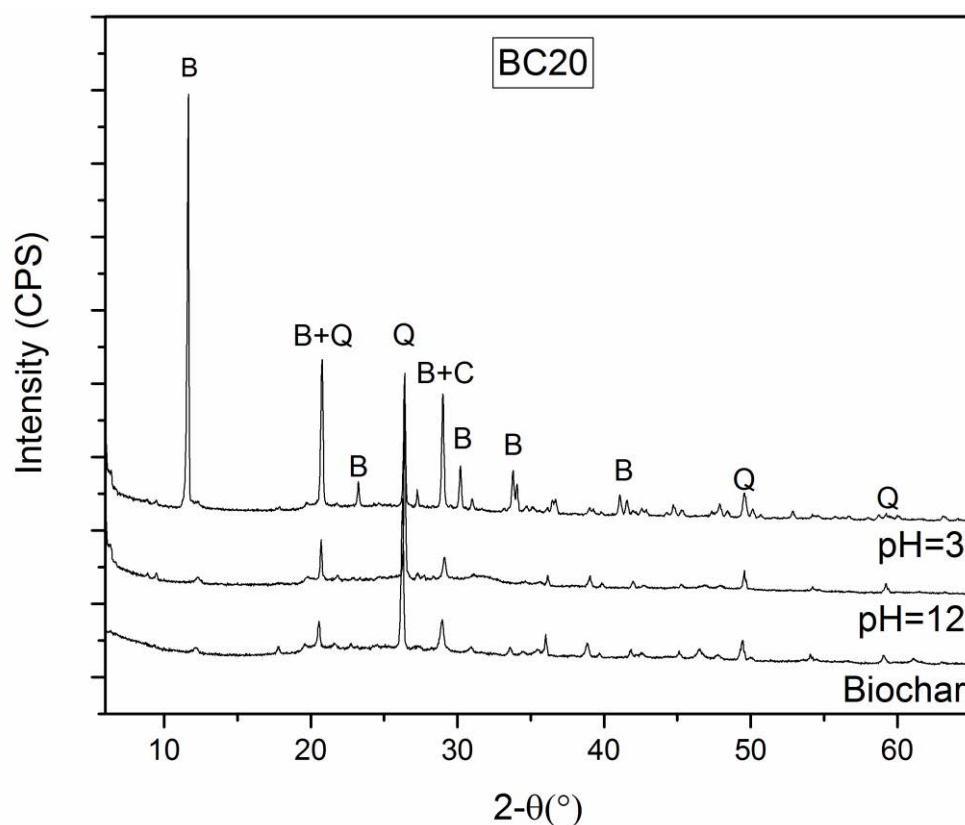


Figure 5.5 – XRD spectrum of the four biochar samples before and after phosphorus removal tests (B – Brushite, Q – Quartz, C – Calcite) (Biochar – before adsorption; pH=2, 3, 4 and 12 – after adsorption).

A mass balance was conducted to determine the maximum phosphorus removal capacity of biochar, assuming that brushite is the main precipitated compound, and the calcium content within biochar obtained by ICP-MS (Table 5.1). The phosphorus removal capacity calculated and obtained were similar for biochar samples BC7 and BC11. However, the phosphorus removal capacity of BC0 was much higher than the value calculated (at pH=4 the Q_e obtained was 28.7 mg-P/g versus estimated 5.0 mg-P/g (only the Ca content was used to calculate the Q_e)). This difference could be attributed to the Al, Fe and Mg content in the biochar, which can be dissolved in low pH solvents and react with the phosphate ionic species. In contrast, the phosphorus removal capacity of BC20 was lower than the value calculated (obtained at pH 3: 78.6 mg-P/L, estimated 89.0 mg-P/L), which can be attributed to the significant presence of calcite, which is less soluble, and also because some of the calcium being dissolved in the solution and not precipitating. In this case, the calcium dissolved in the supernatant was 19.9 mg/L,

and considering this value for the mass balance, the phosphorus removal obtained and estimated had a good agreement (obtained 78.6 mg-P/L, estimated 73.6 mg-P/L).

The statistical significance was analysed by ANOVA, which demonstrated that both factors (initial pH of P-stock solution and percentage calcium in biochar) and their interactions are significant relevant to phosphorus removal capacity ($p < 0.05$) with high F-values. Regression analysis of the experimental data was carried out to obtain an equation to predict the phosphorus removal capacity based on pH and percentage of calcium. The phosphorus removal capacity (Q_e) can be calculated from the equation (5.10):

$$Q_e = 21.87 + 4.75Ca - 2.76pH \quad (5.10)$$

where Ca is the percentage of calcium in biochar and pH represents the initial pH of phosphorus solution. This fitting model describes well the experimental data ($R^2 = 0.85$). The percentage of calcium is the dominant factor as it determines the concentration of Ca^{2+} in solution, but the initial pH is also important due to its impact on concentration and ionic phosphate species. This equation can be useful in the future to estimate the conditions to maximise the phosphorus removal capacity as well as predict operating costs.

This study was carried out with P-stock solutions prepared in the laboratory because they are available, controllable and safe. However, it is crucial to compare the phosphate removal behaviour of the biochar with P-stock solution and with a real effluent to understand the applicability of these results to the real world. For this purpose, the four samples of biochar were tested using both solutions with phosphorus concentrations of 400 mg-P/L and pH 6.0 (these are the characteristics of the effluent collected from a local wastewater treatment plant). One gram of biochar was added to 100 ml of solution and agitated continuously for 24 hours. The phosphorus removal percentage was calculated according to equation (5.2) and is represented in Figure 5.6. The biochar phosphorus removal percentage was higher with the real effluent than with the P-stock solution, which is a good outcome, as all the experiments carried out with a

P-stock solution can be reproduced in a real world with even better results. The increase of phosphorus recovery from a wastewater by biochar can be explained by the higher final pH of the mixture due to biochar, inducing precipitation of phosphorus with co-existing cations in wastewater, such as Al, Ca, Fe and Mg. Also, the NH_4^+ content in wastewater buffers the pH to 9 increasing precipitation of phosphorus compounds.

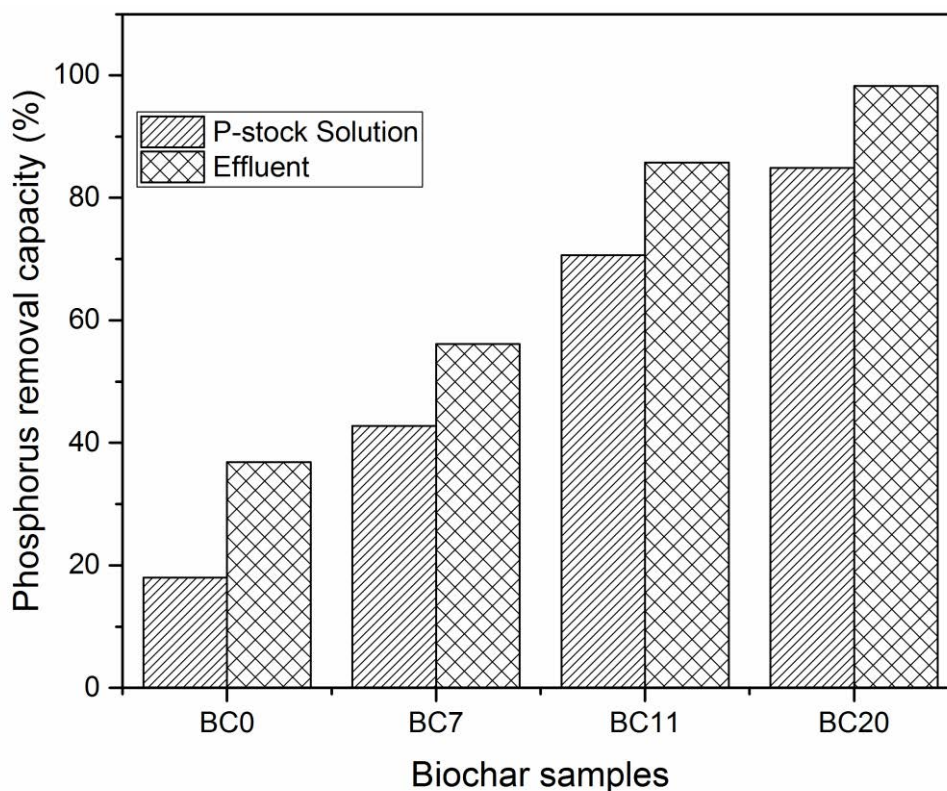


Figure 5.6 – Phosphorus removal by biochar from an effluent and P-stock solution.

5.4 Conclusions

Using biochar produced from biosolids via MWAP is an effective approach for phosphorus recycling as well as for biosolids management. This study demonstrated that Ca-doped biochar enhances phosphorus removal capacity due to the increase of the precipitation process, which is the main mechanism of phosphorus removal. The adsorption results fitted well with the Langmuir isotherm model and pseudo-second-order kinetic model. The initial pH of the phosphorus stock solution plays a key role on

phosphorus removal capacity: a pH of 4 maximises the phosphorus removal capacity. The final product (biochar plus brushite) is a potential substitute for industrial fertilizers.

6 SILVER REMOVAL FROM AQUEOUS SOLUTION BY BIOCHAR

Abstract

The contamination of water with silver has increased due to the widespread applications of products with silver employed as antimicrobial agent. Adsorption is a cost-effective method for silver removal from aqueous solution. In this study biochar, produced from the microwave assisted pyrolysis of biosolids, was used for silver removal from an aqueous solution. The adsorption kinetics, isotherms and thermodynamics were investigated to better understand the silver removal process by biochar. X-ray diffraction results demonstrated that silver removal was a combination two consecutive mechanisms, reduction and physical adsorption. The Langmuir model fitted the experimental data well, showing that silver removal was predominantly a surface mechanism. The thermodynamic investigation demonstrated that silver removal by biochar was an exothermic process. The final nanocomposite Ag-biochar (biochar plus silver) was used for methylene blue adsorption and photodegradation. This study showed the potential of using biochar produced from biosolids for silver removal as a promising solution to mitigate water pollution and an environmentally sustainable approach for biosolids management and reuse.

Keywords: Adsorption kinetics; Ag-biochar composite; Biochar; Particle diffusion; Silver removal.

Highlights

- Biochar surface area was mostly affected by pyrolysis temperature.
- Biochar was successfully applied for silver removal from aqueous solution.
- Reduction and physical adsorption were the mechanisms for silver removal.
- Ag-biochar was used for methylene blue adsorption.

As published in: Antunes, E., J., Brodie, G., Jacob, M. V., Schneider P. A., “*Silver removal from aqueous solution by biochar produced from biosolids via microwave pyrolysis*”, Journal of Environmental Management 2017, 203: 264-272.

6.1 Introduction

The number of applications using nanosilver products has increased significantly due to its antimicrobial ability. As a consequence of the use and disposal of nanosilver products, the contamination of water with silver ions is inevitable. Several methods have been used for silver removal from aqueous solutions, but adsorption is one of the most efficient methods with low energy consumption [209]. Adsorption is a surface process, where ions, molecules or atoms adhere to a surface of the substrate by chemical or physical interactions [163]. Recently, adsorption has gained even more attention due to the potential use of biochar, which is a low-cost adsorbent produced by pyrolysis from different types of biomass, such as agricultural waste, sewage sludge, wood chips, orange peel, saw dust and tea waste [4]. The adsorption capacity of biochar depends mainly on biochar feedstock biomass, pyrolysis technologies and pyrolysis conditions, in particular pyrolysis temperature, which has a great impact on biochar surface area [163, 176, 210].

The adsorption capacity of pollutants by raw biochar is limited; however, biochar production has several advantages compared to other types of adsorbents. Biochar feedstocks are abundantly available at low-cost, and beneficially, biofuel and biogas are produced from biomass while producing biochar [210]. Recently, different physical and chemical activation methods have been explored to increase the adsorption capacity of raw biochar. Chemical modification of biochar is one of the most used methods, which consists of impregnating chemicals onto biochar to enhance the adsorption capacity of a target contaminant. For example, MgO-biochar and AlOOH-biochar have demonstrated a higher phosphorus removal capacity from aqueous solution than unmodified biochar [15, 211]. Chemical activation through an acid/base treatment has been used to increase surface area, modify biochar pore structure and surface functional groups. The common activation chemicals are hydrogen peroxide, phosphoric acid, nitric acid, potassium hydroxide and metal chlorides [176, 212]. For example, hydrogen peroxide modified biochar demonstrated a lead adsorption capacity 20 times higher than unmodified biochar [176]. The physical activation of biochar is a chemical-free process, occurring between 600°C and 1200°C in the presence of steam, air and carbon dioxide [212]. These gases have been used to increase the surface area of biochar and to create and/or enhance porosity within biochar by removing remaining volatile organic compounds.

Biochar adsorption has been explored for removal and recovery of several types of pollutants, such as metals, dyes, antibiotics, pesticides and polynuclear aromatics [2, 201]. The adsorption mechanisms depend on pollutant characteristics and biochar properties, which vary with feedstock and pyrolysis conditions [4, 213]. In general, the main mechanisms for organic contaminant adsorption by biochar are electrostatic interaction, π - π interaction, repulsion and intermolecular hydrogen bonding [176]. Heavy metal removal by biochar can be explained by electrostatic interaction, precipitation, ion exchange, and surface adsorption by biochar surface functional groups (chemisorption) [176, 210]. Precipitation of metals takes place when the biochar is negatively charged, in particular with carbonate and phosphate groups as their release from biochar increases solution pH and consequently metal precipitation [214]. Adsorption of metals by biochar depends on surface functional groups, surface area and pore size. Biochar with high surface area usually exhibits higher metal adsorption capacity [215].

Heavy metal adsorption by biochar from aqueous solution is well reported in the literature because heavy metals are hazardous for the environment and human health, even at low concentrations [2]. Activated carbon has been used for heavy metals removal, but its adsorption capacity is low (a few milligrams per g). Furthermore, using activated carbon has some disadvantages; it is an expensive material, the metal desorption step is very costly and has several environmental issues [2]. Heavy metal adsorption by biochar may be an alternative approach to activated carbon because it has higher adsorption capacity, low-cost production and lower greenhouse gas emissions [216]. In general, lead, copper and cadmium have the highest biochar adsorption capacity while zinc, arsenic and nickel have the lowest adsorption capacity; however, the adsorption capacity depends on biochar properties [217]. The high lead and copper removal capacity by biochar explains the extensive number of studies in copper and lead adsorption by biochar.

Silver adsorption by biochar is not well explored. However, the use of silver has been adopted across in a wide range of applications, such as jewellery, dentistry, clothing and the food industry has increased its concentration in wastewater effluents [218]. Finding a sustainable removal and recovery technology for silver is therefore urgent. Silver is an expensive material and just a few ppm are hazardous for the environment; for example,

the limit of silver in drinking water was fixed at a maximum of 100ppb [209]. Biochar adsorption of silver seems to be one of the most advantageous processes over other treatment methods, such as precipitation and ion-exchange [209]. The regeneration of the adsorbent is usually done by chemical leaching, which is an expensive process and can negatively impact on the environment. Therefore, finding applications for the final material (Ag-biochar) after adsorption is fundamental to mitigate the environmental impacts. The final material has been used successfully as an antimicrobial composite, but more research should be done to find new applications and optimise the recycling cycle of materials and minimise the economic and environmental costs [209, 218]. Finally, recycling resources should be prioritised to avoid future natural resources depletion.

Using biochar for heavy metal removal from aqueous solution has been studied and well reported in the literature. However, the regeneration of the biochar or the reuse of the metal-biochar composite should be investigated to better understand the economic and environmental viability of using biochar for contaminant removal and recovery. Therefore, this work has three main objectives: first, assess the impact of pyrolysis conditions on biochar specific surface area; second, study the adsorption kinetics, isotherms and thermodynamics mechanisms of silver removal by biochar; and third, test the final composite (Ag-biochar) for methylene blue adsorption and degradation, which is a significant environmental problem due to its impact on plants and animals.

6.2 Materials and Methods

This study was performed in three steps. The objective of the first step was to understand the impact of pyrolysis conditions (temperature, time, percentage and size of activated charcoal) on physical properties of biochar (BET, pore size and total pore volume) and assess the impact of these properties on silver removal. In this first step, the Taguchi method was used to study the major effects. Then the biochar with the highest silver removal capacity was selected for the second step. The objective of the second step was to study the adsorption kinetics, isotherms and thermodynamics of silver removal using the biochar sample selected in the previous step. In the last step, the final nanocomposite (Ag-biochar), after silver removal, was tested for methylene blue adsorption and photodegradation. The principal aim of the third step was to find a

potential value-added application for the final composite, instead of pursuing silver recovery from the biochar and subsequent reuse of the biochar.

Using Minitab 17 for statistical analysis, the Taguchi method was employed to find the major effects of pyrolysis conditions on biochar physical properties. Four factors (temperature, residence time, activated charcoal load and size) were considered at three levels, the nine combinations of these factors considered, as represented in Table 6.1. The silver removal by biochar tests were analysed with one-way analysis of variance (ANOVA) where differences were considered significant if $p < 0.05$.

6.2.1 Biochar Preparation

Experimental pyrolysis tests were carried out with biosolids from Euroa Wastewater Treatment facility in Victoria, Australia. A complete characterisation of biosolids used in this study was previously reported [13]. Activated charcoal (AC) was used as a microwave absorber (Sigma Aldrich C2889). Three different activated charcoal sizes were used in this work: the material less than 0.425 mm (fine) was obtained by grinding and sieving the original material, and the other two fractions were obtained by sieving the activated charcoal sample. The particle size of medium AC was between 0.425 and 1.0 mm, and the particles of large AC ranged between 1.0 and 2.0 mm. The specific surface area of these three fractions was similar ($710 \pm 22 \text{ m}^2/\text{g}$), which allowed us to ignore the impact of this variable on the final response.

Biosolids with approximately 40% moisture content were sieved to obtain a sample with a particle size less than 5.2 mm then blended manually with activated charcoal to obtain a uniform distribution of AC throughout the biosolids, ensuring that charcoal particles did not break during the blending process. Mixture samples (60 g) were used for microwave pyrolysis according to the process parameters exhibited in Table 6.1. Duplicate runs were carried out and the final presented values are the average of these two runs. The pyrolysis tests were carried out in a customised single-mode microwave at 600 W [13]. Temperature was monitored by a type K thermocouple and kept at set-point by adjusting the applied net microwave power.

6.2.2 Silver adsorption tests

Silver solutions were prepared by dissolving silver nitrate in single distilled water. Silver adsorption kinetic experiments were conducted in a batch process at room temperature ($22^{\circ}\text{C} \pm 2^{\circ}\text{C}$). Biochar (0.5 g) was added to 100 mL of silver solution with an initial concentration of 500 mg/L and agitated at 350 RPM for different contact times (10 min to 45 hours).

The adsorption isotherms experiments were carried out at 22°C , 35°C and 45°C using silver solutions with initial concentrations varying between 100 and 1000 mg/L. After adsorption tests, the final mixtures were filtered using a 0.45- μm membrane and the silver concentration was measured in the supernatant by inductively coupled plasma - atomic emission spectroscopy (ICP-AES). The silver removal capacity (Q_e in mg/g of biochar) was calculated according to equation (6.1):

$$Q_e = \frac{(C_0 - C_e) \times V}{m} \quad (6.1)$$

where, C_0 (mg/L) is the initial concentration of the silver solution, C_e (mg/L) is the equilibrium concentration of the supernatant after silver removal, V (L) is the volume of Ag solution and m (g) is the amount of biochar employed.

The solid portion (biochar after adsorption tests) was dried at 100°C for posterior X-ray diffraction (XRD) and scanning electron microscopy with energy dispersive X-ray spectrometry (SEM-EDS) analyses. All experiments were repeated at least twice. If the relative difference of two replicates was greater than 5% then one more repetition was done. The presented results are the average of all repeats.

6.2.3 Methylene blue (MB) adsorption and photodegradation

A MB solution (20 mg/L) was prepared and used for the MB photodegradation and adsorption tests. The MB adsorption by biochar was performed by placing a mixture (0.2 g of Ag-biochar in 100 ml of MB solution) on a magnetic stirrer at 150 RPM for one hour and a sample was collected every ten minutes then filtered with a 0.45- μ m membrane. The final concentrations of MB were measured by absorbance using a UV-visible spectrophotometer (Agilent 8453) at 660 nm. The photodegradation of MB by Ag-biochar was examined by placing a mixture under UV-radiation in a photoreactor Model LZC-1. Samples were collected every 10 minutes, filtered and analysed by UV-visible method.

Table 6.1 – Experimental design matrix (L9 orthogonal array), biochar characterisation and silver removal by biochar.

Run	Process variables			Biochar characterisation			Silver removal capacity (mg/L)	
	Temperature (°C)	Residence time (min)	AC load (wt%)	AC size	BET (m ² /g)	Pore size (nm)		Total pore volume (cm ³)
1	400	10	10	Fine	54.60	7.673	0.132	25.80
2	400	20	15	Medium	38.06	6.931	0.096	29.25
3	400	30	20	Large	48.41	7.032	0.109	36.25
4	600	10	15	Large	78.55	6.927	0.119	41.50
5	600	20	20	Fine	148.81	6.789	0.169	27.38
6	600	30	10	Medium	39.67	7.590	0.102	26.93
7	800	10	20	Medium	148.71	6.658	0.150	36.07
8	800	20	10	Large	60.75	7.807	0.126	27.61
9	800	30	15	Fine	150.85	7.294	0.182	24.10

6.2.4 Biochar characterisation

The specific surface area (BET), pore size and total volume of pores were measured using a Micromeritics TriStar 3000 gas adsorption analyser. Prior to gas sorption analyses, samples were degassed overnight at room temperature and then incubated for 1 hour at 250°C.

X-ray diffraction (XRD) was carried out before and after silver adsorption to better understand the mechanisms of silver adsorption. For this purpose a Bruker Phaser D2 X-ray Powder Diffractometer (Cu radiation) was used to collect XRD spectrum between 5° and 65° incidence angle. The concentration of silver in aqueous solutions before and after adsorption by biochar was determined by ICP-AES, using a Varian Liberty Series II Spectrometer.

Scanning electron microscopy (SEM) combined with energy dispersive X-ray spectrometry (EDS) was used to determine the distribution of silver within the biochar after sorption tests. EDS mapping was performed in several biochar particles to check silver distribution in biochar after sorption tests.

6.3 Results and Discussion

6.3.1 The impact of pyrolysis conditions on biochar properties

According to Table 6.1, biochar specific surface area was mostly affected by temperature followed by activated carbon load, while residence time was the variable with least impact on BET. Higher pyrolysis temperatures produce biochar with higher surface area due to enhanced volatile organic compounds (VOC) release, which creates more pores in the final biochar structure. The biochar BET increased with a rise of AC load because AC has a high surface area contributing to increase the BET of final biochar, which is a mixture of biochar and AC. A second effect of the AC load on biochar BET is the heating rate; higher percentages of AC increase the heating rates that may lead to an increase of the gas pressure inside the biosolids particles, creating more pores in the final biochar. The residence time had the opposite effect; higher residence

time decreased the BET due to the shrinkage of particles in particular at high temperatures.

The total volume of pores (TVP) was mostly affected by AC size and pyrolysis temperature and less affected by residence time (Table 6.1). The total volume of pores increased with the increase in pyrolysis temperature due to a higher VOC removal, which contributes to an increase of the BET as mentioned. A significant impact on the TVP was observed by changing the fine to medium AC, but no changes on TVP were observed between medium and large AC. The fine AC produced biochar with higher TVP as this AC had small particles, which create uniform temperature across all sample during pyrolysis contributing to greater VOC release. Biochar samples produced with larger AC particles were not uniformly heated, since the hot spots (AC attracting the microwave energy) were fewer in number (bigger particles means fewer particles) and therefore hotter at the same applied power. They thus transferred thermal energy to the remaining sample by conduction, which would have led to a different heating profile in the sample.

The pore size of biochar was mainly affected by the AC loading; higher AC loads produced biochar with lower pore sizes. Higher AC loading can block the pores on the surface of the biochar and consequently stop the VOC release. The pyrolysis time had the opposite effect; longer pyrolysis time increased the pore size, which is related with a greater VOC removal. Pyrolysis temperature and AC size did not have a strong impact on biochar pore size.

6.3.2 Silver removal study

The silver removal capacity was tested with different biochar samples produced under different process conditions as presented in Table 6.1. These results show that biochar feedstock plays an important role in silver removal from aqueous solution. The specific surface area of biochar ranged between 38 and 151 m²/g, but the silver removal capacity did not increase with the increase of surface area or total volume of pores. The Ag removal capacity by biochar was mainly affected by the activated charcoal size and load, higher AC loads and larger AC particle sizes enhanced Ag removal by biochar.

These findings are similar to previous studies, where biochar with different BET had similar removal capacities. However, biochar produced from different feedstocks, but with similar BET exhibited different copper, lead, zinc and cadmium adsorption capacities [2]. The metal removal seems to depend on surface functional groups, which vary with biochar feedstock, but the pyrolysis conditions have less impact. However, it can be difficult to compare pyrolysis conditions in the literature due to the variety of pyrolysis systems, temperature measurement devices and different pyrolysis times. Table 6.2 shows the silver adsorption capacities of different adsorbents, which are significantly different and vary with the nature of adsorbent material. The biochar used in this study seems to perform well compared with stillage residue biochar and coconut shell activated carbon, but not with the bamboo biochar that has an exceptionally high silver removal capacity.

Table 6.2 – Ag-removal capacity of different adsorbents.

Adsorbent	Q_e (mg/g)	Source
Biosolids biochar	43.9	This study
Bamboo biochar	640.0	[209]
Stillage residue biochar	23.0	[218]
Coconut shell activated carbon	55.0	[219]

6.3.3 Adsorption kinetics

In the previous section results showed that biochar produced from biosolids can effectively remove silver from aqueous solutions, where activated charcoal size has the biggest impact on silver removal. From the Taguchi study, the sample with higher adsorption capacity was selected to better understand the potential mechanisms of Ag adsorption on biochar. Adsorption kinetic experiments were conducted and their data fitted to the two most used theoretical adsorption models, pseudo-first-order and

pseudo-second-order, which are represented by linearized equations (6.2) and (6.3), respectively:

$$\ln(Q_e - Q_t) = \ln Q_e - k_1 t \quad (6.2)$$

$$\frac{t}{Q_t} = \frac{1}{k_2 Q_e^2} + \frac{t}{Q_e} \quad (6.3)$$

where Q_e (mg/g) and Q_t (mg/g) represent the silver removal capacity at equilibrium and at time t , k_1 (h^{-1}) and k_2 (g/mg h) are the reaction rate constants.

The experimental data and the adsorption models are plotted in Figure 6.1, which shows that the pseudo-second-order ($R^2 > 0.99$) adsorption model fits the experimental data better than the pseudo-first-order model (Table 6.3). While the pseudo-first-order model is simpler, the pseudo-second-order model is a more comprehensive process model that can be used to describe multiple adsorption kinetic mechanisms, apart from surface interactions, such as external liquid film diffusion, surface adsorption and precipitation. However, both models did not fitted well the experimental data, but the plot of Q versus $t^{1/2}$ (Figure 6.2) showed a linear dependency of the Ag adsorption capacity against $t^{1/2}$, indicating that the intra-particle model should be considered when analysing the adsorption kinetics. This plot demonstrates multi-linearity, suggesting that each step represents different stages of adsorption. The most applied intra-particle diffusion model was developed by Weber and Morris and represented by equation (6.4):

$$Q_t = k_{id} t^{1/2} + C \quad (6.4)$$

where k_{id} ($\text{g}/(\text{mg h}^{1/2})$) is the intra-particle diffusion rate constant and C (mg/g) is a constant. The kinetic parameters of intra-particle diffusion model are presented in Table 6.3.

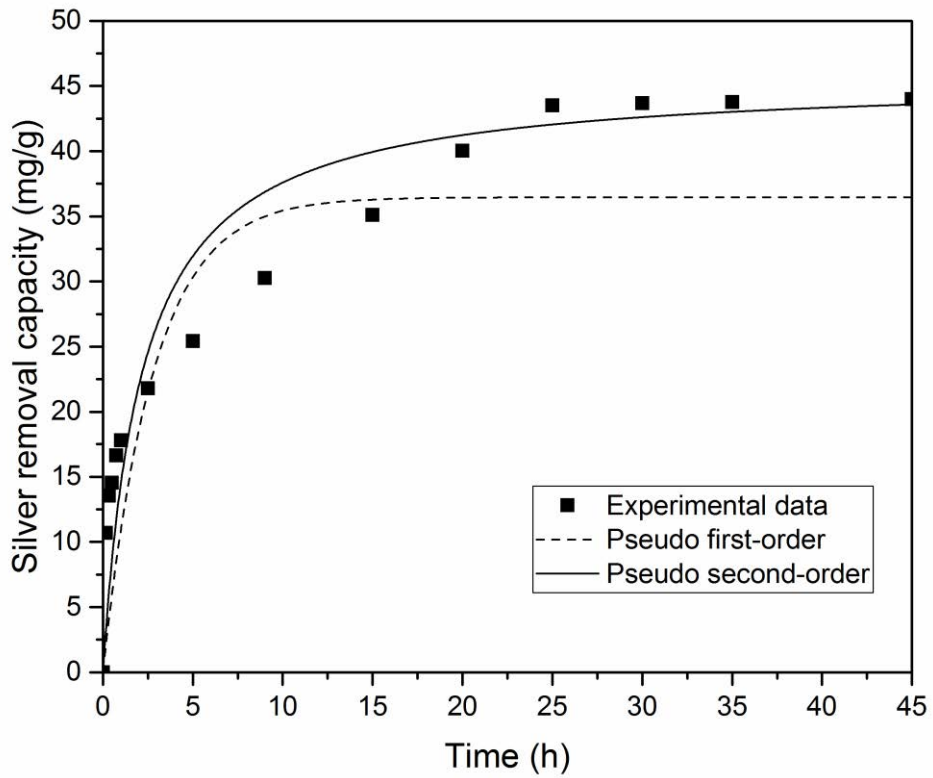


Figure 6.1 – Adsorption kinetics of silver by biochar.

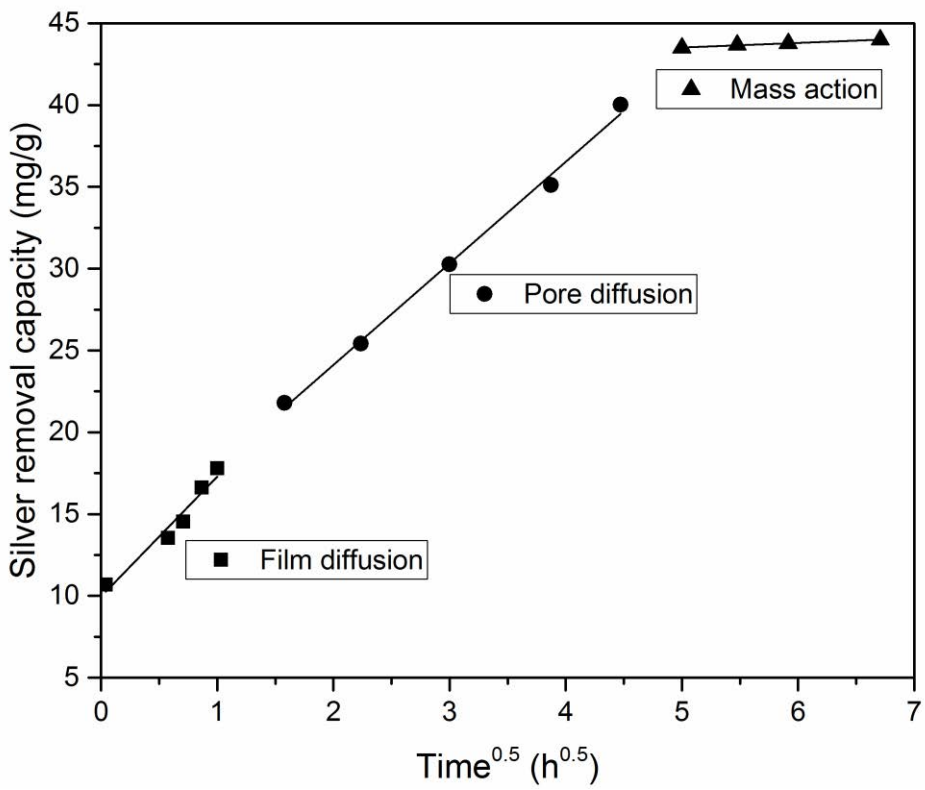


Figure 6.2 – Stages of intra-particle diffusion process of silver in biochar.

Table 6.3 – Adsorption kinetic parameters calculated using different kinetic models.

Kinetic model	Reaction/diffusion rate constant	Constant	R²
Pseudo first-order	$k_1 = 0.3567 \text{ h}^{-1}$	$Q_e = 36.4631 \text{ mg/g}$	0.9550
Pseudo second-order	$k_2 = 0.0102 \text{ g}/(\text{mg h})$	$Q_e = 45.6621 \text{ mg/g}$	0.9918
Intra-particle diffusion	$k_{id} = 5.6809 \text{ g}/(\text{mg h}^{1/2})$	$C = 11.6550 \text{ mg/g}$	0.9637

Table 6.3 shows that the pseudo-second-order model describes the experimental data better than the intra-particle diffusion model, but the plot of Q versus $t^{1/2}$ (Figure 6.2) suggests that three main stages must be considered to explain the overall process of intra-particle diffusion model. The first period (until 1 h) represents film diffusion or external diffusion. The second period (between 1 h and 20 h) corresponds to pore diffusion or internal diffusion, which is characterised by a slower rate due to the lower silver concentration in the solution and the large pore size of the biochar. The third period (after 24 h) is called mass action, corresponding to the adsorption of silver on the interior surface of pores and capillary spaces of biochar [220]. Both film diffusion and pore diffusion can be described by Fick's law [221], equation (6.5):

$$\frac{Q_t}{Q_e} = 6 \left(\frac{D_t}{r^2} \right)^{0.5} \left\{ \pi^{-0.5} + 2 \sum_{n=1}^{\infty} \sum_{n=1}^{\infty} \text{ierfc} \frac{nr}{D_t^{0.5}} \right\} - 3 \frac{D_t}{r^2} \quad (6.5)$$

where r is the adsorbent particle radius, considering that the adsorbent has a spherical shape, D_t is the diffusion rate (cm^2/s).

At small times when $Q_t/Q_e < 0.3$ [222], equation (6.5) can be approximated by equation (6.6), and the first diffusion rate (D_1) can be calculated from the slope of Q_t/Q_e versus $t^{0.5}$.

$$\frac{Q_t}{Q_e} = 6 \left(\frac{D_1}{\pi r^2} \right)^{0.5} t^{0.5} \quad (6.6)$$

At medium and large times, the silver uptakes can be described by equation (6.7):

$$\frac{Q_t}{Q_e} = 1 - \frac{6}{\pi^2} \sum_{n=1}^{\infty} \frac{1}{n^2} \exp\left(\frac{-Dn^2\pi^2 t}{r^2}\right) \quad (6.7)$$

At extended times, equation (6.7) can be simplified as:

$$\left(1 - \frac{Q_t}{Q_e}\right) = \frac{6}{\pi^2} \exp\left(\frac{-D_2\pi^2 t}{r^2}\right) \quad (6.8)$$

Considering $B = (D^2\pi^2/r^2)$ and the linearization of equation (6.8) can be written as:

$$Bt = -0.4977 - \ln\left(1 - \frac{Q_t}{Q_e}\right) \quad (6.9)$$

The Bt ($B \times t$) values calculated for different times were plotted versus t , and the pore diffusion coefficient value (D_2) was determined from the slope (B).

The film diffusion (D_1) and pore diffusion (D_2) coefficients are $1.09 \times 10^{-9} \text{ cm}^2/\text{s}$ and $1.65 \times 10^{-9} \text{ cm}^2/\text{s}$, respectively. These results show that the film diffusion is slower than the pore diffusion, which indicates that film diffusion governs the silver adsorption process by biochar. This conclusion was confirmed by the plot Bt versus t (Figure A1), presenting a linear relationship between Bt and t , but does not pass through the origin.

To further understand the adsorption behaviour, a dimensionless parameter (R_{id}) can be calculated for any time of the adsorption process using the intra-particle diffusion model at time t and t_{ref} :

$$Q_{ref} - Q_t = k_{id}(t_{ref}^{0.5} - t^{0.5}) \quad (6.10)$$

where t_{ref} is the longest time of adsorption, and Q_{ref} is the adsorption at time $t=t_{ref}$. Defining R_{id} as equation (6.11), then equation (6.10) can be rewritten as equation (6.12).

$$R_{id} = \frac{k_{id}t_{ref}^{0.5}}{Q_{ref}} \quad (6.11)$$

$$\frac{Q_t}{Q_{ref}} = 1 - R_{id} \left[1 - \left(\frac{t}{t_{ref}} \right)^{0.5} \right] \quad (6.12)$$

The R_{id} values calculated for the silver adsorption by biochar demonstrated that this adsorption process can be divided in three zones. In general, the R_{id} values are decreasing as the adsorption time increases, from 0.80 to 0.04. For adsorption times up to nine hours, $0.5 < R_{id} < 0.9$, showing that the adsorption is an intermediate process. Between nine hours and twenty hours, the adsorption process can be described as a strong physical adsorption ($0.1 < R_{id} < 0.5$), and after twenty hours the adsorption process is approaching completely initial adsorption. This final adsorption stage can be clearly observed in Figure 6.1, where the adsorption capacity increases very slowly with contact time.

6.3.4 Adsorption isotherms and thermodynamics of adsorption

To better understand the adsorption mechanisms, adsorption isotherms were used to provide an insight into the affinity between sorbent and adsorbent. The adsorption isotherms analyse the effect of initial concentration of silver in solution on silver

removal capacity by biochar, at a constant temperature and pH. For example, at room temperature (22°C), the adsorption capacity of silver by biochar doubled by increasing the initial silver concentration from 100 to 800 mg/L due to the increase of driving force of mass transfer between liquid and solid phase. The two most used isotherm models, Langmuir and Freundlich, (linear equations (6.13) and (6.14), respectively) were used to fit the experimental data obtained at 22, 35 and 45°C. The Langmuir model describes simple mechanisms, such as monolayer adsorption and requires an homogenous surface, while the Freundlich model is more comprehensive, considering the intermolecular interactions between sorbent and adsorbent [223].

$$\frac{C_e}{Q_e} = \frac{1}{Q_m K_L} + \frac{C_e}{Q_m} \quad (6.13)$$

$$\ln Q_e = \ln K_F + \frac{1}{n} \ln C_e \quad (6.14)$$

The adsorption capacity is represented by the model constants (K_F (L/g)^{1/n} and K_L (L/g)), the Freundlich exponent (n) characterises the adsorption intensity and Q_m (mg/g) is the maximum adsorption capacity. The fitting parameters of these two isotherm models and the correlation coefficients are listed on Table 6.4, while Figure 6.3 illustrates the fit of the Langmuir model to the experimental data at varying temperatures.

The Langmuir model describes the experimental data ($R^2 > 0.99$) better than the Freundlich model ($R^2 > 0.92$). The Langmuir model represents an elementary adsorption process, which means that the adsorption sites of biochar are homogenous and no lateral interaction occurred between the absorbed silver molecules [224]. The silver removal by biochar is mainly due to physical adsorption and reduction of silver ions as demonstrated by XRD (Figure 6.6). Moreover, Figure 6.3 shows that the adsorption process depends on temperature, the silver removal capacity and the maximum silver removal adsorption increase as the temperature increases from 22 to 45°C. This conclusion was also confirmed by the variation of Gibbs energy values with

temperature Table 6.5. Conversely, the Langmuir constant rate (K_L) decreased as the temperature increases indicating an exothermic process as demonstrated by the adsorption enthalpy (Table 6.5).

Table 6.4 – Isotherm parameters of Ag adsorption by biochar at different temperatures.

Temperature (°C)	Langmuir			Freundlich			
	K_L	Q_m	R^2	R_L	K_F	$1/n$	R^2
22	0.0096	48.3092	0.9969	0.0947	7.2442	0.2683	0.9284
35	0.0057	63.2911	0.9947	0.1487	5.7875	0.3291	0.9572
45	0.0046	84.0336	0.9934	0.1797	4.7693	0.3947	0.9192

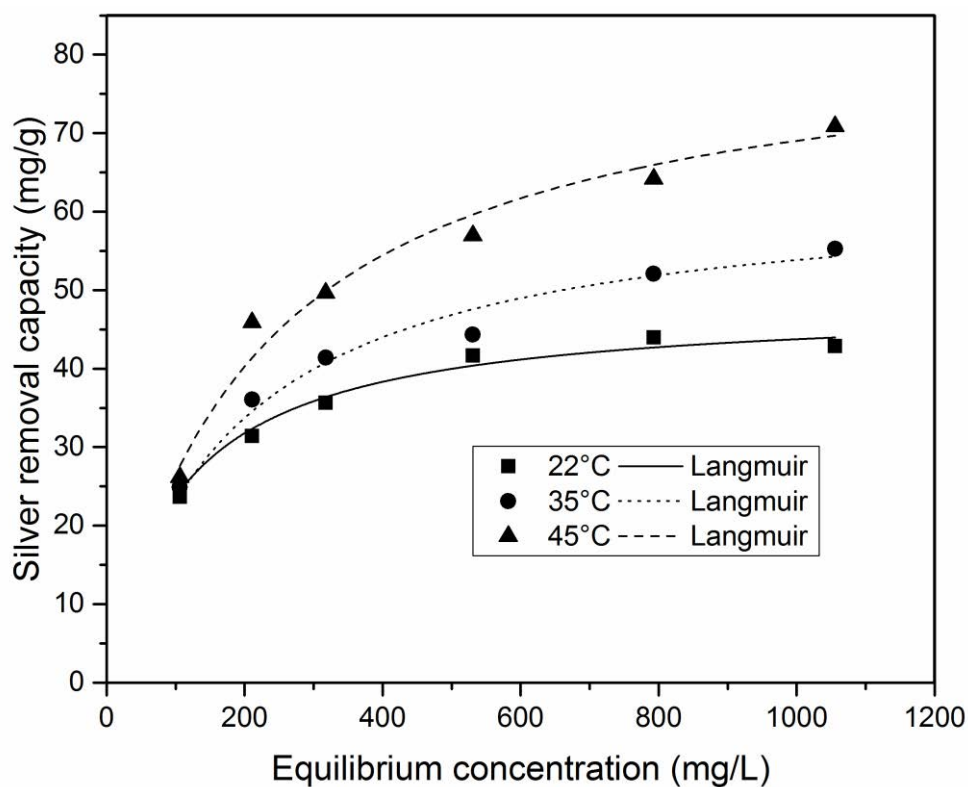


Figure 6.3 – Adsorption isotherms of silver removal by biochar across a range of temperatures.

The equilibrium factor (R_L) calculated by equation (6.15) is a dimensionless parameter used to assess whether the adsorption process is favourable, where K_L is the Langmuir constant and C_0 is the highest silver concentration (1000 mg/L). In this study, the R_L was less than 1 (Table 6.4), indicating that the adsorption of silver by biochar is a favourable process. However, the R_L value decreases with temperature, suggesting that the adsorption process is less favourable at higher temperatures as confirmed by the Gibbs energy results displayed in Table 6.5.

$$R_L = \frac{1}{1 + K_L C_0} \quad (6.15)$$

Thermodynamic parameters (Table 6.5) of the adsorption of silver onto biochar were calculated from Langmuir isotherm using equations (6.16) to (6.18) [225]. The thermodynamic parameters in conjunction with the adsorption kinetics are fundamental to obtain a better understanding of the nature of the Ag removal process using biochar.

$$K = K_L M_{Ag} \quad (6.16)$$

$$\Delta G = -RT \ln(K) \quad (6.17)$$

$$\ln(K) = \frac{\Delta S}{R} - \frac{\Delta H}{RT} \quad (6.18)$$

where ΔG (J/mol) is the Gibbs energy, K_L is the Langmuir constant, M_{Ag} is the molecular weight of silver in mg/mol, R is the ideal gas constant (8.314 J/mol K), T is the temperature in Kelvin (K), ΔS (J/mol K) is the adsorption entropy and ΔH (J/mol) is the adsorption enthalpy. The Gibbs energy was calculated for each temperature using equation (6.17). The adsorption enthalpy and entropy were determined by plotting $\ln(K)$ vs $1/T$ and using equation (6.18), where entropy was calculated via the intercept, and the enthalpy was calculated from the slope. The negative values of ΔG at different

temperatures suggest that the silver adsorption onto biochar is a spontaneous process, which is typical in physical adsorption as confirmed by this study. The ΔG values were in the range between -20 and 0 kJ/mol, which are typical for physical adsorption [226]. These ΔG values demonstrated that the silver removal by biochar was a physical adsorption process. In addition, ΔG increases with temperature indicating that lower temperatures are more favourable to the Ag adsorption than higher temperatures. The negative value of ΔS indicates a decrease in the degree of randomness during the adsorption process of silver by biochar from the aqueous solution.

The negative value of ΔH indicates that the Ag adsorption by biochar is an exothermic process, which confirms that the adsorption is more favourable at lower temperatures [7]. The ΔH value (-25.41 kJ/mol) was less than 50 kJ/mol, which suggests that the van der Waals force was the main interaction between sorbent and adsorbent, and can be attributed to physical adsorption [227]. This result is in line with the findings in adsorption kinetic section (section 5.3.3), where the intra-particle diffusion model described well the experimental data. The physical adsorption was the predominant mechanism for silver removal from aqueous solution, but also the reduction of Ag^+ into Ag nanoparticles was carried out by the biochar surface as demonstrated by XRD results.

Table 6.5 – Thermodynamic parameters of the adsorption of Ag on biochar.

Temperature (°C)	ΔG (kJ/mol)	ΔH (kJ/mol)	ΔS (J/mol K)	R^2
22	-17.03			
35	-16.46	-25.41	-28.57	0.9847
45	-16.40			

6.3.5 Characterisation of Ag-biochar

SEM-EDS and XRD analyses were performed before and after silver adsorption to better understand the adsorption mechanisms. The SEM-EDS mapping analysis (Figure 6.4) indicated that silver is homogeneously distributed in the biochar after silver removal; however, this analysis is just a qualitative indication of silver distribution as this technique works well with flat surfaces, which is not the case for these biochar particles. This figure also reveals that biochar particles have irregular shape and the silver precipitated as nanoparticles on the surface of biochar.

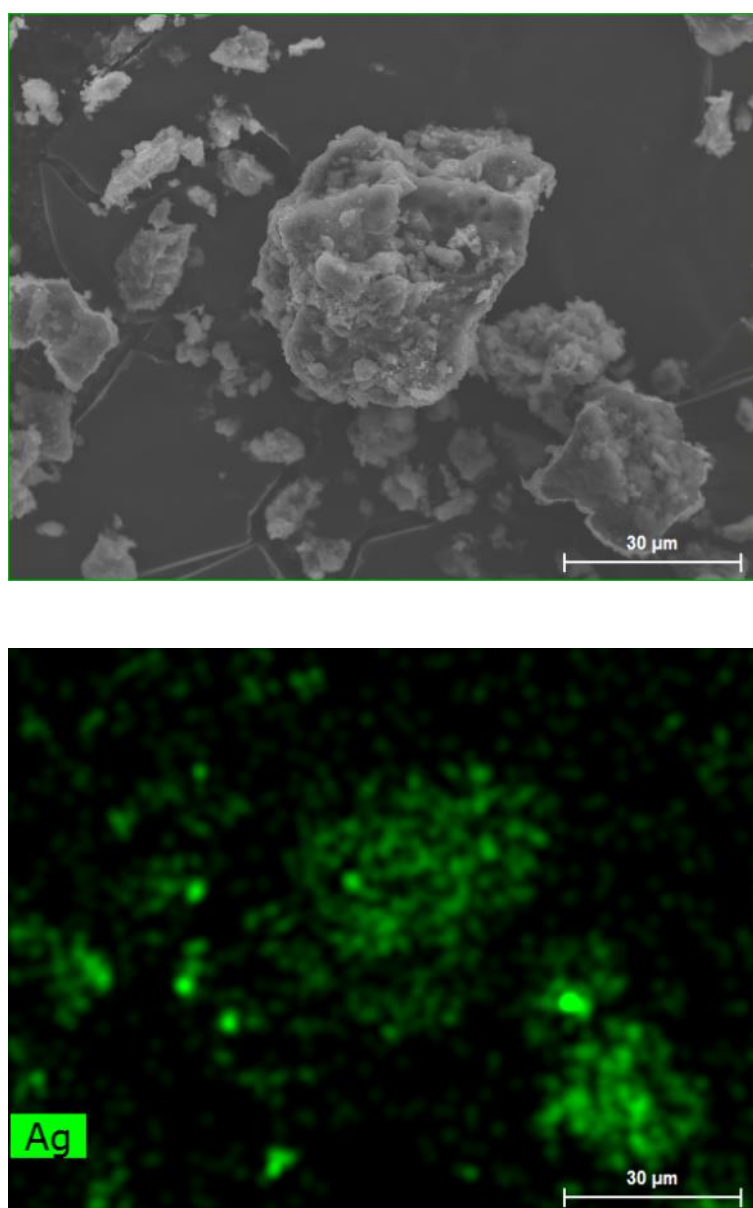


Figure 6.4 – Biochar after silver adsorption (EDS mapping).

The EDS analyses (Figure 6.5) showed that the initial biochar does not contain any silver while after adsorption tests, silver peaks were clearly identified. Besides silver, the SEM-EDS analyses revealed the presence of Ca, Al, Fe, Mg P, Si, C and O which are elements presented in the biosolids and consequently in the biochar.

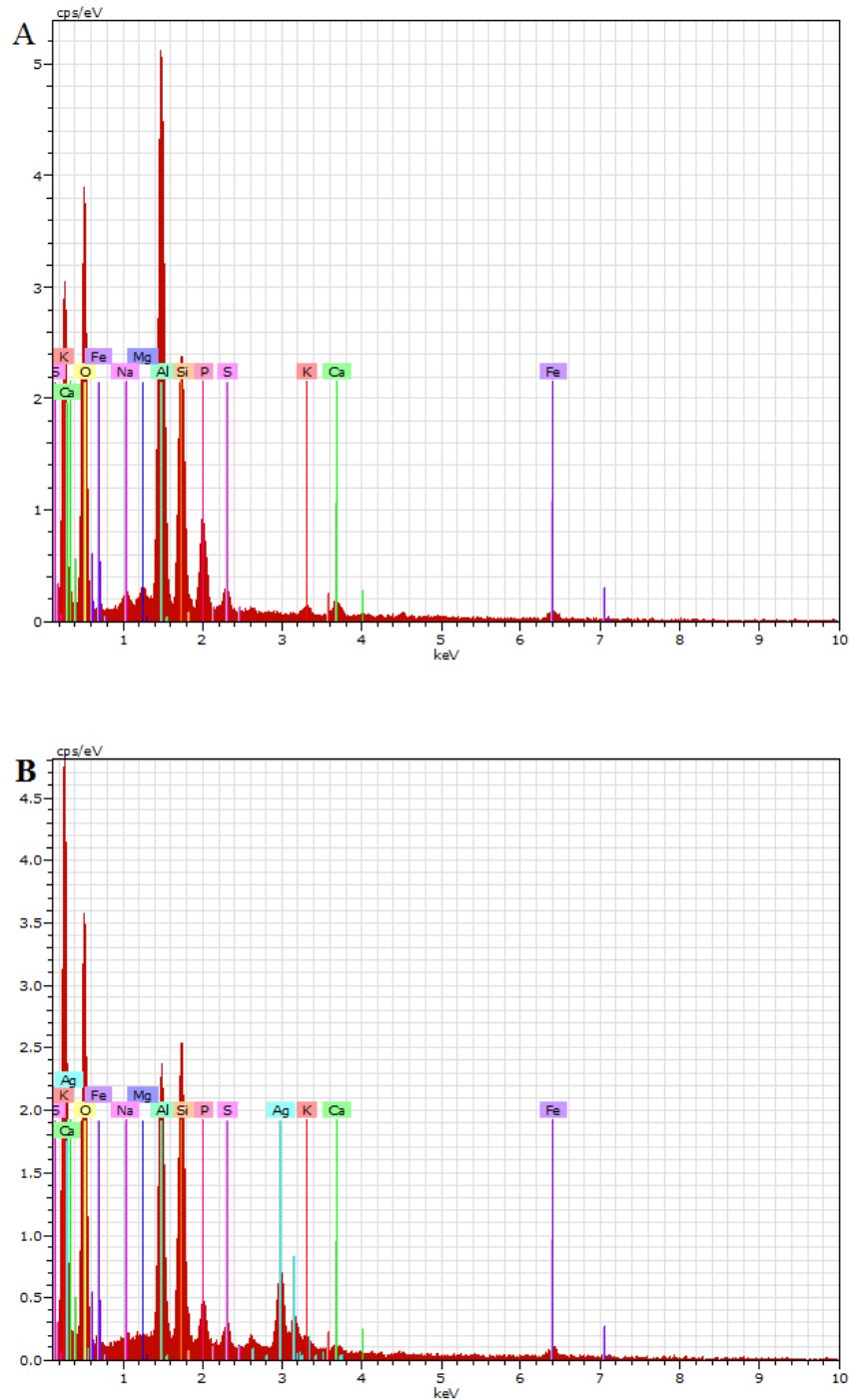


Figure 6.5 – EDS of biochar before adsorption (A) and after silver adsorption (B).

The XRD spectrum analysis of biochar before and after silver adsorption is shown in Figure 6.6. The XRD complements the SEM-EDS analyses, and confirms the silver presence in the biochar after adsorption tests, which was not identified in the original biochar. The presence of metallic silver in biochar indicated that Ag ions in aqueous solution were reduced and then adsorbed on the surface and pores of biochar as reported by other studies [218, 219].

The crystallite size of silver was calculated from the XRD by using the Scherrer equation (6.19), which is used to determine the crystallite size of nanoparticles.

$$D = \frac{K \lambda}{B \cos\theta} \quad (6.19)$$

where, D (nm) is the mean size of the ordered (crystalline) domains, K is the shape factor with a typical value of 0.9, λ is the X-ray wavelength (0.154051 nm for Cu K α radiation), B is the FWHM of diffraction peaks, and θ is the Bragg angle (in degrees). The average size of crystal particles of silver in biochar was 58.8 nm based on the most intense XRD peak. This result is in line with the EDS mapping and confirms that a new nanocomposite (silver nanoparticles on biochar surface) was formed after silver adsorption by biochar. This new nanocomposite could perhaps be used for applications, such as, antimicrobial ability [209, 218], and methylene blue degradation, as demonstrated in this study.

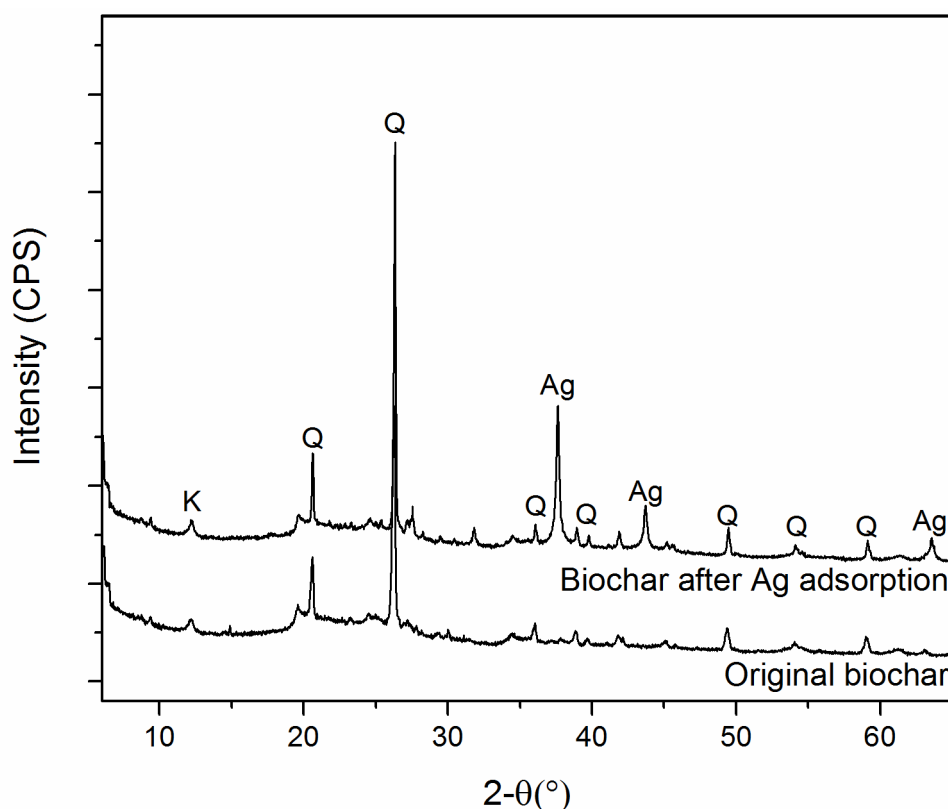


Figure 6.6 – XRD spectrum of biochar before and after silver adsorption (Q: quartz, Ag: silver; K: kaolinite).

6.3.6 Applications of nanocomposite Ag-biochar

The final nanocomposite Ag-biochar was tested for methylene blue adsorption and photocatalytic degradation. The results showed that the methylene blue was removed from aqueous solution mainly due to physical adsorption. The photodegradation of MB by the nanocomposite was residual when compared with physical adsorption for similar reaction times mainly because the physical adsorption process was much faster than photodegradation. For example, for 10 minutes of contact time, the adsorption process reduced the concentration of MB in 50% while the photodegradation reduced in 6%. For longer contact times, the physical adsorption was still much higher than the photodegradation of MB. However, these results showed that the final nanocomposite Ag-biochar is a promising product for MB reduction in water streams.

6.4 Conclusions

The results of this study demonstrated that silver was effectively removed by biochar from an aqueous solution. The intra-particle diffusion model described well the experimental data showing three main steps: external diffusion, internal diffusion and mass action. The Langmuir isotherm model described better the experimental data ($R^2 > 0.99$) than the Freundlich model. The increase of both silver concentration and temperature impacts positively on silver removal onto biochar. The thermodynamic analysis demonstrated that silver adsorption onto biochar is an exothermic process. As the temperature increases, the Gibbs energy increases indicating that the silver removal process is more favourable at lower temperatures. The silver removal process was mainly a physical adsorption mechanism, but XRD analyses demonstrated that the Ag ions were reduced by the biochar surface. Biochar produced from biosolids is a low-cost adsorbent with great potential for silver removal from an aqueous solution and the reuse of the final nanocomposite (Ag-biochar) for methylene blue adsorption and photodegradation is a promising approach to recycle this material.

This study demonstrated that batch adsorption of silver by biochar is an effective approach to mitigate the environmental impact of silver. However, at a large scale, the adsorption should be in a continuous process to deal with the high amount of wastewater, which may require several biochar columns to minimise the downtime of the plant. Therefore, further studies should be carried out in a continuous process to predict the breakthrough point in large scale plants, investigate possible solutions to increase the lifetime of biochar columns and optimise operation conditions.

7 HEAVY METALS IN BIOSOLIDS

Abstract

Heavy metal content in biosolids limits its land application. This study investigated the heavy metal leaching from biosolids compared with biochar produced from the same biosolids via microwave assisted pyrolysis (for 10, 20, 30 and 45 minutes at 500°C and 700°C). The results showed that the heavy metals concentrated in the biochar, except for the longest pyrolysis time (45 minutes) where a small amount of heavy metals volatilised. A modified toxicity characteristic leaching procedure (TCLP) showed that pyrolysis enhanced the heavy metals stability, as the heavy metal leaching from biochar was much lower than that from biosolids. The addition of lime to biosolids before pyrolysis significantly decreased the heavy metals and aluminium leaching. The biochar produced from limed biosolids presented the lowest metal leaching with a total less than 8 mg/kg. Moreover, the aluminium leaching from this biochar was reduced to 13.6 mg/kg. This study showed that biochar produced from limed biosolids can be safely used for land application. The SWOT analysis demonstrated that pyrolysis has a lower environmental impact than incineration, land application and landfilling.

Keywords: aluminium leaching; biochar; biosolids; metal leaching; microwave pyrolysis.

Highlights

- Heavy metals concentrated in biochar during pyrolysis.
- Heavy metal leaching from biochar was much lower than from biosolids.
- Heavy metals and aluminium leaching from biochar produced from limed biosolids is much lower than from biochar obtained from un-limed biosolids.
- Both time and pyrolysis temperature impacted on biochar yield.

As submitted in: Antunes, E., Schumann, J., Jacob, M. V., Schneider P. A., “*Heavy metal leaching from biochar produced from biosolids via microwave assisted pyrolysis: implications for land application*”, Journal of Environmental Chemical Engineering.

7.1 Introduction

Biosolids are the solid waste by-product of the sewage treatment process and contain agronomically important nutrients, such as phosphorus, potassium and nitrogen [56]. Biosolids are rich in organic matter and, when applied to land, increase soil organic carbon content, improve the water holding capacity, water infiltration and ease of cultivation [228]. For this reason, it is desirable to apply biosolids to land to utilise these nutrients. However, the presence of heavy metals in biosolids can prevent them being used in this beneficial manner. Biosolids may contain a range of heavy metals, such as lead, cadmium, chromium, and high amounts of aluminium introduced during the sewage treatment process as coagulant [229]. These heavy metals can leach into the environment when the biosolids are applied to land. Moreover, the presence of heavy metals also increases the difficulty of storing biosolids as there is the risk of soil and water contamination around the storage area.

Heavy metal content, pathogens and persistent organic pollutants in biosolids have forced legislative change and, consequently, biosolids management approaches. For example, in Europe land application of biosolids was the primary disposal method, but public opposition and health risks, because of the contamination of soil and groundwater with heavy metals and emerging organic micro-pollutants, have restricted this approach [230]. Some countries have recently used incineration to convert sludge into energy, since dry sludge calorific value is similar to low-grade coal [53]. In this approach, sludge dewatering is required to enhance the energy balance, but when sludge is combined with coal or other wastes, or when the sludge is incinerated in cement kilns, the energy balance is positive [48]. Air-born emissions and final disposal of ashes are extra problems emerging from this method. Currently, ashes (approximately 30% of dry sludge) have been used for road construction and concrete building materials, which are effective alternatives [231].

Biosolids management costs, pollutant content and global demand for resources are the main reasons for developing new environmentally sustainable solutions to manage biosolids [232]. One solution that prevents the leaching of contaminants to the environment, whilst preserving the beneficial agronomic properties of biosolids, is microwave assisted pyrolysis (MWAP). Pyrolysis is a thermochemical process where an

organic mass is heated in an oxygen-free environment, causing the biomass to thermally decompose into non-condensable gases (collectively called syngas), condensable volatiles (recovered as oils) and a solid biochar product [233]. MWAP is a type of pyrolysis where the heating energy is supplied via microwave energy. The biomass is usually mixed with a material, termed a susceptor, which absorbs then reemits microwave energy as heat, allowing the material to reach temperature for pyrolysis. These susceptors improve energy efficiency of the process by reducing the energy reflection by the sample and to increase the heating rate [70, 107].

The non-condensable and volatile by-products of MWAP are useful for energy and/or chemical production, while the biochar may be used as a solid fuel. However, the biochar also contains a significant amount of ash, leading to slagging problems [234]. The key benefit of the biochar is the heavy metals are incorporated into this char matrix due to the pyrolysis process [67]. Heavy metals are not well incorporated into the fly ash from incineration, presenting a contamination concern [235]. Moreover, investment capital and operating costs of incineration are very high, making pyrolysis a potentially better alternative for biosolids management [236]. As pyrolysis-derived biochar better incorporates heavy metals, their leaching is suppressed allowing the material to be more safely applied to land. Unlike fly ash, biochar also retains the bio-available phosphorus, nitrogen and organic carbon of biosolids, so still provides benefit when used as a soil ameliorant [237, 238].

This study treated biosolids from Victoria, Australia, that have been stored in long-term (more than two decades), open-air stockpiles. Unlike other biomass materials that have been used as a feedstock for MWAP [108], the volatile matter of these biosolids had been significantly degraded due to storage and exposure to the elements. There are over 1.5 million dry tonnes of similar biosolids stockpiled throughout Victoria with no identified method of beneficial use due to the presence of heavy metal contaminants [28]. The goal of this study was to use MWAP produce a biochar from these biosolids that could be applied to land as a soil ameliorant without risk of losses due to leaching. Previous studies have demonstrated that heavy metal leaching from biochar is much lower than from biosolids; however, this study analyses the impact of both pyrolysis time and temperature on subsequent heavy metal leaching from biochar. Also, this study compares the heavy metal leaching between biochar produced from un-limed and limed

biosolids. The three main objectives of this research are: first, explore the impact of pyrolysis conditions on pyrolysis by-products distribution; second, assess the effect of pyrolysis time and temperature on heavy metal content in biochar and heavy metal leaching; and third, evaluate the impact of lime addition to biosolids on heavy metal leaching from biochar. In the last section, a SWOT analysis compared four current biosolids management approaches: pyrolysis, land application, landfilling and incineration. This comparison focused mainly on the environmental impact of these four options.

7.2 Materials and Methods

7.2.1 Biochar production

Biochar was produced from biosolids via microwave assisted pyrolysis at 500°C and 700°C for different pyrolysis times (10, 20, 30 and 45 minutes). The biochar samples were named according to the pyrolysis temperature followed by pyrolysis time, for example: BC500-10 (biochar prepared at 500°C and pyrolysis time of 10 minutes). Prior to pyrolysis, the biosolids (Euroa Wastewater Treatment facility in Victoria, Australia) with approximately 40% moisture content were blended with 10% by weight activated carbon (obtained from Sigma Aldrich - Ref. 242276). Activated carbon was used as a microwave susceptor because dry biosolids are essentially transparent to microwaves. Mixture samples with 80.0 ± 0.5 g were pyrolysed in a customised single-mode microwave with a maximum output of 1.2 kW, described elsewhere [13]. Nitrogen (99.9% purity) with a flow rate of 11 L/min (corresponding to residence time of 6.4 seconds) was used to obtain an inert atmosphere during pyrolysis.

Biochar yield was determined according to equation (7.1):

$$\text{Biochar yield (\%)} = \frac{A - C}{B} \times 100 \quad (7.1)$$

where A is the weight of dry biochar, B is the weight of dry biosolids, and C is the weight of the activated carbon used as a microwave absorber.

Oil yield was determined according to equation (7.2):

$$\text{Oil yield (\%)} = \frac{O}{B} \times 100 \quad (7.2)$$

where O is the dry mass of oil and B is the weight of dry biosolids. The gas yield was calculated by difference.

7.2.2 Chemical composition of biochar

The chemical composition of biochar and supernatant from metal leaching were assessed by Inductively Coupled Plasma - Mass Spectrometry (ICP-MS), using a Varian 820-MS Mass Spectrometer. Before ICP-MS analysis, the biochar samples were dissolved using microwave digestion with nitric acid and hydrogen peroxide.

7.2.3 Heavy metal leaching

The heavy metal leaching from biochar and biosolids was assessed based on the method 1311 – Toxicity characteristic leaching procedure (TCLP) [239]. In this study, 5 g of solid material was used, instead of 100 g as suggested by the method 1311, but the solid mass to extraction fluid ratio was kept as 1:20. Since the pH of all samples (biosolids and biochar) was above 5, just one extraction fluid was prepared. The extraction fluid was prepared by diluting 5.7 ml of glacial acetic acid with distilled water to a volume of 1 L; the pH of extraction fluid was equal to 2.88 ± 0.05 . A quantity of solid material (5 g) was placed in an extraction vessel (pyrex) and 100 ml of the extraction fluid was added. The mixture was agitated for 18 ± 1 h at room temperature ($23 \pm 2^\circ\text{C}$) in a rotary agitation unit. Subsequently, the mixture was filtered using a $0.45 \mu\text{m}$ polytetrafluoroethylene (PTFE) membrane and the heavy metal (As, Cd, Cr, Cu, Ni, Pb and Zn) concentration in the supernatant was analysed by ICP-MS.

7.2.4 Statistical analysis

The impact of pyrolysis temperature and pyrolysis time on heavy metal leaching, and the interactions between these two variables were evaluated using a two-way ANOVA. Statistically significant differences were considered when $p < 0.05$.

7.3 Results and discussion

7.3.1 Pyrolysis by-product yields

The pyrolysis by-product yields obtained with varying pyrolysis conditions are shown in Figure 7.1. In general, the oil yield was very low (less than 1.5%) for any of the pyrolysis conditions, but it increased marginally with pyrolysis time. For both pyrolysis temperatures, the highest mass loss occurs from 0 to 5 min, which is where the least bio-oil was produced, indicating that reactions that produce lighter, non-condensable gases dominate early in pyrolysis. As the pyrolysis proceeds, the mass loss decreases, while the of bio-oil production increases. As the pyrolysis time increases, the gas fraction becomes the predominant by-product from biosolids. At 500°C, the gas fraction reached 48% of the by-products for pyrolysis time of 30 minutes while for 700°C this value was reached within 15 minutes.

For both pyrolysis temperatures, 500°C and 700°C, the oil yield increased until 20 minutes, plateauing at 30 minutes. This suggests that not all the volatile matter was thermally decomposable in the oxygen-free environment. The oil yield obtained at 500°C was higher than at 700°C because, at temperatures above 500°C, the oil yield decreases due to secondary tar reactions, such as thermal cracking, which increases gas yield [109]. The low volatile content in the biosolids feedstock was due to the long storage period and was likely the reason for the low oil yield.

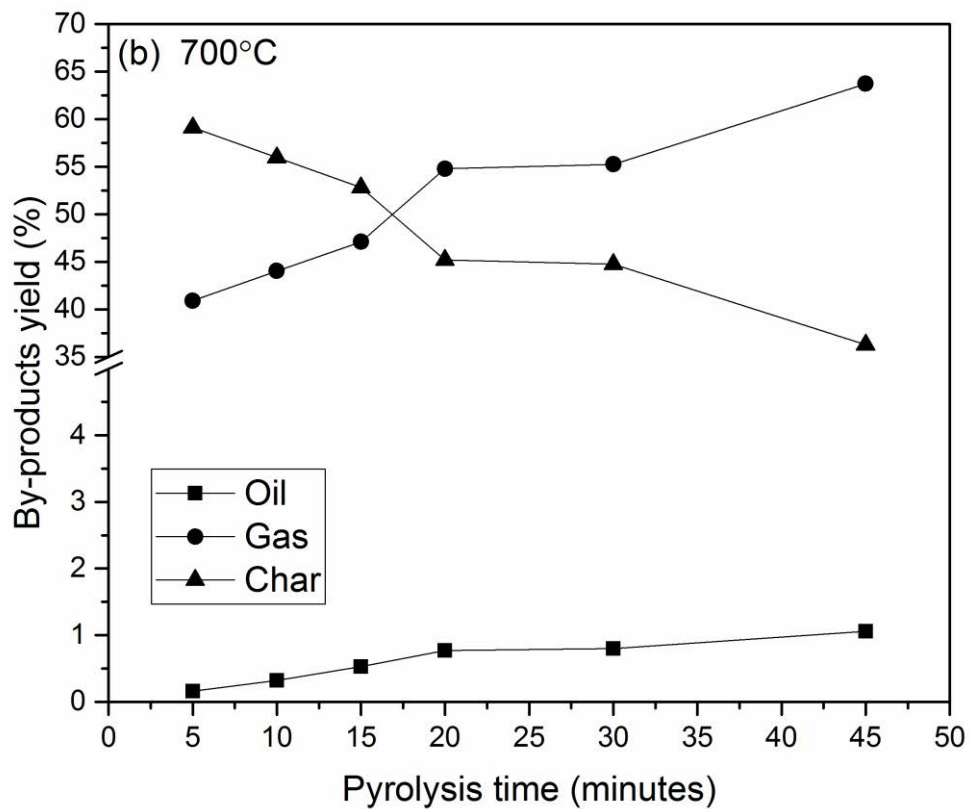
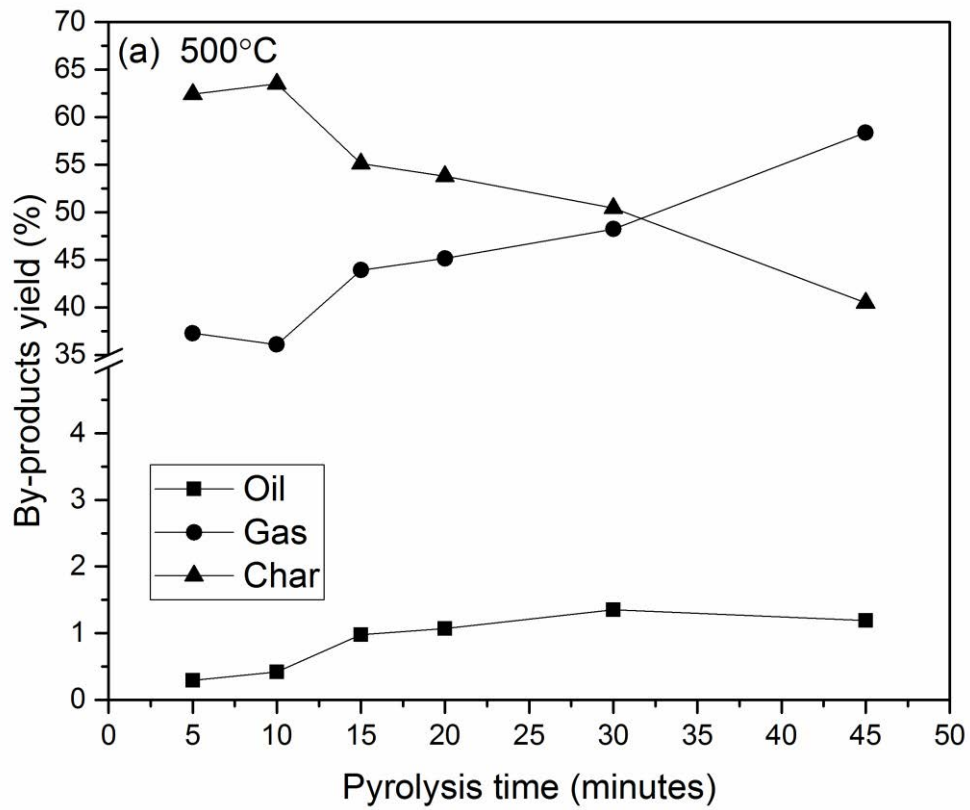


Figure 7.1 – Pyrolysis by-product yields versus pyrolysis time at 500°C (a) and 700°C (b).

Due to the low oil yield, these biosolids are not a good feedstock for oil production, but a promising biomass for biochar and biogas production. The biochar yield decreased with temperature and pyrolysis time and the biogas yield increased at similar ratio. At 700°C the biogas yield increased more with pyrolysis time than at 500°C due to higher volatile organic compound release at higher temperatures. For both pyrolysis temperatures, biochar yield decreased linearly with pyrolysis time at a similar rate and did not plateau, as there was remaining volatile matter in the sample. Of the available volatile matter, only up to 59.54% and 64.77% were pyrolysed, for 500°C and 700°C, respectively. The two-way statistical analyses showed that pyrolysis temperature, pyrolysis holding time and their interactions have significant impact on biochar yield ($p < 0.05$).

7.3.2 Heavy metal in biochar

The heavy metal content in biochar was determined at both 500°C and 700°C for the 10, 20, 30 and 45 minute processing times. Biochar produced at 5 and 15 minutes pyrolysis time were not analysed, since 5 minutes was insufficient for complete pyrolysis and preliminary results indicated that 15 minutes was not significantly different from 10 minutes. The concentration of cadmium in all biochar samples varied between 0.74 and 0.89 mg/kg, below the requirements for biochar land application [187]. The biochar samples produced at 700°C contained a higher proportion of heavy metals than the samples produced at 500°C due to the concentration of the heavy metals in the biochar from the increased mass loss. Figure 7.2 shows that at 700°C the heavy metals concentration increases with pyrolysis time until 30 minutes, but the sample produced with 45 minutes of pyrolysis time contains less heavy metals than the sample produced with 30 minutes. This reduction on the heavy metal concentration is more significant for chromium, nickel and lead, which can be explained by the volatilisation of these elements due to the presence of chloride in the biosolids. This phenomenon of volatilisation of heavy metals was reported by other studies and is related to the heavy metal forms in biosolids, namely, sulphides and chlorides and pyrolysis conditions [36, 240].

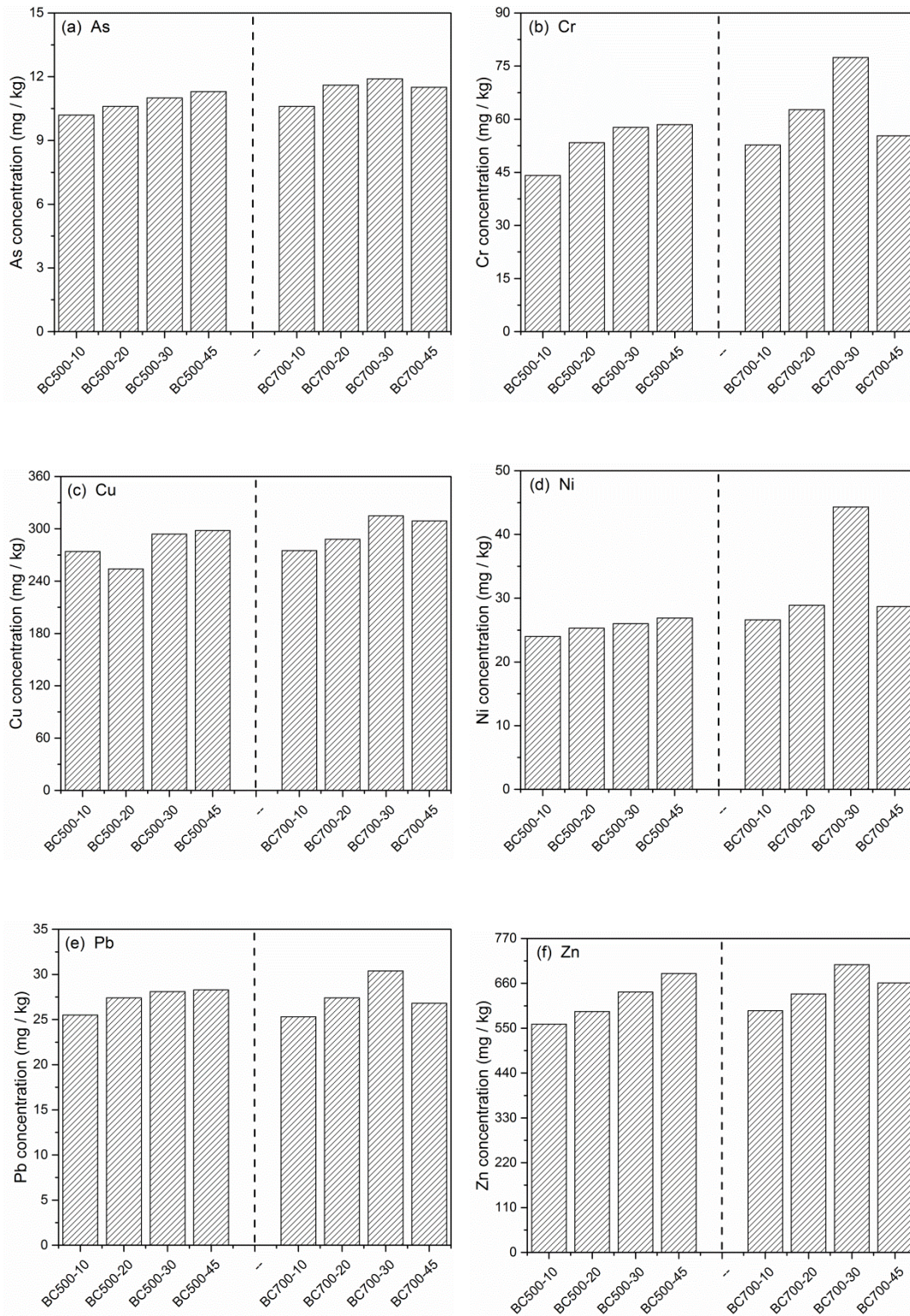


Figure 7.2 – Concentration of heavy metals As (a), Cr (b), Cu (c), Ni (d), Pb (e) and Zn (f) in biochar samples produced at 500°C and 700°C for different pyrolysis times.

The biosolids used in this study were grade C2 due to the concentration of copper, selenium and zinc, while the remainder of the heavy metals present meet the

requirements of grade C1 [177]. The biochar samples produced via microwave pyrolysis have the same trend as the heavy metals did not volatilise during the process except for longer pyrolysis times (45 minutes). However, the concentration of heavy metals in biochar was higher than in biosolids due to the volatile organic matter release during the pyrolysis process, but all biochar samples meet the requirements for land application [187].

7.3.3 Heavy metal leaching from biosolids and biochar

Heavy metal leaching from biosolids and biochar produced under varying pyrolysis conditions was assessed using the TCLP method, indicated in Table 7.1. Heavy metal leaching from biochar is significantly lower compared with the biosolids sample. The Cd and Cr leaching from biochar were very low to below the detection limit of the instrument, while from biosolids was respectively 0.22 and 0.45 mg/kg. The Cu, Ni, Pb and Zn leaching from biosolids was 2.95%, 7.64%, 11.09% and 37.52%, respectively, while the average of all biochar samples produced at 500°C and 700°C was 0.21%, 4.30%, 6.70% and 21.08% respectively. Nickel leaching from biosolids was 7.64%. Nickel did not leach from biochar samples, except for the biochar samples produced with 10 minutes of pyrolysis time. On the other hand, arsenic leaching from biochar samples was higher than from biosolids (4.27%). This is not a problem, though, since the arsenic concentration in biochar and biosolids was lower than 12 mg/kg. The reduction of heavy metal leaching from biochar produced at 500°C and 45 minutes of pyrolysis time was due to the increase of specific surface area and total volume of pores, which enhanced sorption of heavy metals in biochar [188]. Also, the biochar basicity is contributing to stopping metal leaching from biochar because of the presence of alkaline-earth metals (biosolids sample contains 6.9% Ca and 1.9% Mg) [236]. The reduction of Cu leaching from biochar is mainly due to the adsorption of this element by functional groups in biochar [215].

The aluminium content in the biosolids used in this study was 6.2% (based on dry mass of biosolids). The percentage of aluminium is high and may represent a problem for plant growth, since it may be phytotoxic. Therefore, aluminium leaching from biosolids and biochar was assessed and was approximately 800 mg/kg for both products (biosolids and biochar). The data showed that aluminium leaching from biochar is

higher at 700°C than at 500°C and increases with pyrolysis time, which can be explained by the elimination of hydroxide and carboxylic groups at elevated temperatures. However, these aluminium concentrations may well prevent land application of both biosolids and biochar. Aluminium is phytotoxic for plants and also can be combined with phosphorus, limiting its plant uptake.

Table 7.1 – Heavy metal leaching from biosolids and biochar produced with different pyrolysis conditions using TCLP method.

Material	As mg/kg	Cu mg/kg	Ni mg/kg	Pb mg/kg	Zn mg/kg
Biosolids	0.40	6.96	1.89	2.70	205.60
BC500-10	0.76	1.16	1.11	2.30	140.40
BC500-20	0.60	-	-	2.24	125.00
BC500-30	0.80	0.51	-	2.25	124.60
BC500-45	0.82	0.59	-	2.75	124.60
BC700-10	0.78	1.00	1.06	1.49	137.40
BC700-20	0.80	0.68	-	3.20	140.60
BC700-30	1.00	0.76	-	0.87	129.80
BC700-45	0.80	-	-	1.13	118.00

- Below detection limit

7.3.4 Metal leaching from biochar obtained from limed biosolids

Lime addition to sewage sludge has been used as an inexpensive stabiliser. Lime stabilisation increases the pH of sewage sludge, reduces odour generation, vector attraction and pathogen content due to high pH (≥ 12) for extended periods and rise of

temperature [241]. While lime addition also slightly increases biosolids volume, it makes biosolids safer for land application and can be beneficial for acid soils, avoiding an extra addition of agriculture lime. Because of these reasons, lime stabilisation is widely used in municipal wastewater treatment plants. In this study, a comparison of metal leaching from biochar produced from biosolids and biochar produced from limed biosolids was made.

Biosolids and limed biosolids were pyrolysed at 700°C for 20 minutes. These conditions were selected according to previous results that showed biochar with one of the highest heavy metals content. The main crystalline phase of biochar is quartz, which is also the main inorganic chemical compound in the biosolids feedstock used [13]. The lime in biosolids was transformed into calcite (calcium carbonate) during pyrolysis, as lime reacted with carbon dioxide produced during pyrolysis to form calcite (Figure 7.3). Calcite is a stable phase with low solubility in water, which does not present a problem for land application concerning calcium run-off to soil and water.

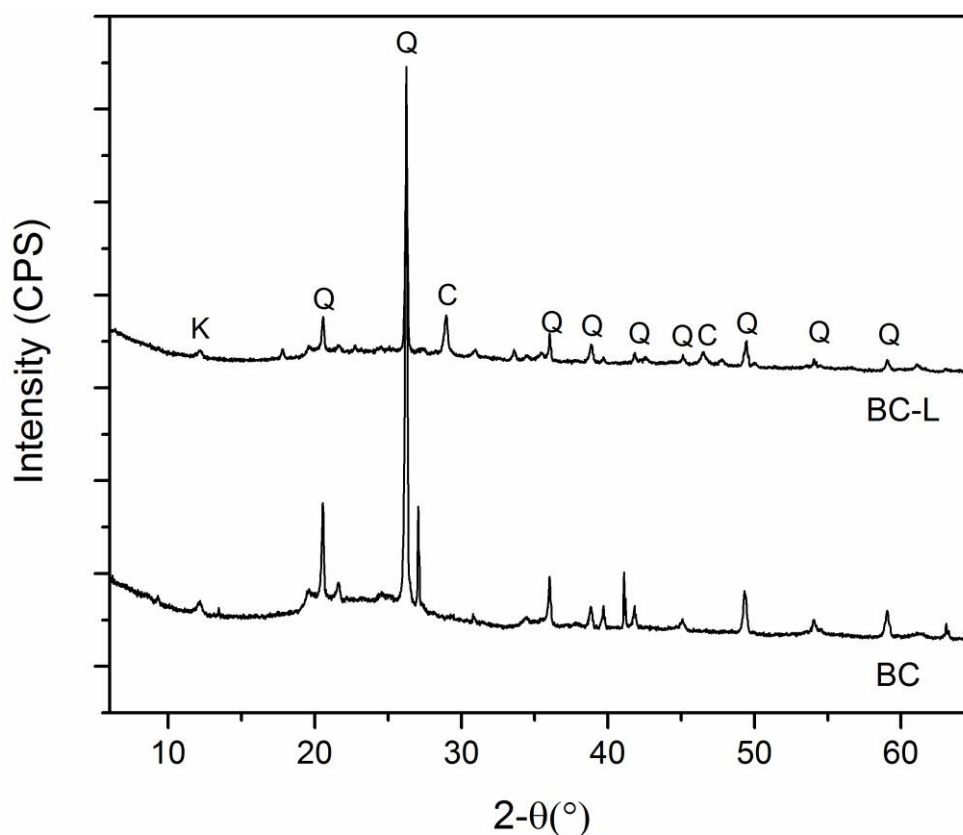


Figure 7.3 – XRD of biochar samples produced from biosolids (BC) and limed biosolids (BC-L) (C – calcite; K – kaolinite; Q - quartz).

The heavy metal leaching from biochar produced from biosolids (BC) and biochar produced from limed biosolids (BC-L) is presented in Table 7.2. It is clear that lime addition significantly reduces the extent of heavy metal leaching from biochar in particular for copper, nickel and zinc. Nickel and cadmium leaching from both biochar samples was lower than the detection limit (0.05 mg/L) of the instrument and much lower than from biosolids (Cd: 0.22 and Ni: 1.86 mg/kg). Lime addition did not impact arsenic and lead leaching from both biochar samples (BC and BC-L). However, lime addition significantly reduced the copper and zinc leaching from biochar, copper leaching reduced 50% while the lead leaching was only 2% compared to the biochar without lime. The heavy metal leaching reduction was likely achieved by two mechanisms: pH buffering by the biochar ($\text{pH} = 10.2 \pm 0.1$) and formation of metal carbonates due to reactions between calcite and heavy metals (CuCaCO_3 , CuCO_3 , ZnCaCO_3 and ZnCO_3). Copper and zinc may be absorbed on the surface of calcite and when in contact with water copper and zinc carbonates may be formed minimising its leaching [242]. The biochar produced from limed biosolids is alkaline ($\text{pH} = 10.2 \pm 0.1$), which neutralizes the pH of solution mitigating the leaching of heavy metals, while BC ($\text{pH} = 7.5 \pm 0.1$) sample has lower alkalinity and the biosolids ($\text{pH} = 6.1 \pm 0.1$) are slightly acid.

The aluminium content in biosolids has not been regulated as it does not represent a problem to humans and plants. The aluminium leaching from biosolids is not taken up by plants, but it may represent a problem for plant growth due to formation of aluminium phosphate compounds making phosphorus unavailable for plants. The aluminium leaching from biochar (BC) produced from biosolids was similar to biosolids at approximately 800 mg/kg. However, the aluminium leaching from biochar (BC-L) produced from lime biosolids reduced significantly to 13.6 mg/kg, which corresponds to only 0.02% of the total aluminium content in the biochar. This reduction is due to the reaction of aluminium compounds with lime during pyrolysis, forming calcium aluminium silicates.

Table 7.2 – Heavy metal leaching from biosolids and biochar produced from biosolids and lime biosolids at 700°C for 20 minutes, using TCLP method.

Material	As mg/kg	Cu mg/kg	Pb mg/kg	Zn mg/kg	Al mg/kg
Biosolids	0.40	6.96	2.70	205.60	884.40
BC	0.80	0.68	3.20	140.60	783.00
BC-L	0.80	0.32	3.71	2.80	13.60

7.3.5 SWOT analysis of biosolids management approaches

Heavy metal leaching from biosolids is only an important factor to consider in biosolids management, they represent a serious threat to all types of life. Other factors such as, greenhouse gas emissions (GHG), resource recycling, groundwater and soil contamination should be considered in the entire process of biosolids management to minimise the environmental impact through pollution mitigation and reduce natural resource extraction. In this section a SWOT (Strengths, Weaknesses, Opportunities and Threats) analysis was performed to evaluate the advantages and key issues of four current biosolids management approaches: pyrolysis, incineration, land application and landfilling. Traditionally, a SWOT analysis is a square (2 by 2 grid) where each quadrant represents one variable, but in this study to summarise and facilitate comparison between the different biosolids management methods, only one table was made where each column represents one variable of the SWOT analysis (Table 7.3). This SWOT analysis was mainly focused on the environmental impact of each biosolids management method and did not consider the economic perspective.

The SWOT analysis is presented in Table 7.3 showing that pyrolysis is the method with more strengths and fewer threats compared to the other three methods. One of the biggest advantages of pyrolysis is the conversion of biosolids into by-products with zero waste production and non-hazardous emissions. The final by-products can be directly used or further processed for many useful applications, for example biochar has been

extensively investigated for contaminant removal, soil amelioration and for activation carbon production. Using biochar for land application instead of biosolids has many advantages. First, the heavy metal leaching from biochar is much lower than from biosolids as demonstrated by this study, while carbon stability is much higher and biochar can reduce heavy metal availability, decreasing metal uptake by plants. Biogas and bio-oil fractions could also be used for energy production, but more research has to be carried out on the bio-oil for diesel production, which can change the environmental and economic scenario of diesel use.

Land application was considered one of the best options for biosolids management as it recycles nutrients and organic matter into soil. However, heavy metal and organic pollutant leaching from biosolids in conjunction with greenhouse gas (GHG) emissions represent a serious environmental threat. This method should be avoided as the heavy metals accumulate in soil and, after decades of biosolids land application, soil may be unsuitable for plant growth. Landfilling has the same problems of land application with fewer benefits making it the less attractive method. Also, this method cannot be implemented in countries with shortage of land.

Incineration has been used as a replacement of land application in Europe. The major advantage of this method is the mass and volume reduction of biosolids, but the disposal of heavily contaminated solid residue (ash) is of concern. This technology needs a strict control of the pollutants emissions, which can be an expensive and challenging process. In countries with no incineration plants like Australia, this is not an option due to the high capital investment, high maintenance costs and no focus on recycling and/or recovery of resources from biosolids.

Table 7.3 – SWOT analysis of biosolids management methods.

	Strengths	Weaknesses	Opportunities	Threats
Pyrolysis	<ul style="list-style-type: none"> - Conversion of waste in value-added products, no waste [231]. - Production of biogas and oil for energy production [53, 84]. - Production of biochar [212]. - Reduction of GHG emissions [243]. - No need for sludge stabilisation; high temperatures destroy pathogens. 	<ul style="list-style-type: none"> - Development of technology for oil processing. - Need of activated carbon or other microwave susceptor (just for microwave pyrolysis). 	<ul style="list-style-type: none"> - Conversion of waste into by-products with great potential. - Recycling/recovery resources avoiding future depletion [118]. - Energy production from waste [53]. - New applications of biochar [212]. 	<ul style="list-style-type: none"> - Lack of environmental legislation for this technology [231].
Land application	<ul style="list-style-type: none"> - Recycling nutrients and organic matter into soil [60]. 	<ul style="list-style-type: none"> - Production of GHG emissions [53]. - Stabilisation of sludge 	<ul style="list-style-type: none"> - Improve soil structure of arable soils [26]. 	<ul style="list-style-type: none"> - Public opposition [60]. - GHG emissions [53].

	<ul style="list-style-type: none"> - Already has a great deal of infrastructure, legislative and logistical support [26, 53]. 	<ul style="list-style-type: none"> - is required [243]. - High water content in sludge, which rises transport costs [28]. 		<ul style="list-style-type: none"> - Soil and water contamination [60].
Landfilling	<ul style="list-style-type: none"> - Recycling nutrients and carbon in forestry. 	<ul style="list-style-type: none"> - Production of GHG emissions [53]. - Land availability [53]. - Transport costs. 	<ul style="list-style-type: none"> - Methane recovery [60]. 	<ul style="list-style-type: none"> - Public opposition. - GHG emissions [53]. - Soil and water contamination [60].
Incineration	<ul style="list-style-type: none"> - High reduction of waste mass/volume [53, 60]. - Energy production [26]. - It is the most well established thermal treatment process for biosolids [231]. 	<ul style="list-style-type: none"> - Production of GHG emissions [60]. - Air pollution (dioxins and furans) [60]. - Heavy metal concentration in final ash [53]. - Sludge dewatering is required to improve energy balance [26]. 	<ul style="list-style-type: none"> - Combine dewatered sludge with other fuels for energy production [244]. - Using ash for brick production for construction [26]. - Phosphorus recovery from ash [245]. 	<ul style="list-style-type: none"> - Ash disposal [53]. - Air pollution [60]. - Energy balance is dependent on downstream dewatering [244].

7.4 Conclusions

Heavy metal content in biosolids is a significant environmental concern, potentially leading to soil and groundwater contamination with implications for all types of life. This study demonstrates that microwave assisted pyrolysis is a potential solution to curb this problem, since the heavy metals concentrating in biochar have a lower leachability than from the untreated biosolids. The biochar produced from limed biosolids have the lowest metal leaching with a total of less than 8 mg/kg of dry biosolids. Besides the reduction of heavy metal leaching, microwave assisted pyrolysis is a promising approach for biosolids management as the waste is converted into pyrolysis by-products (biochar, bio-oil and biogas), creating the idea of non-existent waste and non-hazardous emissions to the atmosphere. The SWOT analysis shows that pyrolysis is a highly favourable solution, reducing GHG emissions, limiting waste, recycling which avoids resource depletion and reduction of CO₂ emissions during its production. However, pyrolysis is not a well-established technology yet, but all of these positive indications are sufficient driving forces to create opportunities in the near future.

8 CONCLUSION AND RECOMMENDATIONS

This chapter reports the overall conclusions of this research. Conclusions are described sequentially, chapter by chapter. The implications of this research are then presented. Finally, recommendations for future work are outlined.

8.1 Dielectric properties and microwave pyrolysis of biosolids

The dielectric properties of biosolids were influenced by microwave frequency, temperature and moisture content. In general, the dielectric constant decreased, while the dielectric loss factor increased, with microwave frequency. Essentially biosolids were transparent to microwave irradiation. As a result a microwave susceptor must be blended with biosolids to enable microwave energy absorption, allowing samples to be heated to above 300°C, necessary for pyrolysis. The selection of an appropriate microwave susceptor will impact on microwave irradiation absorption and reflection, consequently affecting heating rates, pyrolysis by-product composition and distribution and have a significant impact on biochar properties.

Microwave susceptors characterised with a lower loss tangent induced a lower heating rate, as less microwave energy was adsorbed by the sample. However, the biochar formation, above approximately 400°C, triggered higher heating rates of the sample, since biochar is also a good microwave susceptor. A significant part of energy consumption of the microwave pyrolysis process of biosolids occurred during the heating stage as the power consumption at the steady state is usually less than 20% of the heat-up stage. The overall energy consumption is mainly defined by the heating stage energy consumption of the process, so microwave susceptors have a great impact on power consumption as they affect significantly the heating rate.

Three different mechanisms were used to describe the transformation of electromagnetic energy into thermal energy. Wet biosolids were mainly heated due to dipole polarisation. When using a microwave susceptor, such as activated carbon, the microwave heating occurs due to the Maxwell-Wagner mechanism, and the heating results due to an accumulation of charge at the boundaries of the material. The

mechanism of microwave heating of glycerol was mainly ionic polarisation. The heating process of a sample under microwave irradiation can be achieved by three mechanisms: dipole polarisation, Maxwell-Wagner mechanism and ionic polarisation. However, the microwave heating process is very complex; it depends on dielectric properties (which depend on the composition, moisture content, microwave frequency, temperature), bulk density and thermal properties of the sample. The thermal conductivity of the sample is important as the heat is mainly transferred from the microwave susceptor “hot spot” to the cooled surroundings by conduction.

In a single-mode microwaves cavity the sample to be processed disturbs the intensity and distribution of electromagnetic microwave field. Increasing the biosolids sample mass decreased the electromagnetic field intensity and changed the location of the “hot spot” zone. These results illustrate the importance of using numerical techniques to predict the intensity and location of the electromagnetic field, since single-mode microwaves have just one hot spot and samples in the hot spot will have a better coupling with microwaves.

All of variables, including heating rate, pyrolysis temperature, microwave susceptor type, and position of the sample in the microwave cavity, influenced the biochar yield and resultant properties.

8.2 Impact of pyrolysis temperature on biochar properties

Pyrolysis temperature strongly affects biochar yield and its resultant properties. As the pyrolysis temperature increased, the organic composition of the biochar changed as some of the functional groups, such as hydroxyl, carboxyl and amine groups, have weak bonds that brake with temperature. Conversely, the inorganic composition of biochar did not significantly change with pyrolysis temperature; the heavy metal content in biochar increased with increased temperature as the biochar yield decreased due to the accumulation of heavy metals in biochar. The XRD results showed that silica was the main crystalline structure of biosolids and remained the principal phase in biochar.

The specific surface area of biochar was four times higher than biosolids. The specific surface area increased with decreasing biochar yield due to the volatile organic

compounds release, which created porosity and increased surface area. The surface area increase was more significant with pyrolysis temperatures above 500°C. However, other pyrolysis conditions, such as holding time and heating rate, also affected resultant surface area.

Both ash content and volatile content decreased as the pyrolysis temperature increased, due to the greater volatile organic compound removal at increased temperature. In this research, the ash percentage in biochar was quite high (60%) because of the age of biosolids, which had low volatile organic content to begin with.

8.3 Phosphorus recovery by biochar

Phosphorus recovery by biochar depends on the metal content in biochar available to react with phosphate species and precipitate as a salt. In this work, calcium hydroxide (lime) was added to biosolids before microwave pyrolysis. The selection of lime for calcium-rich biochar production was based on addressing three main reasons:

- To enhance phosphorus removal from aqueous solution.
- As some wastewater plants in Australia are already using lime to partially stabilised sewage sludge, this implementation could be easily and cheaply integrated in the future.
- There is a need for alkaline biochar production to avoid agricultural lime land application because agricultural lime has several environmental impacts: CO₂ emissions, soil and groundwater contamination. Its application is also expensive.

The lime reacted with carbon, CO and CO₂ during pyrolysis and calcium carbonate was the main calcium compound in the final biochar.

Phosphorus recovery from aqueous solution was proportional to calcium content in biochar. The biochar without lime addition was able to remove phosphorus (approximately 17 mg-P/g of biochar) due to the presence of other metal elements, such

as magnesium, iron and aluminium. The impact of the initial pH of the phosphorus stock solution influenced phosphorus removal by biochar. In the first phase of the process, acid pH (<2) of phosphorus stock solution increased phosphorus removal due to the better dissolution of calcium carbonate and the release of calcium cations onto the solution. In the second step of the process, higher pH (>8) was required for the precipitation of calcium phosphate salts. The pH of the phosphorus solution increased due to the alkaline property of biochar. As the percentage of calcium in biochar increased, the phosphorus removal capacity increased, and the pH range of maximum phosphorus recovery was also larger. Brushite (calcium hydrogen phosphate dihydrate) was the main salt precipitated on biochar after phosphorus removal.

Calcium-rich biochar was tested with a wastewater stream and the phosphorus removal capacity was higher compared with the tests using phosphorus stock solution. The main reason for this increase was the presence of other metal ions in the wastewater stream that could react with phosphorus species and then precipitate and due to the ammonia content, which increases pH and creates conditions for precipitation. Also, the presence of higher ammonium buffered the pH to 9, creating more suitable conditions for precipitation. Again brushite was the main precipitation salt. While brushite has been recognised as a slow-release fertiliser, plant growth tests should be done to effectively assess the potential of this new product (biochar-brushite).

Phosphorus removal by biochar was well described by a second-order model and by the Langmuir isotherm. Recycling biosolids through microwave pyrolysis is a beneficial approach to deal with an ever-increasing biosolids production, and producing value-added products like biochar rich in phosphorus. Further, this biochar is a potential candidate for phosphorus removal from aqueous solutions, and the final product has many potential benefits for land application apart from its phosphorus content, such as carbon content, surface area and porosity.

8.4 Silver removal by biochar

Silver contamination of wastewater is increasing due to the wide use of silver as an anti-bacterial element. Silver's presence in wastewater streams is an emerging problem, even at low concentrations. An efficient approach for silver removal is adsorption by porous

materials, such as activated carbon and/or biochar. Activated carbon production is expensive and has a significant environmental impact. Biochar production from biomass waste is certainly an approach to be considered in the future, minimises environmental pollution from waste with a bonus of biochar production, which in some cases could replace activated carbon.

Silver was successfully recovered from an aqueous phase using biochar as adsorbent. The maximum adsorption capacity of silver by biochar was 43.9 mg (Ag)/g (biochar). The adsorption process was well described by the intra-particle diffusion model. Experimental data clearly showed three adsorption regimes: film diffusion (external diffusion), pore diffusion (internal diffusion) and mass action. Film diffusion was the fastest stage due to the higher silver concentration in the solution, while mass action was the slowest stage, mainly due to lower silver concentration in the solution and the small surface of pores.

Initial concentration of silver in aqueous solution and temperature of solution played important roles in adsorption. Silver adsorption increased with temperature and with initial concentration of silver in the solution. Thermodynamic analyses demonstrated that this adsorption was a spontaneous process – a common characteristic of the intra-particle diffusion model. The values of ΔG (-20 to 0 kJ/mol) also confirmed that the adsorption of silver onto biochar was a physical process. The final nanocomposite (Ag-biochar) was successfully used for methylene blue degradation/removal from an aqueous solution.

8.5 Heavy metals in biosolids and biochar

Heavy metal content in biosolids limits land application due to contamination of soil and groundwater with these metals. This contamination represents a serious threat to plants, animals and ultimately to humans through the food chain. Microwave assisted pyrolysis is a potential alternative as the heavy metal leaching from biochar is lower than from unprocessed biosolids. Heavy metal leaching from biochar produced from lime-doped biosolids was very low, in total less than 8 mg/kg. Another advantage of pyrolysis is the conversion of biosolids into pyrolysis by-products (biochar, bio-oil and biogas), which creates the concept of non-existent waste. A SWOT analysis

demonstrated that pyrolysis is one the best environmental approaches for biosolids management due to reduced GHG emissions, lower heavy metal leaching from biochar and the potential of using bio-oil and biogas as a renewable energy source.

8.6 Implications of this research

This research has several economic and environmental implications. Using microwave assisted pyrolysis to thermally decompose biosolids into biochar, bio-oil and biogas prevents:

- CO₂ emissions (no CO₂ emissions from transportation of biosolids to disposal site and natural decomposition of biosolids).
- Soil and groundwater contamination with organic compounds, inorganic materials, pathogens and heavy metal due to leaching from biosolids when applied to land.
- Agricultural lime application due to the high pH of biochar, which also increases soil pH.

While not a focus of this study, producing bio-oil and biogas for energy production may also be a significant advantage of this process, and builds a path for recycling energy. The final biochar can be used for many applications apart from land application, such as inorganic and organic contaminant removal from wastewater, energy production, activated carbon production, soil remediation through improving carbon content and sorption of heavy metals, and soil application as a fertiliser.

Recycling key nutrients from the biosolids, particularly phosphorus, is an important advantage of this process. Phosphorus is a fundamental nutrient for plant growth and this process will curtail the depletion of natural resources. Combining the biochar and phosphorus approach will clearly increase plant growth, an essential response to world population growth.

8.7 Recommendations

Single-mode microwaves are difficult to scale-up and, as a result, multi-mode microwave cavities are more common in industry. Laboratory experiments using a multi-mode microwave should be executed to compare pyrolysis by-products yield and distribution with this research. Instead of using a batch process, scaling-up the process as a continuous process is very important.

Due to the poor dielectric properties of biosolids, it is important to find an activated carbon alternative as a microwave susceptor for industrial production because of the prohibitive price of this microwave susceptor. Probably, mixing biosolids with a biomass or biochar produced from other biomass with better dielectric properties will be an advantage, but the impact of this new material on the biochar properties must be investigated.

To minimise the overall pyrolysis costs, the possibility of re-using water vapour and biogas produced during pyrolysis for energy production should be examined as an approach to enhance the global energy balance of pyrolysis process.

All of the experiments of contaminant removal by biochar in this study were carried out as a batch process; therefore, it is recommended to study phosphorus removal as a continuous process. Specifically, assess the feasibility of using biochar columns for phosphorus adsorption from wastewater treatment plants, how the phosphorus can be recycled into agriculture and compare benefits and costs of this approach with current approach. The biochar after phosphorus adsorption should be tested on plant growth and compare the results with the use of industrial fertilisers.

Biochar was successfully used for silver removal from aqueous solutions; the recommendations for future work should be focused on testing this nanocomposite (biochar-silver) for capacitor and antibacterial applications. In this research, biochar was produced from biosolids, but other biomass with higher carbon content could be considered for biochar production for silver removal, which may enhance the outcomes on capacitor applications.

A significant part of the energy consumption of microwave pyrolysis was due to the water evaporation from biosolids. A recommendation for future work is to dry the biosolids prior to microwave pyrolysis using conventional drying or solar drying and compare both costs and processes with microwave technology. The impact of particle size, packing density and porosity on transfer of energy/heat should be analysed to optimise energy consumption of pyrolysis process.

One of the most promising applications of biochar produced from biosolids is land application as a fertiliser. Studying nutrient availability and plant growth using this type of biochar is strongly recommended for future investigation.

This research was carried out with biosolids that were stockpiled for more than two years in Victoria, Australia. The new research must be performed with fresh sewage sludge due to the higher volatiles content, which may enhance the specific surface area of biochar, increase bio-oil and biogas fractions and improve the global energy balance of microwave pyrolysis.

REFERENCES

- [1] L. K. Wang, N. K. Shammass, and Y. T. Hung, *Biosolids engineering and management*: Springer, 2008.
- [2] D. Mohan, A. Sarswat, Y. S. Ok, and C. U. Pittman, "Organic and inorganic contaminants removal from water with biochar, a renewable, low cost and sustainable adsorbent—a critical review," *Bioresource technology*, vol. 160, pp. 191-202, 2014.
- [3] A. Ahmad and A. Idris, "Preparation and characterization of activated carbons derived from bio-solid: a review," *Desalination and Water Treatment*, vol. 52, pp. 4848-4862, 2014.
- [4] M. Ahmad, A. U. Rajapaksha, J. E. Lim, M. Zhang, N. Bolan, D. Mohan, *et al.*, "Biochar as a sorbent for contaminant management in soil and water: a review," *Chemosphere*, vol. 99, pp. 19-33, 2014.
- [5] E. Agrafioti, D. Kalderis, and E. Diamadopoulou, "Arsenic and chromium removal from water using biochars derived from rice husk, organic solid wastes and sewage sludge," *Journal of environmental management*, vol. 133, pp. 309-314, 2014.
- [6] J. Ren, N. Li, L. Li, J.-K. An, L. Zhao, and N.-Q. Ren, "Granulation and ferric oxides loading enable biochar derived from cotton stalk to remove phosphate from water," *Bioresource technology*, vol. 178, pp. 119-125, 2015.
- [7] H. N. Tran, S.-J. You, and H.-P. Chao, "Thermodynamic parameters of cadmium adsorption onto orange peel calculated from various methods: A comparison study," *Journal of Environmental Chemical Engineering*, vol. 4, pp. 2671-2682, 2016.
- [8] M. Carrier, A. G. Hardie, Ü. Uras, J. Görgens, and J. H. Knoetze, "Production of char from vacuum pyrolysis of South-African sugar cane bagasse and its characterization as activated carbon and biochar," *Journal of Analytical and Applied Pyrolysis*, vol. 96, pp. 24-32, 2012.
- [9] X. Wang, X. Xu, X. Liang, Y. Wang, M. Liu, X. Wang, *et al.*, "Adsorption of copper (II) onto sewage sludge-derived materials via microwave irradiation," *Journal of hazardous materials*, vol. 192, pp. 1226-1233, 2011.
- [10] J. Komkiene and E. Baltreinaite, "Biochar as adsorbent for removal of heavy metal ions [Cadmium (II), Copper (II), Lead (II), Zinc (II)] from aqueous phase," *International Journal of Environmental Science and Technology*, vol. 13, pp. 471-482, 2016.

- [11] A. Bogusz, K. Nowak, M. Stefaniuk, R. Dobrowolski, and P. Oleszczuk, "Synthesis of biochar from residues after biogas production with respect to cadmium and nickel removal from wastewater," *Journal of Environmental Management*, vol. 201, pp. 268-276, 2017.
- [12] F.-S. Zhang, J. O. Nriagu, and H. Itoh, "Mercury removal from water using activated carbons derived from organic sewage sludge," *Water research*, vol. 39, pp. 389-395, 2005.
- [13] E. Antunes, J. Schumann, G. Brodie, M. V. Jacob, and P. A. Schneider, "Biochar produced from biosolids using a single-mode microwave: Characterisation and its potential for phosphorus removal," *Journal of Environmental Management*, vol. 196, pp. 119-126, 2017.
- [14] H.-R. Hwang, W.-J. Choi, T.-J. Kim, J.-S. Kim, and K.-J. Oh, "The preparation of an adsorbent from mixtures of sewage sludge and coal-tar pitch using an alkaline hydroxide activation agent," *Journal of Analytical and Applied Pyrolysis*, vol. 83, pp. 220-226, 2008.
- [15] M. Zhang and B. Gao, "Removal of arsenic, methylene blue, and phosphate by biochar/AlOOH nanocomposite," *Chemical engineering journal*, vol. 226, pp. 286-292, 2013.
- [16] L. Kong, Y. Xiong, L. Sun, S. Tian, X. Xu, C. Zhao, *et al.*, "Sorption performance and mechanism of a sludge-derived char as porous carbon-based hybrid adsorbent for benzene derivatives in aqueous solution," *Journal of hazardous materials*, vol. 274, pp. 205-211, 2014.
- [17] P. Devi and A. K. Saroha, "Synthesis of the magnetic biochar composites for use as an adsorbent for the removal of pentachlorophenol from the effluent," *Bioresource technology*, vol. 169, pp. 525-531, 2014.
- [18] S.-y. Wang, Y.-k. Tang, C. Chen, J.-t. Wu, Z. Huang, Y.-y. Mo, *et al.*, "Regeneration of magnetic biochar derived from eucalyptus leaf residue for lead (II) removal," *Bioresource technology*, vol. 186, pp. 360-364, 2015.
- [19] S. Kizito, H. Luo, S. Wu, Z. Ajmal, T. Lv, and R. Dong, "Phosphate recovery from liquid fraction of anaerobic digestate using four slow pyrolyzed biochars: Dynamics of adsorption, desorption and regeneration," *Journal of Environmental Management*, vol. 201, pp. 260-267, 2017.
- [20] D. Cordell, J. Drangert, and S. White, "The story of phosphorus: Global food security and food for thought," *Global Environmental Change*, vol. 19, pp. 292-305, 2009.

- [21] L. A. Guerrero, G. Maas, and W. Hogland, "Solid waste management challenges for cities in developing countries," *Waste management*, vol. 33, pp. 220-232, 2013.
- [22] T. Wang, M. Camps-Arbestain, M. Hedley, and P. Bishop, "Predicting phosphorus bioavailability from high-ash biochars," *Plant and soil*, vol. 357, pp. 173-187, 2012.
- [23] D. Cordell, A. Rosemarin, J. J. Schroder, and A. L. Smit, "Towards global phosphorus security: a systems framework for phosphorus recovery and reuse options," *Chemosphere*, vol. 84, pp. 747-758, 2011.
- [24] L. Shu, P. Schneider, V. Jegatheesan, and J. Johnson, "An economic evaluation of phosphorus recovery as struvite from digester supernatant," *Bioresource Technology*, vol. 97, pp. 2211-6, 2006.
- [25] J. Shao, R. Yan, H. Chen, H. Yang, and D. H. Lee, "Catalytic effect of metal oxides on pyrolysis of sewage sludge," *Fuel Processing Technology*, vol. 91, pp. 1113-1118, 2010.
- [26] H. Wang, S. L. Brown, G. N. Magesan, A. H. Slade, M. Quintern, P. W. Clinton, *et al.*, "Technological options for the management of biosolids," *Environmental Science and Pollution Research-International*, vol. 15, pp. 308-317, 2008.
- [27] S. Petzet and P. Cornel, "Phosphorus Recovery from Wastewater," in *Waste as a Resource*, ed, 2013, p. 110.
- [28] P. Darvodelsky and T. Bridle, "BIOSOLIDS SNAPSHOT."
- [29] S. M. Hong, J. K. Park, and Y. O. Lee, "Mechanisms of microwave irradiation involved in the destruction of fecal coliforms from biosolids," *Water Research*, vol. 38, pp. 1615-1625, 2004.
- [30] S. S. Lam and H. A. Chase, "A review on waste to energy processes using microwave pyrolysis," *Energies*, vol. 5, pp. 4209-4232, 2012.
- [31] R. J. LeBlanc, P. Matthews, and R. P. Richard, *Global atlas of excreta, wastewater sludge, and biosolids management: moving forward the sustainable and welcome uses of a global resource*: Un-habitat, 2009.
- [32] A. Arulrajah, M. Disfani, V. Suthagaran, and M. Imteaz, "Select chemical and engineering properties of wastewater biosolids," *Waste management*, vol. 31, pp. 2522-2526, 2011.
- [33] H. Elliott and G. O'Connor, "Phosphorus management for sustainable biosolids recycling in the United States," *Soil Biology and Biochemistry*, vol. 39, pp. 1318-1327, 2007.

- [34] L. Houdková, J. Boráň, V. Ucekaj, T. Elsäßer, and P. Stehlík, "Thermal processing of sewage sludge–II," *Applied Thermal Engineering*, vol. 28, pp. 2083-2088, 2008.
- [35] R. Singh and M. Agrawal, "Potential benefits and risks of land application of sewage sludge," *Waste management*, vol. 28, pp. 347-358, 2008.
- [36] M. K. Hossain, V. Strezov, K. Y. Chan, A. Ziolkowski, and P. F. Nelson, "Influence of pyrolysis temperature on production and nutrient properties of wastewater sludge biochar," *Journal of Environmental Management*, vol. 92, pp. 223-228, 2011.
- [37] P. Battistoni, A. De Angelis, M. Prisciandaro, R. Boccadoro, and D. Bolzonella, "P removal from anaerobic supernatants by struvite crystallization: long term validation and process modelling," *Water research*, vol. 36, pp. 1927-1938, 2002.
- [38] M. S. Rahaman, D. S. Mavinic, A. Meikleham, and N. Ellis, "Modeling phosphorus removal and recovery from anaerobic digester supernatant through struvite crystallization in a fluidized bed reactor," *Water research*, vol. 51, pp. 1-10, 2014.
- [39] P. Guedes, N. Couto, L. M. Ottosen, and A. B. Ribeiro, "Phosphorus recovery from sewage sludge ash through an electro-dialytic process," *Waste Management*, 2014.
- [40] T. Wang, M. C. Arbestain, M. Hedley, and P. Bishop, "Chemical and bioassay characterisation of nitrogen availability in biochar produced from dairy manure and biosolids," *Organic Geochemistry*, vol. 51, pp. 45-54, 2012.
- [41] D. Cordell, J.-O. Drangert, and S. White, "The story of phosphorus: global food security and food for thought," *Global environmental change*, vol. 19, pp. 292-305, 2009.
- [42] B. Groß, C. Eder, P. Grziwa, J. Horst, and K. Kimmerle, "Energy recovery from sewage sludge by means of fluidised bed gasification," *Waste Management*, vol. 28, pp. 1819-1826, 2008.
- [43] A. Demirbas, "Combustion characteristics of different biomass fuels," *Progress in energy and combustion science*, vol. 30, pp. 219-230, 2004.
- [44] A. Van der Drift and H. Boerrigter, *Synthesis gas from biomass for fuels and chemicals*: ECN Biomass, Coal and Environmental Research, 2006.
- [45] A. Inguanzo, A. Domínguez, J. A. Menéndez, C. Blanco, and J. Pis, "On the pyrolysis of sewage sludge: the influence of pyrolysis conditions on solid, liquid

- and gas fractions," *Journal of Analytical and Applied Pyrolysis*, vol. 63, pp. 209-222, 2002.
- [46] H. J. Park, H. S. Heo, Y.-K. Park, J.-H. Yim, J.-K. Jeon, J. Park, *et al.*, "Clean bio-oil production from fast pyrolysis of sewage sludge: effects of reaction conditions and metal oxide catalysts," *Bioresource technology*, vol. 101, pp. S83-S85, 2010.
- [47] A. Domínguez, J. A. Menéndez, M. Inganzo, and J. Pis, "Production of bio-fuels by high temperature pyrolysis of sewage sludge using conventional and microwave heating," *Bioresource technology*, vol. 97, pp. 1185-1193, 2006.
- [48] Y. Kim and W. Parker, "A technical and economic evaluation of the pyrolysis of sewage sludge for the production of bio-oil," *Bioresource Technology*, vol. 99, pp. 1409-1416, 2008.
- [49] J. Yoder, S. Galinato, D. Granatstein, and M. Garcia-Pérez, "Economic tradeoff between biochar and bio-oil production via pyrolysis," *biomass and bioenergy*, vol. 35, pp. 1851-1862, 2011.
- [50] V. K. Tyagi and S. L. Lo, "Microwave irradiation: A sustainable way for sludge treatment and resource recovery," *Renewable and Sustainable Energy Reviews*, vol. 18, pp. 288-305, 2013.
- [51] N. Mills, P. Pearce, J. Farrow, R. Thorpe, and N. Kirkby, "Environmental & economic life cycle assessment of current & future sewage sludge to energy technologies," *Waste management*, vol. 34, pp. 185-195, 2014.
- [52] G. Houillon and O. Jolliet, "Life cycle assessment of processes for the treatment of wastewater urban sludge: energy and global warming analysis," *Journal of cleaner production*, vol. 13, pp. 287-299, 2005.
- [53] I. Fonts, G. Gea, M. Azuara, J. Ábrego, and J. Arauzo, "Sewage sludge pyrolysis for liquid production: A review," *Renewable and Sustainable Energy Reviews*, vol. 16, pp. 2781-2805, 2012.
- [54] L. M. Ottosen, G. M. Kirkelund, and P. E. Jensen, "Extracting phosphorous from incinerated sewage sludge ash rich in iron or aluminum," *Chemosphere*, vol. 91, pp. 963-9, 2013.
- [55] G. Barry, M. Bell, and G. Pu, "Sustainable biosolids recycling in south east Queensland," 2006.
- [56] M. McLaughlin, M. Bell, D. Nash, D. Pritchard, M. Whatmuff, M. Warne, *et al.*, "Benefits of using biosolid nutrients in Australian agriculture-a national perspective," 2008.

- [57] R. Haynes, G. Murtaza, and R. Naidu, "Inorganic and organic constituents and contaminants of biosolids: implications for land application," *Advances in agronomy*, vol. 104, pp. 165-267, 2009.
- [58] P.-H. Kao, C.-C. Huang, and Z.-Y. Hseu, "Response of microbial activities to heavy metals in a neutral loamy soil treated with biosolid," *Chemosphere*, vol. 64, pp. 63-70, 2006.
- [59] D. Pritchard, N. Penney, M. McLaughlin, H. Rigby, and K. Schwarz, "Land application of sewage sludge (biosolids) in Australia: risks to the environment and food crops," *Water Science and Technology*, vol. 62, p. 48, 2010.
- [60] M. M. Roy, A. Dutta, K. Corscadden, P. Havard, and L. Dickie, "Review of biosolids management options and co-incineration of a biosolid-derived fuel," *Waste Management*, vol. 31, pp. 2228-35, 2011.
- [61] Clarke Energy. (2015, 4 June). *Landfill Gas Composition*. Available: <https://www.clarke-energy.com/landfill-gas/>
- [62] Q. Zhang, J. Chang, T. Wang, and Y. Xu, "Review of biomass pyrolysis oil properties and upgrading research," *Energy conversion and management*, vol. 48, pp. 87-92, 2007.
- [63] T. Bridle and D. Pritchard, "Energy and nutrient recovery from sewage sludge via pyrolysis," *Water Science & Technology*, vol. 50, pp. 169-175, 2004.
- [64] Y. Fernández, A. Arenillas, and J. A. Menéndez, "Microwave heating applied to pyrolysis," in *Advances in induction and microwave heating of mineral and organic materials*, ed: InTech, 2011, pp. 724-752.
- [65] R. Luque, J. A. Menéndez, A. Arenillas, and J. Cot, "Microwave-assisted pyrolysis of biomass feedstocks: the way forward?," *Energy & Environmental Science*, vol. 5, pp. 5481-5488, 2012.
- [66] Y. Tian, W. Zuo, Z. Ren, and D. Chen, "Estimation of a novel method to produce bio-oil from sewage sludge by microwave pyrolysis with the consideration of efficiency and safety," *Bioresource technology*, vol. 102, pp. 2053-2061, 2011.
- [67] E. Agrafioti, G. Bouras, D. Kalderis, and E. Diamadopoulos, "Biochar production by sewage sludge pyrolysis," *Journal of Analytical and Applied Pyrolysis*, vol. 101, pp. 72-78, 2013.
- [68] N. E. Leadbeater and C. B. McGowan, *Laboratory Experiments Using Microwave Heating*: CRC Press, 2013.

- [69] T. N. Wu, "Environmental perspectives of microwave applications as remedial alternatives: Review," *Practice Periodical of Hazardous, Toxic, and Radioactive Waste Management*, vol. 12, pp. 102-115, 2008.
- [70] J. A. Menéndez, A. Arenillas, B. Fidalgo, Y. Fernández, L. Zubizarreta, E. G. Calvo, *et al.*, "Microwave heating processes involving carbon materials," *Fuel Processing Technology*, vol. 91, pp. 1-8, 2010.
- [71] A. A. Salema, Y. K. Yeow, K. Ishaque, F. N. Ani, M. T. Afzal, and A. Hassan, "Dielectric properties and microwave heating of oil palm biomass and biochar," *Industrial Crops and Products*, vol. 50, pp. 366-374, 2013.
- [72] F. Motasemi and M. T. Afzal, "A review on the microwave-assisted pyrolysis technique," *Renewable and Sustainable Energy Reviews*, vol. 28, pp. 317-330, 2013.
- [73] A. A. Salema and F. N. Ani, "Microwave induced pyrolysis of oil palm biomass," *Bioresource Technology*, vol. 102, pp. 3388-95, 2011.
- [74] V. Polshettiwar and R. S. Varma, *Aqueous microwave assisted chemistry: Synthesis and catalysis*: Royal Society of Chemistry, 2010.
- [75] I. Bilecka and M. Niederberger, "Microwave chemistry for inorganic nanomaterials synthesis," *Nanoscale*, vol. 2, pp. 1358-1374, 2010.
- [76] A. Domínguez, Y. Fernandez, B. Fidalgo, J. J. Pis, and J. A. Menéndez, "Bio-syngas production with low concentrations of CO₂ and CH₄ from microwave-induced pyrolysis of wet and dried sewage sludge," *Chemosphere*, vol. 70, pp. 397-403, 2008.
- [77] N. Uphoff, A. S. Ball, E. Fernandes, H. Herren, O. Husson, M. Laing, *et al.*, *Biological approaches to sustainable soil systems*: CRC Press, 2006.
- [78] R. Omar, A. Idris, R. Yunus, K. Khalid, and M. I. Aida Isma, "Characterization of empty fruit bunch for microwave-assisted pyrolysis," *Fuel*, vol. 90, pp. 1536-1544, 2011.
- [79] J. L. Shie, F. J. Tsou, K. L. Lin, and C. Y. Chang, "Bioenergy and products from thermal pyrolysis of rice straw using plasma torch," *Bioresource Technology*, vol. 101, pp. 761-8, 2010.
- [80] Y. F. Huang, W. H. Kuan, S. L. Lo, and C. F. Lin, "Total recovery of resources and energy from rice straw using microwave-induced pyrolysis," *Bioresource Technology*, vol. 99, pp. 8252-8, 2008.
- [81] V. L. Budarin, J. H. Clark, B. A. Lanigan, P. Shuttleworth, S. W. Breeden, A. J. Wilson, *et al.*, "The preparation of high-grade bio-oils through the controlled,

- low temperature microwave activation of wheat straw," *Bioresource Technology*, vol. 100, pp. 6064-8, 2009.
- [82] A. Undri, L. Rosi, M. Frediani, and P. Frediani, "Upgraded fuel from microwave assisted pyrolysis of waste tire," *Fuel*, vol. 115, pp. 600-608, 2014.
- [83] E. A. Grannen, "Microwave pyrolysis of wastes," United States Patent 3,843,457, 22 Oct. 1974, 1974.
- [84] J. A. Menéndez, A. Domínguez, M. Inguanzo, and J. J. Pis, "Microwave pyrolysis of sewage sludge: analysis of the gas fraction," *Journal of Analytical and Applied Pyrolysis*, vol. 71, pp. 657-667, 2004.
- [85] J. A. Menéndez, M. Inguanzo, and J. J. Pis, "Microwave-induced pyrolysis of sewage sludge," *Water research*, vol. 36, pp. 3261-3264, 2002.
- [86] X. Wang, W. Morrison, Z. Du, Y. Wan, X. Lin, P. Chen, *et al.*, "Biomass temperature profile development and its implications under the microwave-assisted pyrolysis condition," *Applied Energy*, vol. 99, pp. 386-392, 2012.
- [87] H. Lu, W. Zhang, S. Wang, L. Zhuang, Y. Yang, and R. Qiu, "Characterization of sewage sludge-derived biochars from different feedstocks and pyrolysis temperatures," *Journal of Analytical and Applied Pyrolysis*, vol. 102, pp. 137-143, 2013.
- [88] S. Petzet, B. Peplinski, and P. Cornel, "On wet chemical phosphorus recovery from sewage sludge ash by acidic or alkaline leaching and an optimized combination of both," *Water Research*, vol. 46, pp. 3769-80, 2012.
- [89] K. Y. Chan and Z. Xu, "Biochar: nutrient properties and their enhancement," *Biochar for environmental management: science and technology*, pp. 67-84, 2009.
- [90] A. A. Kenge, P. H. Liao, and K. V. Lo, "Solubilization of municipal anaerobic sludge using microwave-enhanced advanced oxidation process," *Journal of Environmental Science and Health, Part A*, vol. 44, pp. 502-506, 2009.
- [91] P. H. Liao, W. T. Wong, and K. V. Lo, "Advanced Oxidation Process Using Hydrogen Peroxide/ Microwave System for Solubilization of Phosphate," *Journal of Environmental Science and Health, Part A*, vol. 40, pp. 1753-1761, 2005.
- [92] W. I. Chan, W. T. Wong, P. H. Liao, and K. V. Lo, "Sewage sludge nutrient solubilization using a single-stage microwave treatment," *Journal of Environmental Science and Health, Part A*, vol. 42, pp. 59-63, 2007.

- [93] W. T. Wong, W. I. Chan, P. H. Liao, and K. V. Lo, "A hydrogen peroxide/microwave advanced oxidation process for sewage sludge treatment," *Journal of Environmental Science and Health Part A*, vol. 41, pp. 2623-2633, 2006.
- [94] P. H. Liao, W. Wong, and K. Lo, "Release of phosphorus from sewage sludge using microwave technology," *Journal of Environmental Engineering and Science*, vol. 4, pp. 77-81, 2005.
- [95] W. T. Wong, K. V. Lo, and P. H. Liao, "Factors affecting nutrient solubilization from sewage sludge using microwave-enhanced advanced oxidation process," *Journal of Environmental Science and Health Part A*, vol. 42, pp. 825-829, 2007.
- [96] Y. Yu, I. W. Lo, P. H. Liao, and K. V. Lo, "Treatment of dairy manure using the microwave enhanced advanced oxidation process under a continuous mode operation," *Journal of environmental science and health. Part. B*, vol. 45, pp. 804-9, 2010.
- [97] M. K. Jamali, T. G. Kazi, M. B. Arain, H. I. Afridi, N. Jalbani, G. A. Kandhro, *et al.*, "Speciation of heavy metals in untreated sewage sludge by using microwave assisted sequential extraction procedure," *Journal of Hazardous Materials*, vol. 163, pp. 1157-1164, 2009.
- [98] Y. He, Y. Zhai, C. Li, F. Yang, L. Chen, X. Fan, *et al.*, "The fate of Cu, Zn, Pb and Cd during the pyrolysis of sewage sludge at different temperatures," *Environmental technology*, vol. 31, pp. 567-574, 2010.
- [99] Y. Yao, B. Gao, M. Inyang, A. R. Zimmerman, X. Cao, P. Pullammanappallil, *et al.*, "Biochar derived from anaerobically digested sugar beet tailings: characterization and phosphate removal potential," *Bioresource technology*, vol. 102, pp. 6273-6278, 2011.
- [100] S. P. Galinato, J. K. Yoder, and D. Granatstein, "The economic value of biochar in crop production and carbon sequestration," *Energy Policy*, vol. 39, pp. 6344-6350, 2011.
- [101] D. Beneroso, J. Bermúdez, A. Arenillas, and J. A. Menéndez, "Integrated microwave drying, pyrolysis and gasification for valorisation of organic wastes to syngas," *Fuel*, vol. 132, pp. 20-26, 2014.
- [102] A. Domínguez, J. A. Menéndez, Y. Fernandez, J. J. Pis, J. Nabais, P. Carrott, *et al.*, "Conventional and microwave induced pyrolysis of coffee hulls for the production of a hydrogen rich fuel gas," *Journal of Analytical and Applied Pyrolysis*, vol. 79, pp. 128-135, 2007.

- [103] A. Domínguez, J. A. Menéndez, and J. Pis, "Hydrogen rich fuel gas production from the pyrolysis of wet sewage sludge at high temperature," *Journal of analytical and applied pyrolysis*, vol. 77, pp. 127-132, 2006.
- [104] D. Beneroso, J. Bermúdez, A. Arenillas, and J. A. Menéndez, "Influence of the microwave absorbent and moisture content on the microwave pyrolysis of an organic municipal solid waste," *Journal of Analytical and Applied Pyrolysis*, vol. 105, pp. 234-240, 2014.
- [105] J. Zhang, Y. Tian, J. Zhu, W. Zuo, and L. Yin, "Characterization of nitrogen transformation during microwave-induced pyrolysis of sewage sludge," *Journal of Analytical and Applied Pyrolysis*, vol. 105, pp. 335-341, 2014.
- [106] W. Saw, H. McKinnon, I. Gilmour, and S. Pang, "Production of hydrogen-rich syngas from steam gasification of blend of biosolids and wood using a dual fluidised bed gasifier," *Fuel*, vol. 93, pp. 473-478, 2012.
- [107] W. Zuo, Y. Tian, and N. Ren, "The important role of microwave receptors in bio-fuel production by microwave-induced pyrolysis of sewage sludge," *Waste management*, vol. 31, pp. 1321-1326, 2011.
- [108] C. Yin, "Microwave-assisted pyrolysis of biomass for liquid biofuels production," *Bioresource technology*, vol. 120, pp. 273-284, 2012.
- [109] Q. Xie, P. Peng, S. Liu, M. Min, Y. Cheng, Y. Wan, *et al.*, "Fast microwave-assisted catalytic pyrolysis of sewage sludge for bio-oil production," *Bioresource technology*, vol. 172, pp. 162-168, 2014.
- [110] R. Omar and J. P. Robinson, "Conventional and microwave-assisted pyrolysis of rapeseed oil for bio-fuel production," *Journal of Analytical and Applied Pyrolysis*, vol. 105, pp. 131-142, 2014.
- [111] J. A. Menéndez, M. Inguanzo, P. L. Bernad, and J. J. Pis, "Gas chromatographic–mass spectrometric study of the oil fractions produced by microwave-assisted pyrolysis of different sewage sludges," *Journal of chromatography A*, vol. 1012, pp. 193-206, 2003.
- [112] J. D. Roberts and M. C. Caserio, *Basic principles of organic chemistry*: WA Benjamin, Inc., 1977.
- [113] N. Wang, J. Yu, A. Tahmasebi, Y. Han, J. Lucas, T. Wall, *et al.*, "Experimental Study on Microwave Pyrolysis of an Indonesian Low-Rank Coal," *Energy & Fuels*, vol. 28, pp. 254-263, 2013.
- [114] E. Antunes, M. V. Jacob, G. Brodie, and P. A. Schneider, "Silver removal from aqueous solution by biochar produced from biosolids via microwave pyrolysis," *Journal of Environmental Management*, vol. 203, pp. 264-272, 2017.

- [115] P. Devi and A. K. Saroha, "Utilization of sludge based adsorbents for the removal of various pollutants: a review," *Science of The Total Environment*, vol. 578, pp. 16-33, 2017.
- [116] H. Li, X. Dong, E. B. da Silva, L. M. de Oliveira, Y. Chen, and L. Q. Ma, "Mechanisms of metal sorption by biochars: Biochar characteristics and modifications," *Chemosphere*, vol. 178, pp. 466-478, 2017.
- [117] P. Hadi, M. Xu, C. Ning, C. S. K. Lin, and G. McKay, "A critical review on preparation, characterization and utilization of sludge-derived activated carbons for wastewater treatment," *Chemical engineering journal*, vol. 260, pp. 895-906, 2015.
- [118] K. Smith, G. Fowler, S. Pullket, and N. J. D. Graham, "Sewage sludge-based adsorbents: a review of their production, properties and use in water treatment applications," *Water research*, vol. 43, pp. 2569-2594, 2009.
- [119] B. Hameed, A. M. Din, and A. Ahmad, "Adsorption of methylene blue onto bamboo-based activated carbon: kinetics and equilibrium studies," *Journal of hazardous materials*, vol. 141, pp. 819-825, 2007.
- [120] C. Jindarom, V. Meeyoo, B. Kitiyanan, T. Rirksomboon, and P. Rangsunvigit, "Surface characterization and dye adsorptive capacities of char obtained from pyrolysis/gasification of sewage sludge," *Chemical Engineering Journal*, vol. 133, pp. 239-246, 2007.
- [121] R. Chintala, T. E. Schumacher, L. M. McDonald, D. E. Clay, D. D. Malo, S. K. Papiernik, *et al.*, "Phosphorus Sorption and Availability from Biochars and Soil/Biochar Mixtures," *Clean – Soil, Air, Water*, vol. 42, pp. 626–634, 2014.
- [122] T. Boualem, A. Debab, A. M. de Yuso, and M. Izquierdo, "Activated carbons obtained from sewage sludge by chemical activation: gas-phase environmental applications," *Journal of environmental management*, vol. 140, pp. 145-151, 2014.
- [123] Y. Zhai, X. Wei, G. Zeng, D. Zhang, and K. Chu, "Study of adsorbent derived from sewage sludge for the removal of Cd²⁺, Ni²⁺ in aqueous solutions," *Separation and purification technology*, vol. 38, pp. 191-196, 2004.
- [124] T. Chen, Z. Zhou, R. Han, R. Meng, H. Wang, and W. Lu, "Adsorption of cadmium by biochar derived from municipal sewage sludge: Impact factors and adsorption mechanism," *Chemosphere*, vol. 134, pp. 286-293, 2015.
- [125] E. Gutiérrez-Segura, M. Solache-Ríos, A. Colín-Cruz, and C. Fall, "Adsorption of cadmium by Na and Fe modified zeolitic tuffs and carbonaceous material from pyrolyzed sewage sludge," *Journal of environmental management*, vol. 97, pp. 6-13, 2012.

- [126] R. Xie, W. Jiang, L. Wang, J. Peng, and Y. Chen, "Effect of pyrolusite loading on sewage sludge-based activated carbon in Cu (II), Pb (II), and Cd (II) adsorption," *Environmental Progress & Sustainable Energy*, vol. 32, pp. 1066-1073, 2013.
- [127] T. Chen, Z. Zhou, S. Xu, H. Wang, and W. Lu, "Adsorption behavior comparison of trivalent and hexavalent chromium on biochar derived from municipal sludge," *Bioresource technology*, vol. 190, pp. 388-394, 2015.
- [128] F. Rozada, M. Otero, A. Morán, and A. García, "Adsorption of heavy metals onto sewage sludge-derived materials," *Bioresource Technology*, vol. 99, pp. 6332-6338, 2008.
- [129] M. Otero, F. Rozada, A. Morán, L. Calvo, and A. García, "Removal of heavy metals from aqueous solution by sewage sludge based sorbents: competitive effects," *Desalination*, vol. 239, pp. 46-57, 2009.
- [130] S. Rio, L. Le Coq, C. Faur, D. Lecomte, and P. Le Cloirec, "Preparation of adsorbents from sewage sludge by steam activation for industrial emission treatment," *Process Safety and Environmental Protection*, vol. 84, pp. 258-264, 2006.
- [131] J. Bouzid, Z. Elouear, M. Ksibi, M. Feki, and A. Montiel, "A study on removal characteristics of copper from aqueous solution by sewage sludge and pomace ashes," *Journal of hazardous materials*, vol. 152, pp. 838-845, 2008.
- [132] Q. Lin, H. Cheng, and G. Chen, "Preparation and characterization of carbonaceous adsorbents from sewage sludge using a pilot-scale microwave heating equipment," *Journal of Analytical and Applied Pyrolysis*, vol. 93, pp. 113-119, 2012.
- [133] H. Lu, W. Zhang, Y. Yang, X. Huang, S. Wang, and R. Qiu, "Relative distribution of Pb 2+ sorption mechanisms by sludge-derived biochar," *Water research*, vol. 46, pp. 854-862, 2012.
- [134] M. J. Martín, A. Artola, M. D. Balaguer, and M. Rigola, "Activated carbons developed from surplus sewage sludge for the removal of dyes from dilute aqueous solutions," *Chemical Engineering Journal*, vol. 94, pp. 231-239, 2003.
- [135] X. Wang, N. Zhu, and B. Yin, "Preparation of sludge-based activated carbon and its application in dye wastewater treatment," *Journal of hazardous materials*, vol. 153, pp. 22-27, 2008.
- [136] E. Gutiérrez-Segura, M. Solache-Ríos, and A. Colín-Cruz, "Sorption of indigo carmine by a Fe-zeolitic tuff and carbonaceous material from pyrolyzed sewage sludge," *Journal of Hazardous Materials*, vol. 170, pp. 1227-1235, 2009.

- [137] L. Leng, X. Yuan, H. Huang, J. Shao, H. Wang, X. Chen, *et al.*, "Bio-char derived from sewage sludge by liquefaction: Characterization and application for dye adsorption," *Applied Surface Science*, vol. 346, pp. 223-231, 2015.
- [138] F. Rozada, M. Otero, J. Parra, A. Morán, and A. Garcia, "Producing adsorbents from sewage sludge and discarded tyres: Characterization and utilization for the removal of pollutants from water," *Chemical Engineering Journal*, vol. 114, pp. 161-169, 2005.
- [139] J. Xie, Q. Yue, H. Yu, W. Yue, R. Li, S. Zhang, *et al.*, "Adsorption of reactive brilliant red K-2BP on activated carbon developed from sewage sludge," *Frontiers of Chemistry in China*, vol. 3, pp. 33-40, 2008.
- [140] C. Liu, Z. Tang, Y. Chen, S. Su, and W. Jiang, "Characterization of mesoporous activated carbons prepared by pyrolysis of sewage sludge with pyrolusite," *Bioresource Technology*, vol. 101, pp. 1097-1101, 2010.
- [141] X. Chen, S. Jeyaseelan, and N. Graham, "Physical and chemical properties study of the activated carbon made from sewage sludge," *Waste management*, vol. 22, pp. 755-760, 2002.
- [142] S. Bousba and A. Meniai, "Adsorption of 2-chlorophenol onto sewage sludge based adsorbent: equilibrium and kinetic study," *Chem. Eng*, vol. 35, pp. 859-864, 2013.
- [143] J. Zou, Y. Dai, X. Wang, Z. Ren, C. Tian, K. Pan, *et al.*, "Structure and adsorption properties of sewage sludge-derived carbon with removal of inorganic impurities and high porosity," *Bioresource technology*, vol. 142, pp. 209-217, 2013.
- [144] M. Otero, F. Rozada, L. Calvo, A. Garcia, and A. Moran, "Elimination of organic water pollutants using adsorbents obtained from sewage sludge," *Dyes and Pigments*, vol. 57, pp. 55-65, 2003.
- [145] M. Martin, E. Serra, A. Ros, M. Balaguer, and M. Rigola, "Carbonaceous adsorbents from sewage sludge and their application in a combined activated sludge-powdered activated carbon (AS-PAC) treatment," *Carbon*, vol. 42, pp. 1389-1394, 2004.
- [146] L. Yu and Q. Zhong, "Preparation of adsorbents made from sewage sludges for adsorption of organic materials from wastewater," *Journal of hazardous materials*, vol. 137, pp. 359-366, 2006.
- [147] Y. Jiang, T. Deng, K. Yang, and H. Wang, "Removal performance of phosphate from aqueous solution using a high-capacity sewage sludge-based adsorbent," *Journal of the Taiwan Institute of Chemical Engineers*, 2017.

- [148] L. Kong, Y. Xiong, S. Tian, R. Luo, C. He, and H. Huang, "Preparation and characterization of a hierarchical porous char from sewage sludge with superior adsorption capacity for toluene by a new two-step pore-fabricating process," *Bioresource technology*, vol. 146, pp. 457-462, 2013.
- [149] A. Demirbaş, "Biomass resource facilities and biomass conversion processing for fuels and chemicals," *Energy conversion and Management*, vol. 42, pp. 1357-1378, 2001.
- [150] D. Neves, H. Thunman, A. Matos, L. Tarelho, and A. Gómez-Barea, "Characterization and prediction of biomass pyrolysis products," *Progress in Energy and Combustion Science*, vol. 37, pp. 611-630, 2011.
- [151] Q. Bu, H. Lei, S. Ren, L. Wang, Q. Zhang, J. Tang, *et al.*, "Production of phenols and biofuels by catalytic microwave pyrolysis of lignocellulosic biomass," *Bioresource technology*, vol. 108, pp. 274-279, 2012.
- [152] A. Mudhoo and S. K. Sharma, "Microwave Irradiation Technology In Waste Sludge And Wastewater Treatment Research," *Critical Reviews in Environmental Science and Technology*, vol. 41, pp. 999-1066, 2011.
- [153] Y. Fernández, A. Arenillas, M. Díez, J. Pis, and J. A. Menéndez, "Pyrolysis of glycerol over activated carbons for syngas production," *Journal of Analytical and Applied Pyrolysis*, vol. 84, pp. 145-150, 2009.
- [154] B. Dou, V. Dupont, P. T. Williams, H. Chen, and Y. Ding, "Thermogravimetric kinetics of crude glycerol," *Bioresource technology*, vol. 100, pp. 2613-2620, 2009.
- [155] A. Cross and S. P. Sohi, "A method for screening the relative long-term stability of biochar," *Gcb Bioenergy*, vol. 5, pp. 215-220, 2013.
- [156] K. E. Haque, "Microwave energy for mineral treatment processes—a brief review," *International Journal of Mineral Processing*, vol. 57, pp. 1-24, 1999.
- [157] L. Lu, J. Tang, and X. Ran, "Temperature and moisture changes during microwave drying of sliced food," *Drying Technology*, vol. 17, pp. 414-431, 1999.
- [158] A. a. Metaxas and R. J. Meredith, *Industrial microwave heating*: IET, 1983.
- [159] W. Guo, S. Wang, G. Tiwari, J. A. Johnson, and J. Tang, "Temperature and moisture dependent dielectric properties of legume flour associated with dielectric heating," *LWT-Food Science and Technology*, vol. 43, pp. 193-201, 2010.

- [160] X. Liu, Z. Zhang, and Y. Wu, "Absorption properties of carbon black/silicon carbide microwave absorbers," *Composites Part B: Engineering*, vol. 42, pp. 326-329, 2011.
- [161] A. de la Hoz and A. Loupy, *Microwaves in Organic Synthesis, 2 Volume Set*: John Wiley & Sons, 2013.
- [162] A. Mukherjee and R. Lal, "Biochar impacts on soil physical properties and greenhouse gas emissions," *Agronomy*, vol. 3, pp. 313-339, 2013.
- [163] Y. S. Ok, S. M. Uchimiya, S. X. Chang, and N. Bolan, *Biochar : Production, Characterization, and Applications*: CRC Press, 2015.
- [164] J. Lehmann and S. Joseph, *Biochar for environmental management: science and technology*: Routledge, 2012.
- [165] T. Buckley and E. Domalski, "Evaluation of data on higher heating values and elemental analysis for refuse-derived fuels," in *13th Biennial ASME Solid Waste Processing Conf., Philadelphia, PA*, 1988, pp. 16-24.
- [166] S. Okumura, T. Tasaki, and Y. Moriguchi, "Economic growth and trends of municipal waste treatment options in Asian countries," *Journal of Material Cycles and Waste Management*, vol. 16, pp. 335-346, 2014.
- [167] R. Majumder, S. J. Livesley, D. Gregory, and S. K. Arndt, "Biosolid stockpiles are a significant point source for greenhouse gas emissions," *Journal of Environmental Management*, vol. 143, pp. 34-43, 2014.
- [168] N. Saqib and M. Bäckström, "Distribution and leaching characteristics of trace elements in ashes as a function of different waste fuels and incineration technologies," *Journal of Environmental Sciences*, vol. 36, pp. 9-21, 2015.
- [169] H. Lin and X. Ma, "Simulation of co-incineration of sewage sludge with municipal solid waste in a grate furnace incinerator," *Waste management*, vol. 32, pp. 561-567, 2012.
- [170] "Fact sheet - biosolids profile," A. W. Association, Ed., ed: Australian Government 2013.
- [171] G. Brodie, R. Destefani, P. A. Schneider, L. Airey, and M. V. Jacob, "Dielectric Properties of Sewage Biosolids: Measurement and Modeling," *Journal of Microwave Power and Electromagnetic Energy*, vol. 48, pp. 147-157, 2014.
- [172] S. Sohi, E. Krull, E. Lopez-Capel, and R. Bol, "A review of biochar and its use and function in soil," *Advances in agronomy*, vol. 105, pp. 47-82, 2010.

- [173] K. Crombie and O. Mašek, "Pyrolysis biochar systems, balance between bioenergy and carbon sequestration," *GCB Bioenergy*, vol. 7, pp. 349-361, 2015.
- [174] Y. Yang, Y. Zhao, and P. Kearney, "Influence of ageing on the structure and phosphate adsorption capacity of dewatered alum sludge," *Chemical Engineering Journal*, vol. 145, pp. 276-284, 2008.
- [175] A. Babatunde and Y. Zhao, "Equilibrium and kinetic analysis of phosphorus adsorption from aqueous solution using waste alum sludge," *Journal of Hazardous Materials*, vol. 184, pp. 746-752, 2010.
- [176] A. U. Rajapaksha, S. S. Chen, D. C. Tsang, M. Zhang, M. Vithanage, S. Mandal, *et al.*, "Engineered/designer biochar for contaminant removal/immobilization from soil and water: Potential and implication of biochar modification," *Chemosphere*, vol. 148, pp. 276-291, 2016.
- [177] E. P. A. Victoria, "Guidelines for environmental management: Biosolids land application," *Southbank, EPA Victoria*, 2004.
- [178] K. E. Wright, "Internal precipitation of phosphorus in relation to aluminum toxicity," *Plant physiology*, vol. 18, p. 708, 1943.
- [179] E. Delhaize and P. R. Ryan, "Aluminum toxicity and tolerance in plants," *Plant physiology*, vol. 107, p. 315, 1995.
- [180] B. B. Kaudal, D. Chen, D. B. Madhavan, A. Downie, and A. Weatherley, "Pyrolysis of urban waste streams: Their potential use as horticultural media," *Journal of Analytical and Applied Pyrolysis*, vol. 112, pp. 105-112, 2015.
- [181] Y. Cao and A. Pawłowski, "Sewage sludge-to-energy approaches based on anaerobic digestion and pyrolysis: Brief overview and energy efficiency assessment," *Renewable and Sustainable Energy Reviews*, vol. 16, pp. 1657-1665, 2012.
- [182] M. E. Oliveira and A. S. Franca, "Finite element analysis of microwave heating of solid products," *International communications in heat and mass transfer*, vol. 27, pp. 527-536, 2000.
- [183] E. Thostenson and T.-W. Chou, "Microwave processing: fundamentals and applications," *Composites Part A: Applied Science and Manufacturing*, vol. 30, pp. 1055-1071, 1999.
- [184] J. Robinson, S. Kingman, D. Irvine, P. Licence, A. Smith, G. Dimitrakakis, *et al.*, "Understanding microwave heating effects in single mode type cavities—theory and experiment," *Physical Chemistry Chemical Physics*, vol. 12, pp. 4750-4758, 2010.

- [185] O. Mašek, V. Budarin, M. Gronnow, K. Crombie, P. Brownsort, E. Fitzpatrick, *et al.*, "Microwave and slow pyrolysis biochar—Comparison of physical and functional properties," *Journal of Analytical and Applied Pyrolysis*, vol. 100, pp. 41-48, 2013.
- [186] M. Tripathi, J. Sahu, P. Ganesan, and T. Dey, "Effect of temperature on dielectric properties and penetration depth of oil palm shell (OPS) and OPS char synthesized by microwave pyrolysis of OPS," *Fuel*, vol. 153, pp. 257-266, 2015.
- [187] I. B. Initiative, "Standardized Product Definition and Product Testing Guidelines for Biochar That Is Used in Soil," ed: IBI biochar standards, 2015.
- [188] J. H. Park, G. K. Choppala, N. S. Bolan, J. W. Chung, and T. Chuasavathi, "Biochar reduces the bioavailability and phytotoxicity of heavy metals," *Plant and soil*, vol. 348, pp. 439-451, 2011.
- [189] L. E. De-Bashan and Y. Bashan, "Recent advances in removing phosphorus from wastewater and its future use as fertilizer (1997–2003)," *Water research*, vol. 38, pp. 4222-4246, 2004.
- [190] B. E. Rittmann, B. Mayer, P. Westerhoff, and M. Edwards, "Capturing the lost phosphorus," *Chemosphere*, vol. 84, pp. 846-53, 2011.
- [191] Y. Zhang, E. Desmidt, A. Van Looveren, L. Pinoy, B. Meesschaert, and B. Van der Bruggen, "Phosphate separation and recovery from wastewater by novel electro dialysis," *Environmental science & technology*, vol. 47, pp. 5888-5895, 2013.
- [192] S. Hukari, L. Hermann, and A. Nätörp, "From wastewater to fertilisers—Technical overview and critical review of European legislation governing phosphorus recycling," *Science of The Total Environment*, vol. 542, pp. 1127-1135, 2016.
- [193] C. Fang, T. Zhang, P. Li, R. Jiang, S. Wu, H. Nie, *et al.*, "Phosphorus recovery from biogas fermentation liquid by Ca–Mg loaded biochar," *Journal of Environmental Sciences*, vol. 29, pp. 106-114, 2015.
- [194] A. Oehmen, P. C. Lemos, G. Carvalho, Z. Yuan, J. Keller, L. L. Blackall, *et al.*, "Advances in enhanced biological phosphorus removal: from micro to macro scale," *Water research*, vol. 41, pp. 2271-300, 2007.
- [195] H. Dai, X. Lu, Y. Peng, H. Zou, and J. Shi, "An efficient approach for phosphorus recovery from wastewater using series-coupled air-agitated crystallization reactors," *Chemosphere*, vol. 165, pp. 211-220, 2016.

- [196] S. Kataki, H. West, M. Clarke, and D. C. Baruah, "Phosphorus recovery as struvite from farm, municipal and industrial waste: Feedstock suitability, methods and pre-treatments," *Waste Management*, vol. 49, pp. 437-454, 2016.
- [197] M. Zhang, B. Gao, Y. Yao, Y. Xue, and M. Inyang, "Synthesis of porous MgO-biochar nanocomposites for removal of phosphate and nitrate from aqueous solutions," *Chemical Engineering Journal*, vol. 210, pp. 26-32, 2012.
- [198] K. A. Krishnan and A. Haridas, "Removal of phosphate from aqueous solutions and sewage using natural and surface modified coir pith," *Journal of Hazardous Materials*, vol. 152, pp. 527-535, 2008.
- [199] C. Takaya, L. Fletcher, S. Singh, U. Okwuosa, and A. Ross, "Recovery of phosphate with chemically modified biochars," *Journal of Environmental Chemical Engineering*, vol. 4, pp. 1156-1165, 2016.
- [200] B. Chen, Z. Chen, and S. Lv, "A novel magnetic biochar efficiently sorbs organic pollutants and phosphate," *Bioresource technology*, vol. 102, pp. 716-23, 2011.
- [201] D. H. K. Reddy, K. Vijayaraghavan, J. A. Kim, and Y.-S. Yun, "Valorisation of post-sorption materials: Opportunities, strategies, and challenges," *Advances in Colloid and Interface Science*, vol. 242, pp. 35-58, 2016.
- [202] J. L. Field, C. M. Keske, G. L. Birch, M. W. DeFoort, and M. F. Cotrufo, "Distributed biochar and bioenergy coproduction: a regionally specific case study of environmental benefits and economic impacts," *GCB Bioenergy*, vol. 5, pp. 177-191, 2013.
- [203] T. O. West and A. C. McBride, "The contribution of agricultural lime to carbon dioxide emissions in the United States: dissolution, transport, and net emissions," *Agriculture, Ecosystems & Environment*, vol. 108, pp. 145-154, 2005.
- [204] S. Fan, Y. Wang, Z. Wang, J. Tang, J. Tang, and X. Li, "Removal of methylene blue from aqueous solution by sewage sludge-derived biochar: Adsorption kinetics, equilibrium, thermodynamics and mechanism," *Journal of Environmental Chemical Engineering*, vol. 5, pp. 601-611, 2017.
- [205] J. Chen, H. Kong, D. Wu, X. Chen, D. Zhang, and Z. Sun, "Phosphate immobilization from aqueous solution by fly ashes in relation to their composition," *Journal of Hazardous Materials*, vol. 139, pp. 293-300, 2007.
- [206] S. Lu, S. Bai, L. Zhu, and H. Shan, "Removal mechanism of phosphate from aqueous solution by fly ash," *Journal of Hazardous Materials*, vol. 161, pp. 95-101, 2009.

- [207] S. Arifuzzaman and S. Rohani, "Experimental study of brushite precipitation," *Journal of Crystal Growth*, vol. 267, pp. 624-634, 2004.
- [208] R. E. Wuthier, G. S. Rice, J. E. Wallace Jr, R. L. Weaver, R. Z. LeGeros, and E. D. Eanes, "In vitro precipitation of calcium phosphate under intracellular conditions: formation of brushite from an amorphous precursor in the absence of ATP," *Calcified tissue international*, vol. 37, pp. 401-410, 1985.
- [209] Y. Zhou, B. Gao, A. R. Zimmerman, and X. Cao, "Biochar-supported zerovalent iron reclaims silver from aqueous solution to form antimicrobial nanocomposite," *Chemosphere*, vol. 117, pp. 801-805, 2014.
- [210] X.-f. Tan, Y.-g. Liu, Y.-l. Gu, Y. Xu, G.-m. Zeng, X.-j. Hu, *et al.*, "Biochar-based nano-composites for the decontamination of wastewater: A review," *Bioresource technology*, vol. 212, pp. 318-333, 2016.
- [211] K.-W. Jung and K.-H. Ahn, "Fabrication of porosity-enhanced MgO/biochar for removal of phosphate from aqueous solution: application of a novel combined electrochemical modification method," *Bioresource technology*, vol. 200, pp. 1029-1032, 2016.
- [212] K. Qian, A. Kumar, H. Zhang, D. Bellmer, and R. Huhnke, "Recent advances in utilization of biochar," *Renewable and Sustainable Energy Reviews*, vol. 42, pp. 1055-1064, 2015.
- [213] W. Ding, X. Dong, I. M. Ime, B. Gao, and L. Q. Ma, "Pyrolytic temperatures impact lead sorption mechanisms by bagasse biochars," *Chemosphere*, vol. 105, pp. 68-74, 2014.
- [214] M. Inyang, B. Gao, Y. Yao, Y. Xue, A. R. Zimmerman, P. Pullammanappallil, *et al.*, "Removal of heavy metals from aqueous solution by biochars derived from anaerobically digested biomass," *Bioresource technology*, vol. 110, pp. 50-56, 2012.
- [215] X. Zhang, H. Wang, L. He, K. Lu, A. Sarmah, J. Li, *et al.*, "Using biochar for remediation of soils contaminated with heavy metals and organic pollutants," *Environmental Science and Pollution Research*, vol. 20, pp. 8472-8483, 2013.
- [216] H. A. Alhashimi and C. B. Aktas, "Life cycle environmental and economic performance of biochar compared with activated carbon: A meta-analysis," *Resources, Conservation and Recycling*, vol. 118, pp. 13-26, 2017.
- [217] D. L. Sparks, *Advances in agronomy* vol. 118: Academic Press, 2012.
- [218] Y. Yao, B. Gao, F. Wu, C. Zhang, and L. Yang, "Engineered biochar from biofuel residue: characterization and its silver removal potential," *ACS applied materials & interfaces*, vol. 7, pp. 10634-10640, 2015.

- [219] F. V. Silva-Medeiros, N. Consolin-Filho, M. Xavier de Lima, F. P. Bazzo, M. A. S. Barros, R. Bergamasco, *et al.*, "Kinetics and thermodynamics studies of silver ions adsorption onto coconut shell activated carbon," *Environmental technology*, vol. 37, pp. 3087-3093, 2016.
- [220] W. Cheung, Y. Szeto, and G. McKay, "Intraparticle diffusion processes during acid dye adsorption onto chitosan," *Bioresource technology*, vol. 98, pp. 2897-2904, 2007.
- [221] A. E. Ofomaja, "Intraparticle diffusion process for lead (II) biosorption onto mansonia wood sawdust," *Bioresource technology*, vol. 101, pp. 5868-5876, 2010.
- [222] H. Qiu, L. Lv, B.-c. Pan, Q.-j. Zhang, W.-m. Zhang, and Q.-x. Zhang, "Critical review in adsorption kinetic models," *Journal of Zhejiang University-Science A*, vol. 10, pp. 716-724, 2009.
- [223] V. Bolis, "Fundamentals in adsorption at the solid-gas interface. Concepts and thermodynamics," in *Calorimetry and Thermal Methods in Catalysis*, ed: Springer, 2013, pp. 3-50.
- [224] K. Foo and B. Hameed, "Insights into the modeling of adsorption isotherm systems," *Chemical Engineering Journal*, vol. 156, pp. 2-10, 2010.
- [225] P. S. Ghosal and A. K. Gupta, "Determination of thermodynamic parameters from Langmuir isotherm constant-revisited," *Journal of Molecular Liquids*, vol. 225, pp. 137-146, 2017.
- [226] Z. Liu and F.-S. Zhang, "Removal of lead from water using biochars prepared from hydrothermal liquefaction of biomass," *Journal of Hazardous Materials*, vol. 167, pp. 933-939, 2009.
- [227] E. Worch, *Adsorption technology in water treatment: fundamentals, processes, and modeling*: Walter de Gruyter, 2012.
- [228] Y. Chan, "Increasing soil organic carbon of agricultural land," *Primefact*, vol. 735, pp. 1-5, 2008.
- [229] T. Okuda, W. Nishijima, M. Sugimoto, N. Saka, S. Nakai, K. Tanabe, *et al.*, "Removal of coagulant aluminum from water treatment residuals by acid," *Water research*, vol. 60, pp. 75-81, 2014.
- [230] G. Mininni, A. Blanch, F. Lucena, and S. Berselli, "EU policy on sewage sludge utilization and perspectives on new approaches of sludge management," *Environmental Science and Pollution Research*, vol. 22, pp. 7361-7374, 2015.

- [231] M. Samolada and A. Zabaniotou, "Comparative assessment of municipal sewage sludge incineration, gasification and pyrolysis for a sustainable sludge-to-energy management in Greece," *Waste management*, vol. 34, pp. 411-420, 2014.
- [232] S. Alanya, J. Dewulf, and M. Duran, "Comparison of overall resource consumption of biosolids management system processes using exergetic life cycle assessment," *Environmental science & technology*, vol. 49, pp. 9996-10006, 2015.
- [233] K. Sichone, M. C. Lay, T. White, C. J. R. Verbeek, H. Kay, and L. E. van den Berg, "Pilot scale pyrolysis-determination of critical moisture content for sustainable organic waste pyrolysis," 2012.
- [234] Y. Niu, H. Tan, and S. e. Hui, "Ash-related issues during biomass combustion: Alkali-induced slagging, silicate melt-induced slagging (ash fusion), agglomeration, corrosion, ash utilization, and related countermeasures," *Progress in Energy and Combustion Science*, vol. 52, pp. 1-61, 2016.
- [235] M. Cyr, M. Coutand, and P. Clastres, "Technological and environmental behavior of sewage sludge ash (SSA) in cement-based materials," *Cement and Concrete Research*, vol. 37, pp. 1278-1289, 2007.
- [236] I. Hwang, Y. Ouchi, and T. Matsuto, "Characteristics of leachate from pyrolysis residue of sewage sludge," *Chemosphere*, vol. 68, pp. 1913-1919, 2007.
- [237] T. Liu, B. Liu, and W. Zhang, "Nutrients and heavy metals in biochar produced by sewage sludge pyrolysis: its application in soil amendment," *Polish Journal of Environmental Studies*, vol. 23, pp. 271-275, 2014.
- [238] C. Adam, B. Peplinski, M. Michaelis, G. Kley, and F. G. Simon, "Thermochemical treatment of sewage sludge ashes for phosphorus recovery," *Waste Management*, vol. 29, pp. 1122-1128, 2009.
- [239] EPA, "Method 1311. Toxicity Characteristic Leaching procedure," ed: USA Norm, 1992.
- [240] H. Yuan, T. Lu, D. Zhao, H. Huang, K. Noriyuki, and Y. Chen, "Influence of temperature on product distribution and biochar properties by municipal sludge pyrolysis," *Journal of Material Cycles and Waste Management*, vol. 15, pp. 357-361, 2013.
- [241] P. Samaras, C. Papadimitriou, I. Haritou, and A. Zouboulis, "Investigation of sewage sludge stabilization potential by the addition of fly ash and lime," *Journal of Hazardous Materials*, vol. 154, pp. 1052-1059, 2008.
- [242] P. Papadopoulos and D. Rowell, "The reactions of copper and zinc with calcium carbonate surfaces," *European Journal of Soil Science*, vol. 40, pp. 39-48, 1989.

- [243] L. Miller-Robbie, B. A. Ulrich, D. F. Ramey, K. S. Spencer, S. P. Herzog, T. Y. Cath, *et al.*, "Life cycle energy and greenhouse gas assessment of the co-production of biosolids and biochar for land application," *Journal of Cleaner Production*, vol. 91, pp. 118-127, 2015.
- [244] W. Rulkens, "Sewage sludge as a biomass resource for the production of energy: overview and assessment of the various options," *Energy & Fuels*, vol. 22, pp. 9-15, 2007.
- [245] M. Franz, "Phosphate fertilizer from sewage sludge ash (SSA)," *Waste Management*, vol. 28, pp. 1809-18, 2008.
- [246] M. Heckenmüller, D. Narita, and G. Klepper, "Global availability of phosphorus and its implications for global food supply: an economic overview," Kiel Working Paper 2014.

APPENDIX

Table A1 - Chemical composition of biochar produced at different pyrolysis temperature.

Element	Units	300°C	400°C	500°C	600°C	700°C	800°C
Al	Mean (mg/kg)	65610	73190	76290	75330	72500	81190
	±	150	680	860	220	160	1250
As	Mean (mg/kg)	12.2	12.8	13.0	14.9	13.0	12.7
	±	0.3	0.3	0.3	0.2	0.3	0.3
Ca	Mean (mg/kg)	6930	7960	8310	8210	8570	8530
	±	10	60	70	40	20	110
Cd	Mean (mg/kg)	0.769	0.912	0.875	0.911	0.930	0.908
	±	0.038	0.023	0.024	0.037	0.032	0.034
Co	Mean (mg/kg)	7.50	7.71	8.03	8.97	8.14	8.50
	±	0.11	0.19	0.11	0.22	0.11	0.20
Cr	Mean (mg/kg)	58.0	57.6	64.7	73.2	54.5	65.4
	±	0.4	1.5	1.0	1.4	1.1	2.5
Cu	Mean (mg/kg)	336	345	355	384	368	360
	±	4	6	5	5	5	7
Fe	Mean (mg/kg)	20360	20730	22260	22220	22620	24940
	±	190	90	280	160	120	470
Hg	Mean (mg/kg)	1.11	1.05	0.908	1.20	1.26	1.01
	±	0.36	0.21	0.029	0.14	0.09	0.28
Mg	Mean (mg/kg)	2070	2360	2400	2370	2430	2600
	±	10	20	20	10	10	30
Mo	Mean (mg/kg)	2.76	3.19	3.42	3.82	3.00	3.02
	±	0.11	0.09	0.10	0.17	0.11	0.13
Ni	Mean (mg/kg)	28.1	29	30.5	36.1	29.9	31.8
	±	0.5	0.8	0.4	0.7	0.5	0.6
Pb	Mean (mg/kg)	25.7	27.5	27.1	30.8	32.0	29.4
	±	0.7	0.3	0.4	0.6	0.7	0.7
Se	Mean (mg/kg)	14.6	14.7	16.3	15.3	15.7	14.8
	±	1.3	1.6	1.0	1.4	1.4	1.0
Zn	Mean (mg/kg)	720	774	799	858	827	808
	±	13	16	12	14	15	14
P	Mean (mg/kg)	13810	16450	16660	16480	16950	17220
	±	20	80	180	50	70	270
K	Mean (mg/kg)	1030	1540	1760	1650	1890	2190
	±	100	60	40	30	70	100

Table A2 - Chemical composition of biosolids

Element	Units	Biosolids
Al	Mean (mg/kg) ±	62300 157
As	Mean (mg/kg) ±	9.36 0.2
Ca	Mean (mg/kg) ±	6142 21
Cd	Mean (mg/kg) ±	0.684 0.018
Co	Mean (mg/kg) ±	6.72 0.09
Cr	Mean (mg/kg) ±	52.9 0.7
Cu	Mean (mg/kg) ±	236 4
Fe	Mean (mg/kg) ±	18995 18
Hg	Mean (mg/kg) ±	0.424 0.016
Mg	Mean (mg/kg) ±	1895 8
Mo	Mean (mg/kg) ±	2.52 0.11
Ni	Mean (mg/kg) ±	24.7 0.3
Pb	Mean (mg/kg) ±	24.3 0.5
Se	Mean (mg/kg) ±	3.29 0.21
Zn	Mean (mg/kg) ±	548 7
P	Mean (mg/kg) ±	13300 112
K	Mean (mg/kg) ±	1910 46

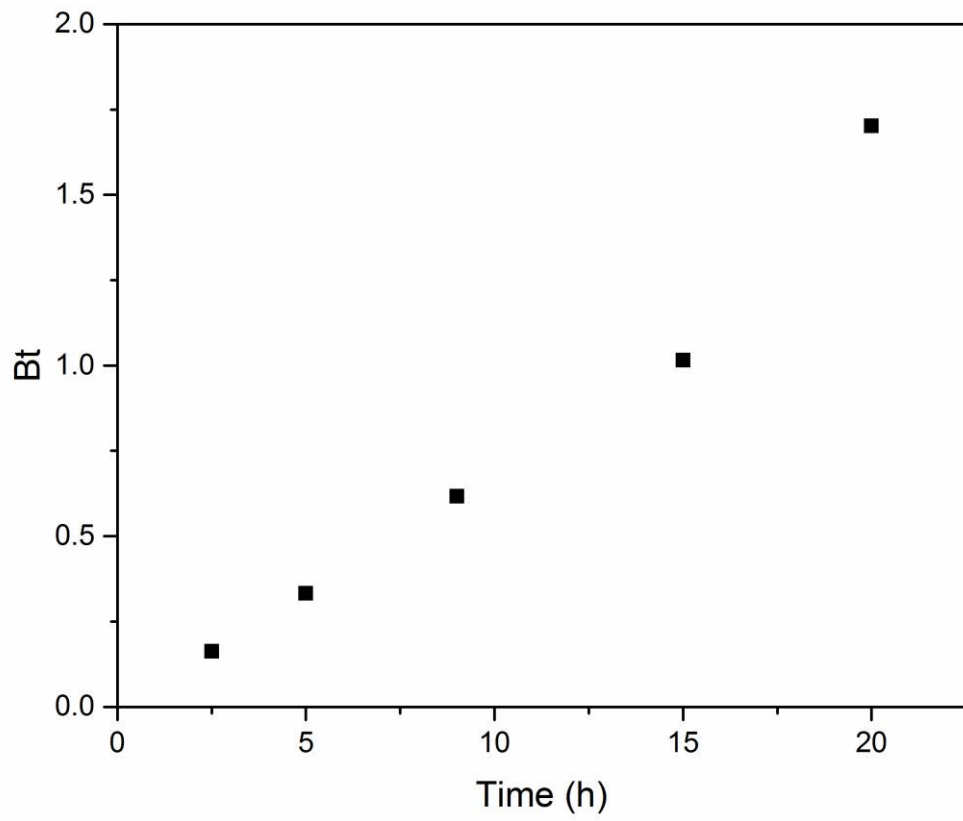


Figure A1 – Boyd plot (Bt versus t).

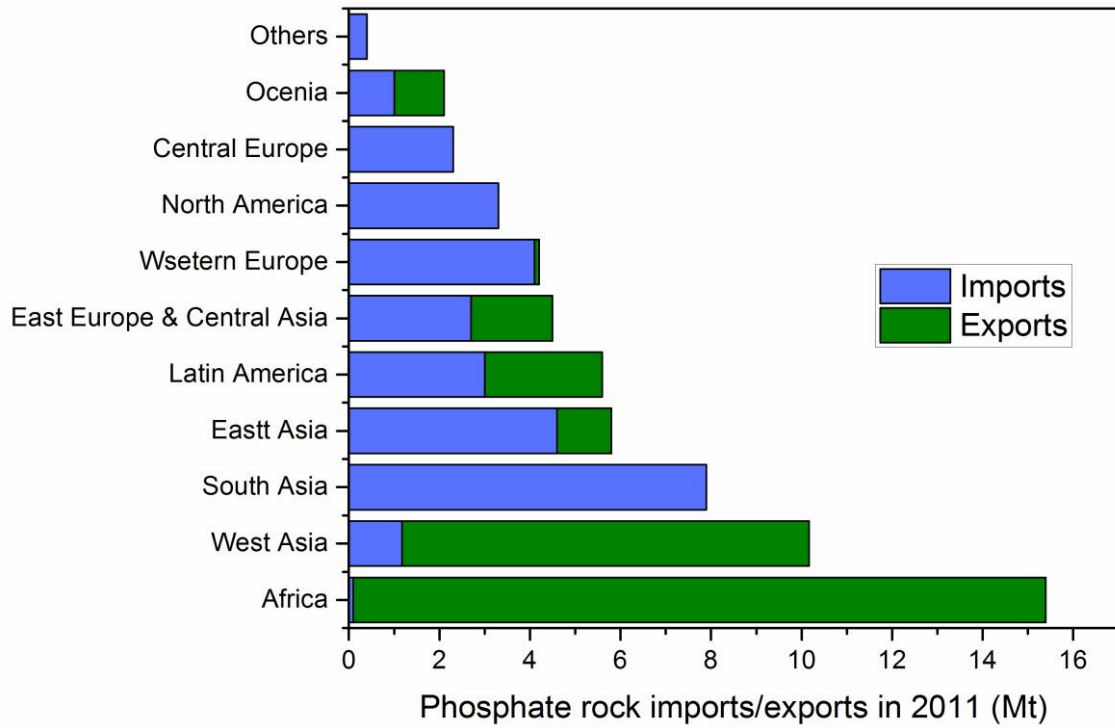


Figure A2 – Phosphate rock exports and imports by region (2011) [246].

Table A3 - Contaminant upper limits for classifying biosolids as grade C1 or C2 (values are mg/kg dry weight) [177].

Contaminant	Grade C1 and RSCL⁽¹⁾	Grade C2
As	20	60
Cd	1	10
Cr⁽²⁾	400	3000
Cu	100 (150) ⁽³⁾	2000
Pb	300	500
Hg	1	5
Ni	60	270
Se	3	50
Zn	200 (300) ⁽⁴⁾	2500

(1) RSCL-Receiving soil contaminant limits.

(2) Chromium (III) limit due to expectation that this will be the dominant form.

(3) 150 mg/kg copper limit for biosolids products composted to AS 4454.

(4) 300 mg/kg zinc limit for biosolids products composted to AS 4454.